Enclosure 4

CENPD-188-A, "HERMITE - A Multi-Dimensional Space-Time Kinetics Code for PWR Transients"

(Non-Proprietary)

Westinghouse Electric Company
1000 Westinghouse Drive
Cranberry Township, PA 16066

CENPD-188-A

HERMITE

A MULTI-DIMENSIONAL SPACE-TIME KINETICS CODE FOR PWR TRANSIENTS

P.E. ROHAN
S.G. WAGNER
S.E. RITTERBUSCH

March, 1976
Reprinted July, 1976

POWER SYSTEMS
COMBUSTION ENGINEERING, INC.

UNITED STATES
NUCLEAR REGULATORY COMMISSION
WASHINGTON, D. C. 20555

JUN 1 0 1976

Mr. A. E. Scherer
Licensing Manager (460-4)
Nuclear Power Systems Division
Combustion Engineering, Inc.
1000 Prospect Hill Road
Windsor, Connecticut 06095

Dear Mr. Scherer:

The Nuclear Regulatory Commission (NRC) staff has completed its review of Combustion Engineering topical report CENPD-188 entitled, "HERMITE - a Multidimensional Space-Time Kinetics Code for PWR Transients."

We conclude that CENPD-188 describes an acceptable neutron kinetics computer code for solving the few-group transient diffusion equations in one, two, and three dimensions. We also conclude that CENPD-188 is acceptable for reference in license applications.

Should NRC criteria or regulations change such that our conclusions concerning CENPD-188 are invalidated, you will be notified and given an opportunity to revise and resubmit your topical report, should you so desire.

It is requested that when this report is resubmitted as an approved report that our approval letter and its enclosed evaluation be incorporated as part of the document. The staff does not intend to repeat its review of this report when it appears as a reference in a particular license application.

Sincerely,

Olan D. Parr

Olan D. Parr, Chief
Light Water Reactors
Branch No. 3
Division of Project Management

Enclosure:
Staff Evaluation of
CENPD-188

TOPICAL REPORT EVALUATION

Report No.:	CENPD-188
Report Title:	HERMITE - A Multi-Dimensional Space-Time Kinetics Code for PWR Transients (Nonproprietary)
Report Date:	March 1976
Originating Organization:	Combustion Engineering, Inc.
Reviewed By:	Core Performance Branch
Date of Evaluation:	June 1976

SUMMARY OF TOPICAL REPORT

This report describes the HERMITE space-time kinetics computer code which was developed by CE for the analysis of design and off-design transients in large PWR's. The three-dimensional, four-group, time-dependent neutron diffusion equation is solved by a finite element method and includes feedback effects of fuel temperature, coolant temperature, coolant density and control rod motion. The heat conduction equation in the pellet, gap and clad is solved by a finite difference method. Continuity and energy conservation equations are solved for the coolant enthalpy and density.

Extensive verification calculations have been performed and are summarized in this report. HERMITE was applied to the three-dimensional analysis of the control rod ejection accident and results were compared to the corresponding two-dimensional analysis.

A description of the code input is also included as an appendix.

SUMMARY OF STAFF EVALUATION

We have reviewed the subject report, including the mathematical models and analytical procedures and methods. The HERMITE code described in this report is one of the more sophisticated neutron kinetics computer codes because of its three-dimensional capabilities. For this reason, the large computer time required to analyze typical reactivity transients may restrict the code's use as a standard design tool but enable it to be extremely useful in evaluating the accuracy (or conservatism) of less-sophisticated calculational methods, such as point kinetics, used to analyze accidents as suggested in Appendix A-12 of Regulatory Guide 1.77.

The verification of the HERMITE code was accomplished by comparing numerical results from HERMITE to those from existing computer codes which utilize accepted calculational methodology. For example, verification of HERMITE's steady-state neutronics model was accomplished via comparison of eigenvalues and static power distributions from HERMITE and PDQ. Thermal-hydraulic feedback effects were not included and the comparisons showed good agreement. Similarly, HERMITE's transient neutronics calculations without feedback were verified by comparing HERMITE and TWIGL for a control rod ejection accident. The test problem was a two-dimensional representation and again the comparisons showed good agreement. HERMITE's thermal-hydraulic model was decoupled from the neutronics portion of the code and showed good agreement in comparisons with CE's STRIKIN-II transient heat transfer code.

HERMITE results for transient neutronics calculations with thermal feedback (Doppler only) were verified via comparison with two-dimensional TWIGL calculations for control rod ejection accidents initiated from both zero and full power conditions and the comparison was good.

At present, only transients initiated by control rod motion are treated. It is anticipated that future modifications to the code will allow other transients of interest to be analyzed in three-dimensions.

Although no comparisons were performed with other existing three-dimensional space-time kinetics codes, the staff feels that the good agreement obtained by two-dimensional steady-state comparisons with PDQ and two-dimensional kinetics comparisons with TWIGL substantiate acceptable results in the extrapolation of HERMITE to three-dimensions.

STAFF POSITION

The subject report describes an acceptable neutron kinetics computer code for solving the few-group transient diffusion equations in one, two and three dimensions. It has been used to support the CE Control Element Assembly Ejection Analysis Topical Report (CENPD-190, January 1976) and may be referenced in future license applications and topical reports.

LEGAL NOTICE

This report was prepared as an account of work sponsored by Combustion Engineering, Inc. Neither Combustion Engineering nor any person acting on its behalf:

a. Makes any warranty or representation, express or implied including the warranties of fitness for a particular purpose or merchantability, with respect to the accuracy, completeness, or usefulness of the information contained in this report, or that the use of any information, apparatus, method, or process disclosed in this report may not infringe privately owned rights; or

b. Assumes any liabilities with respect to the use of, or for damages resulting from the use of, any information, apparatus, method or process disclosed in this report.

Acknowledgement

The authors would like to acknowledge the contributions of C. M. Kang to the development of prototype versions of the HERMITE code. R. A. Shober's contribution to the initial programming of this version of HERMITE is also gratefully acknowledged.

Approvals

G. B. Peeler, Supervisor
Nuclear Safety

P. E. Rohan, Section Manager
Physics & Computer Analysis

W. C. Coppersmith, Manager
Nuclear Safety

R. R. Lee, Manager
Physics & Computer Analysis

W. R. Corcoran, Director
Nuclear Safety

S. Visner, Director
Physics & Computer Analysis

3/22/76
Date

6/25/76
Date

ABSTRACT

This report describes the HERMITE space-time kinetics computer code. This code was developed for the analysis of design and off-design transients in large PWR's by means of a numerical solution to the multi-dimensional, few-group, time-dependent neutron diffusion equation including feedback effects of fuel temperature, coolant temperature, coolant density and control rod motion. The time-dependent neutron diffusion equation is solved by a finite element method. The heat conduction equation in the pellet, gap and clad is solved by a finite difference method. Continuity and energy conservation equations are solved for the coolant enthalpy and density.

Extensive verification calculations have been performed and are summarized in this report. HERMITE was applied to the three-dimensional analysis of the control element assembly ejection incident, and results were compared to the corresponding two-dimensional analysis. An input description is included as an appendix.

TABLE OF CONTENTS

Section	Title	Page
1.0	INTRODUCTION	1-1
2.0	THE MODELS INCORPORATED IN HERMITE	2-1
	2.1 The Neutronics Model	2-1
	2.1.1 Derivation of the Equations	2-1
	2.1.2 Solution of the Equations	2-7
	2.2 The Thermal-Hydraulic Model	2-10
	2.2.1 Fuel Pin Heat Conduction Model	2-11
	2.2.2 Coolant Model	2-19
	2.2.3 Clad-Coolant Heat Transfer	2-22
	2.2.4 Physical Properties of Fuel, Gas Gap, Clad and Coolant	2-24
	2.3 The Cross Section Representation	2-28
	2.4 References for Section 2.0	2-31
3.0	THE HERMITE COMPUTER CODE	3-1
	3.1 Structure of the HERMITE Code	3-1
	3.2 Features and Options in the HERMITE Code	3-2
	3.3 Reference for Section 3.0	3-5
4.0	VERIFICATION OF THE HERMITE MODELS	4-1
	4.1 Verification of HERMITE's Neutronics Model Without Thermal Feedback	4-1
	4.1.1 HERMITE and PDQ Eigenvalues and Static Power Distributions	4-1
	4.1.2 HERMITE and PDQ Control Element Assembly Worths	4-4
	4.1.3 HERMITE and TWIGL Transient Neutronics	4-4
	4.2 Verification of HERMITE's Thermal-Hydraulic Model	4-5
	4.3 Verification of HERMITE's Neutronics Model with Thermal Feedback	4-6
	4.3.1 HERMITE and TWIGL Full Power Control Element Assembly Ejection Incidents	4-7

TABLE OF CONTENTS (Cont.)

Section	Title	Page
	4.3.2 HERMITE and TWIGL Zero Power Control Element Assembly Ejection Incidents	4-7
	4.4 References for Section 4.0	4-9
5.0	THREE-DIMENSIONAL ANALYSIS OF THE CONTROL ELEMENT ASSEMBLY EJECTION INCIDENT	5-1
	5.1 Full Power Control Element Assembly Ejection Incident	5-1
	5.2 Zero Power Control Element Assembly Ejection Incident	5-3
6.0	NOMENCLATURE	6-1
	6.1 Neutronics and Cross Section Nomenclature for Sections 2.1 and 2.3	6-1
	6.2 Thermal-Hydraulic Nomenclature for Section 2.2	6-4

LIST OF APPENDICES

Appendix	Title	Page
A	HERMITE Input Description	A-i

LIST OF TABLES

Table	Title	Page
4-1	HERMITE and PDQ Control Element Assembly Worths (%Δρ)	4-10
4-2	Thermal-Hydraulic Calculation for a Full Power Control Element Assembly Ejection Incident - A Comparison of HERMITE and STRIKIN-II Results	4-11
4-3	Thermal-Hydraulic Calculation for a Full Power Control Element Assembly Ejection Incident - A Comparison of HERMITE Results for Fuel Pins with Nineteen and Nine Radial Nodes	4-12
4-4	Thermal-Hydraulic Calculation for a Zero Power Control Element Assembly Ejection Incident - A Comparison of HERMITE and STRIKIN-II Results	4-13
4-5	Thermal-Hydraulic Calculation for a Zero Power Control Element Assembly Ejection Incident - A Comparison of HERMITE Results for Fuel Pins with Nineteen and Nine Radial Nodes	4-14
5-1	Central Control Element Assembly Static Worths (%Δρ)	5-6

LIST OF FIGURES

Figure	Title	Page
2-1	Finite Element Basis Function	2-33
2-2	Mesh Structure for a Thermal-Hydraulic Flow Channel	2-34
3-1	HERMITE Overlay Structure and Overlay Functions	3-6
3-2	Steady-State Problem Logic Diagram	3-7
3-3	Transient Problem Logic Diagram	3-8
4-1	217 Fuel Assembly Core, Full Power Control Element Pattern for HERMITE Verification	4-15
4-2	HERMITE and PDQ Power Distribution Differences for a 4 x 4 Mesh, 217 Fuel Assembly Core at Full Power	4-16
4-3	HERMITE Power Distribution Differences for a 2 x 2 Mesh, 217 Fuel Assembly Core at Full Power	4-17
4-4	HERMITE and PDQ Power Distribution Differences for a 2 x 2 Mesh, 241 Fuel Assembly Core at Full Power	4-18
4-5	241 Fuel Assembly Core, Zero Power Control Element Pattern for HERMITE Verification	4-19
4-6	HERMITE and PDQ Power Distribution Differences for a 2 x 2 Mesh, 241 Fuel Assembly Core at Zero Power	4-20
4-7	241 Fuel Assembly Core, Full Power Control Element Pattern for HERMITE Verification	4-21
4-8	Full Power CEA Ejection Transient, Total Core Power Without Feedback	4-22

LIST OF FIGURES (Cont.)

Figure	Title	Page
4-9	Full Power CEA Ejection Transient, Core Power Forcing Function for Thermal-Hydraulic Model Verification	4-23
4-10	Zero Power CEA Ejection Transient, Core Power Forcing Function for Thermal-Hydraulic Model Verification	4-24
4-11	Full Power CEA Ejection Transient, Total Core Power With Feedback	4-25
4-12	Zero Power CEA Ejection Transient, Total Core Power With Feedback	4-26
5-1	Full Power CEA Ejection Transient, Total Core Power	5-7
5-2	Full Power CEA Ejection Transient, Central Assembly Power	5-8
5-3	Full Power CEA Ejection Transient, Central Assembly Power Distribution at t = 0.004 Seconds	5-9
5-4	Full Power CEA Ejection Transient, Central Assembly Power Distribution at t = 0.012 Seconds	5-10
5-5	Full Power CEA Ejection Transient, Central Assembly Power Distribution at t = 0.028 Seconds	5-11
5-6	Full Power CEA Ejection Transient, Central Assembly Power Distribution at t = 0.044 Seconds	5-12
5-7	Full Power CEA Ejection Transient, Core Power After Step Ejection of the CEA	5-13
5-8	3D Full Power CEA Ejection Transient, Maximum Node Power Relative to Average Node Power	5-14

LIST OF FIGURES (Cont.)

Figure	Title	Page
5-9	3D Full Power CEA Ejection Transient, Location of Maximum Node Power	5-15
5-10	Zero Power CEA Ejection Transient, Total Core Power	5-16
5-11	Zero Power CEA Ejection Transient, Central Assembly Power	5-17
5-12	Zero Power CEA Ejection Transient, Core Average Fuel Temperature	5-18
5-13	Zero Power CEA Ejection Transient, Central Assembly Average Fuel Temperature	5-19
5-14	Zero Power CEA Ejection Transient, Central Assembly Power Distribution at t = 0.004 Seconds	5-20
5-15	Zero Power CEA Ejection Transient, Central Assembly Power Distribution at t = 0.012 Seconds	5-21
5-16	Zero Power CEA Ejection Transient, Central Assembly Power Distribution at t = 0.024 Seconds	5-22
5-17	Zero Power CEA Ejection Transient, Central Assembly Power Distribution at t = 0.044 Seconds	5-23
5-18	3D Zero Power CEA Ejection Transient, Maximum Node Power Relative to Average Node Power	5-24
5-19	3D Zero Power CEA Ejection Transient, Location of Maximum Node Power	5-25

1.0 INTRODUCTION

As the size of large power reactors increases, space-time effects during reactor transients become more important. In order not to penalize reactor performance unduly with overly conservative design methods, it is desirable to have the capability of performing detailed space-time neutronics calculations for both design and off-design transients.

The HERMITE computer code has been developed to meet this objective. It solves the few-group, space and time dependent neutron diffusion equation including feedback effects of fuel temperature, coolant temperature, coolant density and control rod motion. The neutronics equations are solved by a finite element method. The fuel temperature model explicitly represents the pellet, gap and clad regions of the fuel pin, and the governing heat conduction equations are solved by a finite difference method. Continuity and energy conservation equations are solved in order to determine the coolant temperature and density. Each of these models is described in detail in Section 2.

Section 3 describes the HERMITE program's structure, and includes calculation flow diagrams. Sections 4 and 5 describe the verification of HERMITE's calculations and the application of HERMITE to three-dimensional full power and zero power control element assembly (CEA) ejection transients. Section 6 defines the nomenclature used in this report. An input description for HERMITE is included in Appendix A.

2.0 THE MODELS INCORPORATED IN HERMITE

2.1 THE NEUTRONICS MODEL

2.1.1 Derivation of the Equations

The solution of the space and time dependent neutron diffusion equation is obtained by a finite element method developed by Kang and Hansen, references 2-1 and 2-2. The starting point is the multigroup diffusion equations:

$$\nabla \cdot D_g \nabla \Psi_g(\underline{r},t) - \Sigma_g^T \Psi_g(\underline{r},t) + \Sigma_{g-1}^r \Psi_{g-1}(\underline{r},t)$$

$$+(1-\beta)\chi_g \sum_{g'=1}^{G} \frac{\nu_{g'}}{\lambda} \Sigma_{g'}^f \Psi_{g'}(\underline{r},t) + \sum_{n=1}^{N} \lambda_n \chi_g \exp(-\lambda_n t) C_{n,o}(\underline{r})$$

$$+\sum_{n=1}^{N} \chi_g \sum_{g'=1}^{G} \lambda_n \beta_n \int_o^t ds \exp(-\lambda_n(t-s)) \frac{\nu_{g'}}{\lambda} \Sigma_{g'}^f \Psi_{g'}(\underline{r},s)$$

$$= \frac{1}{v_g} \frac{\partial \Psi_g(\underline{r},t)}{\partial t}, \qquad g=1,\ldots,G \qquad (2\text{-}1)$$

where

$$C_{n,o}(\underline{r}) = \frac{\beta_n}{\lambda_n} \sum_{g'=1}^{G} \frac{\nu_{g'}}{\lambda} \Sigma_{g'}^f \Psi_{g'}(\underline{r},o). \qquad (2\text{-}2)$$

The nomenclature is conventional and is defined in Section 6.0.

The boundary conditions on $\Psi_g(\underline{r},t)$, may be either:

$$\Psi_g(\underline{r}_s,t) = 0 \qquad (2\text{-}3)$$

or

$$\frac{\partial}{\partial n} \Psi_g(\underline{r},t) \Big|_{\underline{r}_s} = 0, \qquad (2\text{-}4)$$

where $\underline{r}_s$ denotes points on the boundary and $\partial/\partial n$ denotes an outward pointing derivative normal to the reactor surface. At interfaces, flux and current continuity conditions are imposed. That is, the two quantities

$$\Psi_g(\underline{r},t)\Big|_{\underline{r}_I} \qquad \text{and} \qquad D_g \frac{\partial \Psi_g(\underline{r},t)}{\partial n}\Big|_{\underline{r}_I}$$

are continuous at all points $\underline{r}_I$ on interfaces.

Equation 2-1 is converted to the "weak" or "variational" form by multiplying it by a test function, v, and integrating this product over the region of solution, R. Expressed in the conventional inner product notation, the first term of equation 2-1 becomes:

$$\int_R v \nabla \cdot D_g \nabla \Psi_g(\underline{r},t)\, d\underline{r} = (v, \nabla \cdot D_g \nabla \Psi_g).$$

Since Ψ_g will ultimately be approximated by functions which are not twice differentiable, it is necessary to convert this term to a form which has less restrictive smoothness requirements. Using the identity

$$v \nabla \cdot D_g \nabla \Psi_g = \nabla \cdot v D_g \nabla \Psi_g - D_g \nabla v \cdot \nabla \Psi_g, \qquad (2\text{-}5)$$

the divergence theorem, and imposing the "essential" boundary condition that v be zero whenever $\partial\Psi_g/\partial n$ is non-zero on the boundary, the first term of equation 2-1 becomes:

$$-(\nabla v, D_g \nabla \Psi_g).$$

The weak form of the multigroup diffusion equation is now written as

$$\begin{aligned}
&-(\nabla v, D_g \nabla \Psi_g) - (v, \Sigma_g^T \Psi_g) + (v, \Sigma_{g-1}^r \Psi_{g-1}) \\
&+ (1-\beta)(v, \chi_g \sum_{g'=1}^{G} \frac{\nu_{g'}}{\lambda} \Sigma_{g'}^f \Psi_{g'}) + \sum_{n=1}^{N} \lambda_n \chi_g \exp(-\lambda_n t)(v, C_{n,o}) \\
&+ \sum_{n=1}^{N} \chi_g \sum_{g'=1}^{G} \lambda_n \beta_n \int_o^t ds \exp(-\lambda_n(t-s))(v, \frac{\nu_{g'}}{\lambda} \Sigma_{g'}^f \Psi_{g'}) \\
&= (v, \frac{1}{v_g} \frac{\partial}{\partial t} \Psi_g). \qquad (2\text{-}6)
\end{aligned}$$

The functions Ψ_g and v must be continuous and have first-order spatial derivatives which are square integrable in the region of solution. A *function Ψ_g is a solution to equation 2-6 if it satisfies the equation for* all admissible test functions, v.

In selecting admissible trial solution functions for equation 2-6, it is not necessary to impose current continuity at interfaces since the exact solution will naturally satisfy this condition. For the same reason it is not necessary to impose the zero-current condition, $\partial\Psi_g/\partial n = 0$, on the applicable boundaries.

In the finite element method, the neutron flux $\Psi_g(\underline{r},t)$ is expanded in a set of known basis functions $u_m(\underline{r})$:

$$\Psi_g(\underline{r},t) = \sum_{m=1}^{M} \Psi_{g,m}(t)\, u_m(\underline{r}). \qquad (2\text{-}7)$$

The test functions, v, are restricted to those which are linear combinations of the basis functions.

The particular finite element method employed in the HERMITE code uses piecewise linear basis functions in each spatial dimension. In three space dimensions these functions are defined by the following relationships:

$$u_m(\underline{r}) = u_i(x)\, u_j(y)\, u_k(z)$$

$$u_i(x) = \begin{cases} (x - x_{i-1})/(x_i - x_{i-1}); & x_{i-1} \le x \le x_i \\ (x_{i+1} - x)/(x_{i+1} - x_i); & x_i \le x \le x_{i+1} \\ 0 \quad ; & \text{elsewhere.} \end{cases} \qquad (2\text{-}8)$$

This function is shown in Figure 2-1. Similar definitions apply to $u_j(y)$ and $u_k(z)$.

If the mesh points in the x-direction are numbered 0, 1, 2, ..., I, and similarly for the y- and z-directions, then there are (I+1)*(J+1)*(K+1) mesh points and basis functions. That is,

$$M = (I+1)*(J+1)*(K+1) \qquad (2\text{-}9)$$

in equation 2-7. From the definition of the basis functions, equation 2-8, and the flux expansion, equation 2-7, one sees that the expansion coefficient $\Psi_{g,m}(t)$ is the value of the group g flux at mesh point $\underline{r}_m = (x_i, y_j, z_k)$ at time t. The zero-flux boundary condition, where applicable, is imposed by setting $\Psi_{g,m} = 0$ and $v_m = 0$. This has the effect of reducing the number of unknowns, M, in an obvious manner.

The flux expansion of equation 2-7 is substituted into equation 2-6 and each of the basis functions $u_m(\underline{r})$ is used as a test function, v, in the spatial integrations. This procedure is called Galerkin weighting and ensures that equation 2-6 will be satisfied for all test functions which are linear combinations of the basis functions, and which meet the required boundary conditions. The result of the substitution is a set of G x M coupled, first-order, ordinary differential equations in time for $\Psi_{g,m}(t)$. Written in matrix form the equations are:

$$V \frac{\partial}{\partial t} \underline{\Psi}(t) = [-L(t) + S(t) + (1-\beta) F(t)] \underline{\Psi}(t)$$
$$+ \sum_{n=1}^{N} \lambda_n \{\underline{C}_{n,o} \exp(-\lambda_n t) + \beta_n \int_0^t ds \exp(-\lambda_n (t-s)) F(s) \underline{\Psi}(s)\}. \qquad (2\text{-}10)$$

$\underline{\Psi}(t)$ is a vector with G x M components. Each component, $\Psi_{g,m}(t)$, is the flux in group g at mesh point $\underline{r}_m$ and time t. $\underline{C}_{n,o}$ is also a vector with G x M components. Each component,

$$C_{ngmo} = \frac{\beta_n}{\lambda_n} \chi_g \left(u_m, \sum_{g'=1}^{G} \frac{\nu_{g'}}{\lambda} \Sigma^f_{g'} \Psi_{g',m}(0)\right), \qquad (2\text{-}11)$$

is the appropriately weighted and integrated initial delayed neutron precursor concentration. The quantities V, L, S and F are all (GM x GM) matrices whose elements are

$$V_{g'gm'm} = \delta_{g'g} \left(u_{m'}, \frac{1}{v_g} u_m\right), \qquad (2\text{-}12)$$

$$L_{g'gm'm} = \delta_{g'g} \{ (\nabla u_{m'}, D_g \nabla u_m) + (u_{m'}, \Sigma_g^T u_m) \}, \quad (2\text{-}13)$$

$$S_{g'gm'm} = \delta_{g'g-1} (u_{m'}, \Sigma_{g-1}^r u_m) \quad (2\text{-}14)$$

and

$$F_{g'gm'm} = \chi_g (u_{m'}, \frac{\nu_{g'}}{\lambda} \Sigma_{g'}^f u_m). \quad (2\text{-}15)$$

where $\delta_{g'g}$ is the Kronecker delta function. With this notation, $\underline{C}_{n,o}$ can be written as:

$$\underline{C}_{n,o} = \frac{\beta_n}{\lambda_n} F(0) \underline{\Psi}(0). \quad (2\text{-}16)$$

Equation 2-10 is discretized in time by assuming that the flux, $\Psi_{g,m}(t)$, is a linear function of time between t_p and t_{p+1}:

$$\Psi_{g,m}(t) = \Psi_{g,m}(t_p) u_p(t) + \Psi_{g,m}(t_{p+1}) u_{p+1}(t) \quad (2\text{-}17)$$

where

$$u_p(t) = \begin{cases} \dfrac{t - t_{p-1}}{t_p - t_{p-1}} ; & t_{p-1} \leq t \leq t_p \\ \dfrac{t_{p+1} - t}{t_{p+1} - t_p} ; & t_p \leq t \leq t_{p+1} \\ 0 ; & \text{elsewhere.} \end{cases} \quad (2\text{-}18)$$

These temporal basis functions have the same form as the spatial basis functions described earlier. Equation 2-17 is substituted into equation 2-10 and the result is integrated over the time interval (t_p, t_{p+1}). The matrices in equation 2-10 are time-dependent because of thermal-hydraulic effects and control rod movement. During the integration they are assumed to have their value at time t_p and to remain constant over the time interval (t_p, t_{p+1}).

The resulting set of discrete equations is

$$\{V(t_p) - \frac{\Delta t_p}{2}[-L(t_p) + S(t_p)] - \gamma_p F(t_p)\} \underline{\Psi}(t_{p+1})$$

$$= \{V(t_p) + \frac{\Delta t_p}{2}[-L(t_p) + S(t_p)] + \alpha_p F(t_p)\} \underline{\Psi}(t_p)$$

$$+ \sum_{n=1}^{N} [\exp(-\lambda_n t_p) - \exp(-\lambda_n t_{p+1})] \underline{S}_{p,n} \qquad (2\text{-}19)$$

where

$$\underline{S}_{o,n} = \frac{\beta_n}{\lambda_n} F(0) \underline{\Psi}(0) = \underline{C}_{n,o} \ , \qquad (2\text{-}20)$$

$$\underline{S}_{p,n} = \underline{S}_{p-1,n} + F(t_{p-1}) [\mu_{p,n} \underline{\Psi}(t_{p-1}) + \epsilon_{p,n} \underline{\Psi}(t_p)] \ , \qquad (2\text{-}21)$$

$$\gamma_p = \frac{\Delta t_p}{2} + \sum_{n=1}^{N} \frac{\beta_n}{\lambda_n} \{-1 - \frac{1}{\lambda_n \Delta t_p}(\exp(-\lambda_n \Delta t_p) - 1)\} \ , \qquad (2\text{-}22)$$

$$\alpha_p = \frac{\Delta t_p}{2} + \sum_{n=1}^{N} \frac{\beta_n}{\lambda_n} \{1 + (1 + \frac{1}{\lambda_n \Delta t_p})(\exp(-\lambda_n \Delta t_p) - 1)\} \ , \qquad (2\text{-}23)$$

$$\mu_{p,n} = \frac{\beta_n}{\Delta t_{p-1}} \{-\frac{1}{\lambda_n^2} \exp(\lambda_n t_p)$$

$$- (\frac{\Delta t_{p-1}}{\lambda_n} + \frac{1}{\lambda_n^2}) \exp(\lambda_n t_{p-1})\} \qquad (2\text{-}24)$$

and

$$\epsilon_{p,n} = \frac{\beta_n}{\Delta t_{p-1}} \{(\frac{\Delta t_{p-1}}{\lambda_n} - \frac{1}{\lambda_n^2}) \exp(\lambda_n t_p)$$

$$+ \frac{1}{\lambda_n^2} \exp(\lambda_n t_{p-1})\}. \qquad (2\text{-}25)$$

Equation 2-19 represents a set of algebraic equations for the G x M unknowns $\Psi_{g,m}(t_{p+1})$ at each time point t_{p+1}. The initial condition for this system is obtained by assuming that the reactor is critical and in the steady state at $t_o = 0$. The code solves the steady-state form of equation 2-19 to obtain the initial flux distribution, $\underline{\Psi}(0)$, and eigenvalue, λ,

$$\{-L + S + \frac{1}{\lambda} \hat{F}\} \Psi(0) = 0, \qquad (2\text{-}26)$$

where $1/\lambda$ has been factored out of F by defining

$$\hat{F} = \lambda F. \qquad (2\text{-}27)$$

2.1.2 Solution of the Equations

Equations 2-19 and 2-26 are solved by iterative methods. The familiar technique of outer iterations on the fission source is used. By this method, the neutron fluxes may be solved one group at a time beginning with the highest energy group (g=1). Within each group inner iterations on the spatial flux distribution are carried out. The analysis proceeds in the following manner for each group g.

Equations 2-19 and 2-26 can both be written in the general form

$$A_g \underline{\Psi}_g = \underline{k}_g. \qquad (2\text{-}28)$$

In the steady state,

$$A_g = L_g \qquad (2\text{-}29)$$

and

$$\underline{k}_g = S_{g-1}\, \underline{\Psi}_{g-1}(0) + \frac{1}{\lambda} (\hat{F}\, \underline{\Psi}(0))_g. \qquad (2\text{-}30)$$

L_g and S_{g-1} are the appropriate blocks of L and S for computing the group g flux, $\underline{\Psi}_g$. $(\hat{F}\, \underline{\Psi}(0))_g$ is the group g component of the fission source vector.

In the transient,

$$A_g = V_g + \frac{\Delta t_p}{2} L_g \tag{2-31}$$

and

$$\underline{k}_g = \{V_g - \frac{\Delta t_p}{2} L_g\} \underline{\Psi}(t_p)$$

$$+ \frac{\Delta t_p}{2} S_{g-1} [\underline{\Psi}_{g-1}(t_{p+1}) + \underline{\Psi}_{g-1}(t_p)]$$

$$+ [\gamma_p F \underline{\Psi}(t_{p+1}) + \alpha_p F \underline{\Psi}(t_p)]_g$$

$$+ \sum_{n=1}^{N} [\exp(-\lambda_n t_p) - \exp(-\lambda_n t_{p+1})] (\underline{S}_{p,n})_g \tag{2-32}$$

For one-dimensional problems the A_g matrix is tridiagonal, and equation 2-28 can be solved for $\underline{\Psi}_g$ by well known methods. See for example, reference 2-11. For two-dimensional and three-dimensional problems A_g is a 9- or 27-stripe matrix. For these problems an iterative method for solving equation 2-28 is used. The method chosen is that of successive over-relaxation. The matrix A_g is split into three parts:

$$A_g = L_g + \mathcal{D}_g + U_g \tag{2-33}$$

where L_g is a 3- or 12-stripe lower triangular matrix, $\mathcal{D}_g$ is a 3-stripe diagonal matrix, and U_g is a 3- or 12-stripe upper triangular matrix. If the inner iteration counter is denoted by ℓ, then the successive over-relaxation algorithm is used in the following form. First,

$$\mathcal{D}_g \underline{x} = \underline{k}_g - L_g \underline{\Psi}_g^{\ell+1} - U_g \underline{\Psi}_g^{\ell} \tag{2-34}$$

is solved for $\underline{x}$. Since $\mathcal{D}_g$ is tridiagonal, this is analogous to solving a one-dimensional problem along each line of the mesh in the x-direction. Next, $\underline{\Psi}_g^{\ell+1}$ is determined from

$$\underline{\Psi}_g^{\ell+1} = (1-\omega)\ \underline{\Psi}_g^{\ell} + \omega\ \underline{x} \qquad (2\text{-}35)$$

where ω is the over-relaxation parameter. $\underline{\Psi}_g^{\ell+1}$ (instead of Ψ_g^{ℓ}) appears on the right hand side of equation 2-34 because of the structure of the matrices $\mathcal{D}_g$ and L_g.

After a fixed number of inner iterations, L, are performed, the vector $S_g\underline{\Psi}_g^{L}$ is recomputed for t=0 or $t=t_{p+1}$ as appropriate. Then the inner iterations are performed for the next lower energy group. When inner iterations for all groups are completed, the outer or fission source iteration is advanced by recomputing $F\underline{\Psi}$ for t=0 or $t=t_{p+1}$. One steady-state outer iteration may be regarded as an approximate solution of the following problem

$$\underline{\Psi}^{(m+1)} = (L - S)^{-1}\ \frac{1}{\lambda^{(m)}}\ \hat{F}\underline{\Psi}^{(m)} \qquad (2\text{-}36)$$

where m is the outer iteration counter. The vector $\underline{\Psi}^{(m+1)}$ is only approximately known because only a finite number of inner iterations, are performed to invert (L-S). Since it is desired to estimate λ for steady-state problems, an iteration index has been included with λ also. To obtain the next estimate of λ, the length of the fission source, $\frac{1}{\lambda}\hat{F}\ \underline{\Psi}$, is held constant. Thus we choose

$$\lambda^{(m+1)} = \lambda^{(m)}\ \frac{|\ \hat{F}\ \underline{\Psi}^{(m+1)}\ |}{|\ \hat{F}\ \underline{\Psi}^{(m)}\ |}. \qquad (2\text{-}37)$$

A problem analogous to equation 2-36 is solved for a transient outer iteration. The inner iterations and outer iterations are repeated until a pointwise flux convergence criterion is satisfied and the solution to equation 2-28 is obtained.

2.2 THE THERMAL-HYDRAULIC MODEL

The purpose of the thermal-hydraulic calculation is to include the effects of the changing core thermal-hydraulic conditions in the neutronics calculation. This objective is accomplished by modifying the diffusion equation cross sections using calculated values of fuel temperature, coolant temperature, and coolant density.

In the HERMITE thermal-hydraulic calculation, the core is modeled as a collection of closed, parallel flow channels. Each flow channel is defined by a portion of the cross sectional area of the core. This cross sectional area may represent a part of a fuel assembly, a whole fuel assembly, or a group of fuel assemblies and corresponds to a specified region of the horizontal plane of the neutronics mesh structure.

For flexibility in editing, the cross sectional areas of the channels may overlap but the user is required to specify a subset of the channels, called "primary" channels, which cover the active region of the core with no overlapping. Only primary channel data is used to modify cross sections.

In one- or three-dimensional problems where the axial dimension is explicitly modeled, the core is divided into axial nodes which consist of one or more finite element mesh intervals. The bottom and top reflectors (if present) are each assigned an axial node. The power generated in each axial node of each channel is determined during the neutronics calculation.

Within each flow channel all fuel pins are assumed to behave identically, and within each axial node all fuel pins are assumed to be operating at the same average linear heat rate. Within a fuel pin the one-dimensional radial heat conduction equation is solved for the temperature distribution at each axial node. As an alternative to solving the heat conduction equation for steady-state problems, HERMITE provides the option of determining the average fuel temperature at each axial node from one of two empirical correlations. Material properties are determined from temperature dependent correlations.

In the coolant, the axial continuity and conservation of energy equations are solved simultaneously with the equation of state. Axial expansion of the coolant and homogeneous, two-phase slip flow are modeled. Subcooled, saturated, superheated, and supercritical coolant properties are determined from the 1967 ASME Steam Tables. The core pressure, channel inlet temperatures, and channel inlet flow rates are specified by the user.

The fuel pin and coolant models are coupled by the clad surface heat flux calculation. The heat flux is determined by a two-regime heat transfer model which selects either the forced convection to subcooled water or nucleate boiling heat transfer regime. Heat is also added directly to the coolant as a fraction of the node power.

The time points for the thermal-hydraulic calculation are the initial time (t = 0.0) and a subset of the time points used for the neutronics calculation.

2.2.1 Fuel Pin Heat Conduction Model

HERMITE models three regions within a fuel pin: fuel pellet, gas gap, and cladding. The fuel and cladding are assumed to be concentric cylinders of uniform homogeneous material. Heat generation in the pellet is assumed to be radially and azimuthally uniform. No heat is generated in the gap or clad although an input fraction of the heat may be deposited directly in the coolant. Temperature is assumed to be azimuthally and axially uniform within an axial node. Axial heat conduction is ignored. The conductivities and specific heats of fuel and clad are spatially varying functions of temperature. Density is assumed constant for a given material. Gap conductance is an input function of linear heat rate (kw/ft generated) for steady-state calculations. For transient calculations an option exists to vary the gap conductance with gap temperature, as discussed in Section 2.2.4.3. There is no heat storage in the gap.

Radial mesh points are defined to include the centerline and all physical interfaces. Within the pellet and within the clad, additional equally spaced mesh points are allowed.

The model employs a finite difference approximation to the radial heat conduction equation:

$$\rho C_p \frac{\partial T}{\partial t} = - \frac{1}{r} \frac{\partial}{\partial r} rq'' + q''' . \qquad (2\text{-}38)$$

The nomenclature is conventional and is defined in Section 6.0.

At any radius the heat flux is

$$q'' = -k \frac{\partial}{\partial r} T. \qquad (2\text{-}39)$$

In the gap, equations 2-38 and 2-39 may be reduced to an equation of the form

$$q'' = h_{gap} (T_{FS} - T_{IC}) \qquad (2\text{-}40)$$

where q" is evaluated at the center of the gap. Specification of h_{gap} is discussed in Section 2.2.4.3. Here and elsewhere FS refers to the outer fuel pellet surface and IC refers to the inside clad surface, and w denotes the outer clad surface or "wall".

The boundary condition at the centerline is

$$q''_o = 0 . \qquad (2\text{-}41)$$

The heat flux at the outer clad surface, q''_w, is known in the steady state, but is an unknown, dependent on T_w and surface heat transfer conditions, during a transient.

Both temperature and heat flux are continuous over $0 \leq r \leq r_w$.

The steady-state (initial) condition is

$$\left. \frac{\partial T}{\partial t} \right|_{t \leq 0} = 0 . \qquad (2\text{-}42)$$

The volumetric heat generation rate in the fuel is computed as follows:

$$q''' = (1 - R_c)\, Q/(\pi\, r_{FS}^2\, \Delta z\, N_{pins}) \qquad (2\text{-}43)$$

2.2.1.1 Formulation of the Discretized Equations

Before writing the discretized version of equation 2-38, it is useful to outline some notation and further assumptions. In the figure below, radial mesh point r_j is pictured in radial region j which is bounded by two radii r_{j-} and r_{j+}.

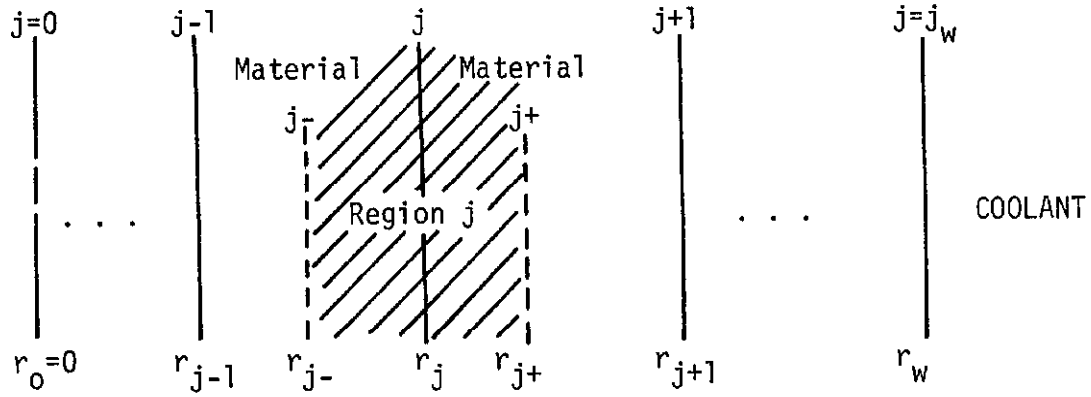

FUEL PIN RADIAL MESH

Region boundaries are given by

$$r_{j-} = \begin{cases} (r_j + r_{j-1})/2; & j>0 \\ 0 & ; j=0 \text{ (centerline)} \end{cases} \qquad (2\text{-}44)$$

$$r_{j+} = \begin{cases} (r_j + r_{j+1})/2; & j<j_w \\ r_w & ; j=j_w \text{ (clad-coolant interface).} \end{cases} \qquad (2\text{-}45)$$

It can be seen that the central and outermost regions are one-half of one mesh interval thick. The area of region j is given by

$$V_j = \pi (r_{j+}^2 - r_{j-}^2). \quad (2\text{-}46)$$

The areas for the two subregions on the + or - side of r_j are given by

$$V_{j-} = \pi (r_j^2 - r_{j-}^2) \quad (2\text{-}47)$$

and

$$V_{j+} = \pi (r_{j+}^2 - r_j^2). \quad (2\text{-}48)$$

From the definitions of r_{j+} and r_{j-}, it can be seen that V_{w+} and V_{o-} degenerate to zero.

The temperatures at the radii, r_j, are denoted by

$$T_j = T(r_j). \quad (2\text{-}49)$$

To estimate heat fluxes into and out of region j, it is necessary to estimate the conductivities at region boundaries. This is done as follows:

$$k_{j+} = [k(T_{j+1}) + k(T_j)]/2 \quad (2\text{-}50)$$

and

$$k_{j-} = [k(T_j) + k(T_{j-1})]/2. \quad (2\text{-}51)$$

Both conductivities in each sum are evaluated for the material (fuel or clad) on the appropriate side of r_j.

The volumetric heat capacity for region j is evaluated at T_j for the appropriate material:

$$(\rho C_p)_j = \rho C_p(T_j). \quad (2\text{-}52)$$

For the two gap interfaces, a volume weighted average of the fuel or clad heat capacity and the gap heat capacity (which is zero) is used:

$$(\rho\ C_p)_{IC} = \rho_{Zr}\ C_{p,Zr}\ V_{IC+}/V_{IC} \tag{2-53}$$

and

$$(\rho\ C_p)_{FS} = \rho_{UO2}\ C_{p,UO2}\ V_{FS-}/V_{FS} \tag{2-54}$$

Similarly, the heat generation rate for node FS must be adjusted:

$$q'''_j = \begin{cases} q''' & ; \quad j<j_{FS} \\ q'''\ V_{FS-}/V_{FS} & ; \quad j=j_{FS} \\ 0 & ; \quad \text{otherwise.} \end{cases} \tag{2-55}$$

Integration of the heat conduction equation, 2-38, over region j yields the following energy balance

$$V_j(\rho\ C_p)_j\ \frac{\partial\ T_j}{\partial t} = 2\pi\ r_{j-}\ q''_{j-} - 2\pi\ r_{j+}\ q''_{j+} + V_j\ q'''_j\ . \tag{2-56}$$

Time steps are denoted as follows:

$$0 = t_o < t_1 <\ldots< t_n < t_{n+1}. \tag{2-57}$$

The subscript or superscript n applied to any of the above quantities refers to time t_n. Thus

$$T_j^n = T(r_j,\ t_n),\ \text{etc.} \tag{2-58}$$

The time step size is

$$\Delta t_n = t_n - t_{n-1};\quad n\geq 1. \tag{2-59}$$

During each time step, material properties are held constant at their values at time t_{n-1}. For example,

$$(C_p)_j^{n-1} = C_p\,(T_j^{n-1}); \qquad t_{n-1} < t \leq t_n. \tag{2-60}$$

Assuming linear variation of temperature and heat source in time, equation 2-56 is integrated over time to yield

$$V_j(\rho\, C_p)_j^{n-1}\left\{\frac{T_j^n - T_j^{n-1}}{\Delta t_n}\right\}$$

$$= \pi\, r_{j-}\,\{(q")_{j-}^n + (q")_{j-}^{n-1}\} - \pi\, r_{j+}\,\{(q")_{j+}^n + (q")_{j+}^{n-1}\}$$

$$+ \frac{V_j}{2}\{(q"')_j^n + (q"')_j^{n-1}\}. \tag{2-61}$$

The steady-state equation may be obtained from equation 2-56 or 2-61 by assuming all quantities are invariant in time:

$$0 = 2\pi\, r_{j-}(q")_{j-}^o - 2\pi\, r_{j+}(q")_{j+}^o + V_j(q"')_j^o. \tag{2-62}$$

The following values for heat flux are substituted into equations 2-61 and 2-62 depending on the region. At the centerline

$$q"_o = 0. \tag{2-63}$$

At the center of the gap

$$q"_{FS+} = q"_{IC-} = h_{gap}\,(T_{FS} - T_{IC}). \tag{2-64}$$

At the clad-coolant interface, $q"_W$ (which is equivalent in this notation to $q"_{W+}$) is known in the steady state but is an unknown in the transient. At all other region boundaries

$$q"_{j+} = k_{j+}\,(T_{j+1} - T_j)/(r_{j+1} - r_j) \tag{2-65}$$

and

$$q"_{j-} = k_{j-}\,(T_{j-1} - T_j)/(r_{j-1} - r_j). \tag{2-66}$$

2.2.1.2 Solution of the Discretized Equations

When the above substitutions are made for q" in equations 2-61 or 2-62, a tridiagonal system of equations in T_j and q''_w is obtained. This system has j_w+1 equations in j_w+2 unknowns. This apparent inconsistency is resolved differently in the steady state and in the transient.

In the steady state, the last equation ($j=j_w$) is linearly dependent on the others and is eliminated. The clad-coolant heat flux, q''_w, is determined by energy conservation and the steady-state condition:

$$(q'')^o_w = (1 - R_c)\, Q^o/(2\pi r_w\, \Delta z\, N_{pins}). \qquad (2\text{-}67)$$

This equation divides the power being deposited in fuel pellets by the total fuel pin surface area for the thermal-hydraulic node. T^o_w is evaluated as a function of $(q'')^o_w$ using the appropriate heat transfer correlation (see Section 2.2.3). The remaining j_w equations are solved for the j_w unknowns, T^o_o through $T^o_{j_w-1}$, by standard methods for tridiagonal systems. Since the conductivities are functions of the temperatures, iterations are performed until a consistent set of k_j and T_j values is found. Convergence is assumed after i iterations if

$$|T^i_j - T^{i-1}_j| \le \varepsilon_{TF} \qquad (2\text{-}68)$$

for all j. The error criterion, ε_{TF}, is specified by the user.

In the transient, the additional unknown, q''_w, is present. Here, forward elimination is performed until one equation in two unknowns remains:

$$a_1 = a_2\, q''_w + T_w\ . \qquad (2\text{-}69)$$

This equation is then solved simultaneously with the appropriate heat transfer correlation (see Section 2.2.3). Once q''_w and T_w are known, backward substitution is used to calculate all of the T_j's.

2.2.1.3 Volume Weighted Average Fuel Temperature

Cross sections are functions of the volume-averaged fuel temperature in a thermal-hydraulic node. From the detailed spatial fuel temperature distribution T_j, the average fuel temperature T_{FUEL} is computed using the formula

$$T_{FUEL} = \sum_{j=0}^{j=FS} a_j T_j \qquad (2\text{-}70)$$

where

$$a_j = \begin{cases} 1/(4 \cdot j_{FS}^2) & ; \ j = 0 \\ j/(j_{FS}^2) & ; \ 1 \le j \le j_{FS} - 1 \\ (2 \cdot j_{FS} + 1)/(4 \cdot j_{FS}^2); & j = j_{FS}. \end{cases} \qquad (2\text{-}71)$$

The quadrature formula chosen for the numerical integration is such that the result is exact for the steady-state case of constant thermal conductivity within each radial node.

For use in cross section computation, T_{FUEL} is converted from Fahrenheit to Kelvin and the square root is taken.

2.2.1.4 Fuel Temperature by Correlation

The user may optionally request that the average fuel temperature, T_{FUEL}, be computed by one of two correlations rather than by the fuel pin heat conduction model described above. This option is available only for steady-state problems which do not initiate transients and is provided primarily for the purpose of comparison to other existing codes. Both correlations give T_{FUEL} as a function of q', the generated linear heat rate (which includes heat deposited in the coolant):

$$q' = Q/(\Delta z \cdot N_{pins}). \qquad (2\text{-}72)$$

The first correlation is

$$T_{FUEL} = C_1 [1 - C_2 \exp(-C_3 q')] - C_1 (1 - C_2) + T_w. \qquad (2\text{-}73)$$

The second correlation is a polynomial:

$$T_{FUEL} = C_1 + C_2\, q' + C_3(q')^2 + C_4(q')^3. \qquad (2\text{-}74)$$

In both correlations, the user specifies the constants, C_i.

2.2.2 Coolant Model

HERMITE solves the one-dimensional axial continuity and energy conservation equations for each channel. The continuity or conservation of mass equation is

$$\frac{\partial \rho(z,t)}{\partial t} = - \frac{\partial G(z,t)}{\partial z} \quad . \qquad (2\text{-}75)$$

The reader is referred to Section 6.0 for nomenclature.

The conservation of energy equation, neglecting friction, kinetic energy, potential energy and pressure change terms, is

$$\rho(z,t)\, \frac{\partial h}{\partial t} = - G(z,t)\, \frac{\partial h(z,t)}{\partial z} + q'''(z,t). \qquad (2\text{-}76)$$

The coolant equations are coupled to the fuel by q''' which combines direct heating and heat passing through the clad surface. In the transient, the latter term depends on coolant conditions, heat transfer regime and clad temperature.

The equations of state relating density and other coolant properties to enthalpy at the system pressure is represented in tabular form (See Section 2.2.4.4).

2.2.2.1 Discretized Equations

Each channel is divided into axial nodes consisting of one or more intervals from the finite element neutronics mesh. The coolant enthalpy, density, and mass flow rate are calculated for each node interface z_k, at each time point, t_n.

For a particular time step and a particular axial node, the following definitions and variable transformations are utilized:

$$\Delta t = t_n - t_{n-1}, \tag{2-77}$$

$$\Delta z = z_k - z_{k-1}, \tag{2-78}$$

$$\tau = (t - t_{n-1})/\Delta t \tag{2-79}$$

and

$$\eta = (z - z_{k-1})/\Delta z. \tag{2-80}$$

Equation 2-75 becomes

$$\frac{1}{\Delta t} \frac{\partial \rho(\eta,\tau)}{\partial \tau} = - \frac{1}{\Delta z} \frac{\partial G(\eta,\tau)}{\partial \eta}, \tag{2-81}$$

while equation 2-76 becomes

$$\frac{\rho(\eta,\tau)}{\Delta t} \frac{\partial h(\eta,\tau)}{\partial \tau} = - \frac{G(\eta,\tau)}{\Delta z} \frac{\partial h(\eta,\tau)}{\partial \eta} + q'''(\eta,\tau). \tag{2-82}$$

At the core inlet the coolant mass velocity, enthalpy and density are known for all time points from the boundary conditions. The solution proceeds from the core inlet to the core outlet for each flow channel at each time point. G, h and ρ are known for all axial mesh points η at the previous time point, $\tau = 0$; and also at the next lower axial mesh point $\eta = 0$ for the current time point $\tau = 1$. This is illustrated in Figure 2-2. G, h, and ρ are determined for point $\eta = 1$, $\tau = 1$ by the following procedure.

G(1,1) is calculated from equation 2-81 by assuming that the time derivative of density at the node inlet is constant over the whole node:

$$G(1,1) = G(0,1) + \frac{\Delta z}{\Delta t} [\rho(0,0) - \rho(0,1)]. \tag{2-83}$$

In the steady state this degenerates to

$$G(1) = G(0) = G_{inlet}. \tag{2-84}$$

Equation 2-82 is approximated by assuming that q"' is constant and by making the following substitutions for the other two terms:

$$\rho(\eta,\tau)\,\frac{\partial h(\eta,\tau)}{\partial \tau} \tilde{=} \rho(1,0)\,[h(1,1) - h(1,0)] \qquad (2\text{-}85)$$

and

$$G(\eta,\tau)\,\frac{\partial h(\eta,\tau)}{\partial \eta} \tilde{=} G(1,1)\,[h(1,0) - h(0,0)]. \qquad (2\text{-}86)$$

Density is evaluated at the outlet of the node at the previous time step. Mass velocity is evaluated at the outlet at the present time step. The time and space enthalpy derivatives are taken at the outlet of the node and the beginning of the time step, respectively. By defining

$$R = [G(1,1)\ \Delta t]/[\rho(1,0)\Delta z], \qquad (2\text{-}87)$$

the conservation of energy equation can be written as

$$h(1,1) \tilde{=} h(1,0) - R[h(1,0) - h(0,0)] + q"'\ \Delta t/\rho(1,0). \qquad (2\text{-}88)$$

In the steady state, the time derivative is zero and

$$h(1) = h(0) + q"'\ \Delta z/G_{inlet}. \qquad (2\text{-}89)$$

The formula for q"' uses the heat flux at time t_{n-1} and an average of the direct heating terms at times t_{n-1} and t_n:

$$q"' = q''_{w,\tau=0} \cdot (2\ \pi\ r_w\ N_{pins}/A) + R_C\ (Q_{\tau=0} + Q_{\tau=1})/(2A\ \Delta z). \qquad (2\text{-}90)$$

In the steady state, heat is deposited in the coolant at the same rate as it is generated so

$$q"' = Q/(A\Delta z). \qquad (2\text{-}91)$$

Finally, the density $\rho(1,1)$ is determined as a function of h(1,1),

$$\rho(1,1) = \rho\ (h(1,1),P), \qquad (2\text{-}92)$$

from the water property tables described in Section 2.2.4.4. At this time

$$T(1,1) = T\ (h(1,1),\ P) \qquad (2\text{-}93)$$

is also determined for editing purposes.

2.2.2.2 Average Coolant Conditions

For cross section modifications and for heat transfer calculations, certain "bulk" or average coolant conditions are defined and computed as follows:

$$h_B = [h(0,1) + h(1,1)]/2,$$

$$\rho_B = \rho(h_B,P) \qquad (2\text{-}94)$$

and

$$T_B = T(h_B,P).$$

The bulk viscosity, specific heat, thermal conductivity and quality are also computed (See Section 2.2.4.4). Both ρ_B and T_B are used in cross section modifications. ρ_B is converted to gm/cm^3 for this purpose.

2.2.3 Clad-Coolant Heat Transfer

The clad surface temperature and heat flux couple the fuel pin heat conduction equation and the coolant conservation of energy equation. A simultaneous solution is required between these equations and the appropriate heat transfer correlation. In the steady state these equations are decoupled by the fact that the heat flux is known. In the transient the coolant conditions are determined using the old value of the heat flux. Then equation 2-69 from Section 2.2.1 is solved simultaneously with the appropriate heat transfer correlation described below.

Two heat transfer regimes are modeled in the present version of HERMITE. The regimes will be discussed first, followed by the regime selection rules.

2.2.3.1 Forced Convection to Subcooled Water (Regime 1)

Forced convection to subcooled water is modeled using the Dittus-Boelter correlation:

$$q''_W = h_{DB} (T_W - T_B) \qquad (2\text{-}95)$$

where

$$h_{DB} = 0.023 (k_B/D) Re_B^{0.8} Pr_B^{0.4}. \qquad (2\text{-}96)$$

Equations 2-95 and 2-69 are solved simultaneously for T_W in the transient.

2.2.3.2 Nucleate Boiling (Regime 2)

In the nucleate boiling regime the Jens-Lottes correlation is used:

$$T_W = T_{sat} + 60 (q''_W/10^6)^{0.25} \exp(-P/900). \qquad (2\text{-}97)$$

Equations 2-97 and 2-69 are solved simultaneously using a Newton-Raphson iteration procedure in the transient.

2.2.3.3 Selection of the Heat Transfer Regime

In steady state, where q''_W is known, regime 1 is tried first. If $T_W < T_{sat}$, regime 1 is selected. If $T_W \geq T_{sat}$, regime 2 is compared with regime 1 and the regime yielding the lowest T_W is selected.

In the transient, the regime selected for the previous time step is tentatively selected. If the previous regime was regime 1 and $T_W < T_{sat}$, it

is accepted. If the previous regime was regime 2, it is accepted if $T_w > T_{sat}$. Otherwise, the regime yielding the higher heat flux is selected.

2.2.4 Physical Properties of Fuel, Gas Gap, Clad and Coolant

2.2.4.1 Fuel Properties

The fuel conductivity [Btu/ft-hr-°F] is calculated using the Lyons correlation (reference 2-9) converted to English units:

$$k(T) = 3978.696/(692.32 + T) + 60.716 \times 10^{-13} (459.69 + T)^3. \quad (2\text{-}98)$$

The fuel specific heat [Btu/lb-°F] is calculated from the following temperature-dependent functions (reference 2-8).

T <2240°F:

$$C_p(T) = 0.0726 + 3.33 \times 10^{-6} T - 4.74 \times 10^{+3}/(T + 459.69)^2 \quad (2\text{-}99)$$

T $\geq$2240°F:

$$C_p(T) = -.18426 + 3.8303 \times 10^{-4} T - 2.0447 \times 10^{-7} T^2 + 4.6457 \times 10^{-11} T^3 - 3.6289 \times 10^{-15} T^4. \quad (2\text{-}100)$$

The stack height density of fuel in gm/cc is input by the user and converted to the appropriate units internally.

2.2.4.2 Clad Properties

The clad conductivity [Btu/ft-hr-°F] is computed according to the formula from reference 2-9.

$$k(T) = 7.693 + 4.499 \times 10^{-3}T - 2.242 \times 10^{-6}T^2 + 1.047 \times 10^{-9}T^3. \quad (2\text{-}101)$$

The clad specific heat [Btu/lb-°F] is linearly interpolated between the valves given in the following table.

Temp (°F)	Specific Heat [Btu/lb-°F]
68	0.07010
1068	0.08210
1112	0.08611
1468	0.08611
1670	0.19726
1787	0.08511
10000	0.08523

This data is based on the specific heats by Eldridge (reference 2-10).

The clad density [gm/cc] is input by the user and converted to the appropriate units internally.

2.2.4.3 Gas Gap Properties

The steady-state gap conductance is determined from an input table of h_{gap} [Btu/hr-ft^2-°F] versus linear heat rate [kw/ft]. The user may input several tables and assign a table to each thermal-hydraulic channel. The transient gap conductance is based on the steady-state conductance and on the temperature dependence of the conductivity of helium (reference 2-7):

$$h_{gap}(t) = h_{gap}(0)\,[(T_{gap}(t) + C1)/(T_{gap}(0) + C1)]^{C2} \quad (2\text{-}102)$$

where C1 and C2 are input by the user and,

$$T_{gap} = (T_{IC} + T_{FS})/2. \quad (2\text{-}103)$$

2.2.4.4 Coolant Properties

Coolant physical properties are determined from steam-water property tables at the operating pressure. A programmed version of the 1967 ASME Steam Tables (references 2-4 and 2-5) is used to generate the tables used in HERMITE.

The tabulated properties are

- h = Specific enthalpy (Btu/lbm),
- T = Temperature (°F),
- v = Specific volume (ft^3/lbm),
- μ = Viscosity (lbm/ft-hr),
- C_p = Specific heat (Btu/lbm-°F)

and k = Thermal conductivity (Btu/hr-ft-°F).

For subcritical pressures and temperatures, the user specifies a range and number of equally spaced temperature increments below and up to saturation. Saturated liquid and vapor values are tabulated automatically and the user may optionally specify a range and number of equally spaced superheated temperatures beginning at saturation. For supercritical pressures the user specifies a lower and upper temperature and a number of equally spaced temperatures. Except for the specific volume in the two phase region, values are retrieved from the table using linear interpolation. Either temperature or enthalpy may be used as the independent variable.

In the saturated two phase region, the specific volume and density are calculated from the void fraction. The void fraction is calculated from the slip ratio. The expression for slip ratio is based on results given by Thom in reference 2-6:

$$\gamma = (v_g/v_f)^{.17}. \quad (2\text{-}104)$$

The void fraction is obtained from the following relationship:

$$\alpha = 1/\{1 + \gamma\ (v_f/v_g)\ [(1-x)/x]\} \qquad (2\text{-}105)$$

where x is the quality:

$$x = (h - h_f)/(h_g - h_f). \qquad (2\text{-}106)$$

The density may then be calculated,

$$\rho = (1 - \alpha)/v_f + \alpha/v_g, \qquad (2\text{-}107)$$

and used to compute specific volume

$$v = 1/\rho. \qquad (2\text{-}108)$$

2.3 THE CROSS SECTION REPRESENTATION

Reactor core thermal-hydraulic conditions influence, or feed back into, the neutronics calculations through changes in cross sections. In general the cross sections need to be functions of fuel temperature, coolant temperature, and coolant density. Because transients can involve large temperature and density changes, a flexible cross section representation is required to account accurately for these variations.

In the most general case, the macroscopic constants used in the diffusion equation can be functions of a number of indpendent variables. The independent variables may be number densities of isotopic species such as U-235, hydrogen, etc., or changes in fuel temperature, coolant temperature and coolant density. Computation of these thermal-hydraulic variables was described in Section 2.2.

The code computes macroscopic constants used in the diffusion equation from the following formula:

$$\Sigma = \sum_j N_j \{\sigma_j(N_1,N_2,N_3)\, g_j(N_4,N_5,N_6) + \sum_n \delta\sigma_j^n\,(N_7,N_8,N_9)\, g_j^n\,(N_{10},N_{11},N_{12})\, \Delta X_n\}, \qquad (2\text{-}109)$$

where:

Σ macroscopic cross section (transport, absorption, removal, or fission) used in the neutron diffusion equation.

j index labeling isotopic species such as U-235, hydrogen, etc.

n index labeling thermal-hydraulic quantities. Currently these may include fuel temperature, coolant temperature and coolant density.

N_j number density of isotopic species j in atoms/barn-centimeter.

$\sigma_j(N_1,N_2,N_3)$ microscopic cross section in barns of nuclide j. σ_j may be a constant or a function of up to three of the number densities, N_j, or thermal-hydraulic variations, ΔX_n. This is indicated symbolically by the arguments N_1,N_2,N_3.

$g_j(N_4,N_5,N_6)$ this is called a g-factor multiplier on the microscopic cross section. It defaults to a value of 1.0 and is included in the representation for flexibility. g_j may be a function of up to any three of the number densities, N_j, or thermal-hydraulic variations, ΔX_n.

$\delta\sigma_j^n(N_7,N_8,N_9)$ this is the change in the microscopic cross section σ_j per unit change in the thermal-hydraulic variable X_n. $\delta\sigma_j^n$ may be a constant or a function of up to three of the number densities, N_j, or thermal-hydraulic variations, ΔX_n.

$g_j^n(N_{10},N_{11},N_{12})$ this is a g-factor multiplier on the change in microscopic cross section $\delta\sigma_j^n$. It defaults to 1.0 and is included in the representation for flexibility. g_j^n may be a function of up to three of the number densities, N_j, or thermal-hydraulic variations, ΔX_n.

ΔX_n is the variation in the thermal-hydraulic variable X_n from an input reference value,

$$\Delta X_n = X_n - X_{n,\,ref}$$

X_n fuel temperature, coolant temperature or coolant density. For fuel temperature, X_n is the square root of the fuel temperature in degrees Kelvin. For coolant temperature, X_n is in degrees Fahrenheit, and for coolant density it is in grams per cm^3. This is the density of pure water and is not, for example, the homogenized density of water in a fuel-water mixture.

Equation 2-109 is valid for transport, absorption, removal and fission cross sections. For $\nu\Sigma^f$ and $\kappa\Sigma^f$, a slightly different expression employing the product rule for derivatives is used. For $\nu\Sigma^f$, the expression is

$$\nu\Sigma^f = \sum_j N_j \{\nu_j \sigma_j^f g_j^f + \sum_n [\nu_j \delta\sigma_j^{fn} + \sigma_j^f \delta\nu_j^n] \Delta X_n g_j^{fn}\}. \qquad (2\text{-}110)$$

Each of the quantities ν_j, σ_j^f, g_j^f, g_j^{fn}, $\delta\sigma_j^{fn}$ and $\delta\nu_j^n$ may be a function of up to three number densities, N_j, or variations, ΔX_n. A similar expression holds for $\kappa\Sigma^f$.

Often it is not necessary to use the cross section representation in its most general form. Usually g-factors are not used and the code defaults them to unity. Certain nuclides may be designated as being macroscopic quantities. For these nuclides the code automatically sets the number density to unity.

When control rods are present in the core, the user selects a specific nuclide to represent the cross sections of the control rods. The number density of this nuclide is given a value of 0.0 if the control rod is not present in a mesh rectangle, a value of 1.0 if it is present, and a value between 0.0 and 1.0 if it is partially present. Thus, the control rod cross sections are, in effect, positive or negative changes in macroscopic quantities. Control rods may be assigned fission cross sections and thermal feedback variations if required to reflect spectral effects on macroscopic constants.

The mesh used for cross section representation may be finer than the mesh used for the finite element basis functions. The cross section mesh is known as the fine mesh, and the basis function mesh is known as the finite element or coarse mesh. Cross sections and material compositions are assumed to be spatially constant throughout a fine mesh rectangle. There may be one or more fine mesh rectangles in a coarse mesh rectangle.

2.4 REFERENCES FOR SECTION 2.0

2-1 C. M. Kang and K. F. Hansen, "Finite Element Methods for Reactor Analysis", Nucl. Sci. and Eng., 51, pp. 456-495, 1973.

2-2 C. M. Kang and K. F. Hansen, "Finite Element Methods for Space Time Reactor Analysis", MIT-3903-5, MITNE-135, November, 1971.

2-3 "STRIKIN-II, A Cylindrical Geometry Fuel Rod Heat Transfer Program", CENPD-135P, August, 1974.

2-4 R. B. McClintock and G. J. Silvestri, "Formulations and Iterative Procedures for the Calculation of Properties of Steam", ASME, New York, 1968.

2-5 R. B. McClintock and G. J. Silvestri, "Some Improved Steam Property Calculation Procedures", 69-WA/Pwr-2, 1969.

2-6 J. R. S. Thom, "Prediction of Pressure Drop During Forced Circulation Boiling of Water", Int. J. Heat and Mass Transfer, 7, pp. 700-724, 1964.

2-7 J. C. Hocevar and T. W. Wineinger, "THETAI-B, A Computer Code for Nuclear Reactor Core Thermal Analysis", IN-1445, February, 1971.

2-8 H. C. Brassfield, et al., "Recommended Property and Reaction Kinetics Data for Use in Evaluating a Light Water Cooled Reactor Loss-of-Coolant Incident Involving Zircaloy-4 or 304-SS Clad UO_2", GEMP-482, 1968.

2-9 "High Temperature Properties of Zircaloy and UO_2 for Use in LOCA Evaluation Models", CENPD-136, July, 1974.

2-10 E. A. Eldridge and H. W. Deem, "Specific Heats and Heats of Transformation of Zircaloy-2 and Low Nickel Zircaloy-2", BMI-1803, May, 1967.

2-11 Robert D. Richtmyer and K.W. Morton, "Difference Methods For Initial-Value Problems", p. 198ff, Interscience Publishers, New York, 2nd Edition, 1967.

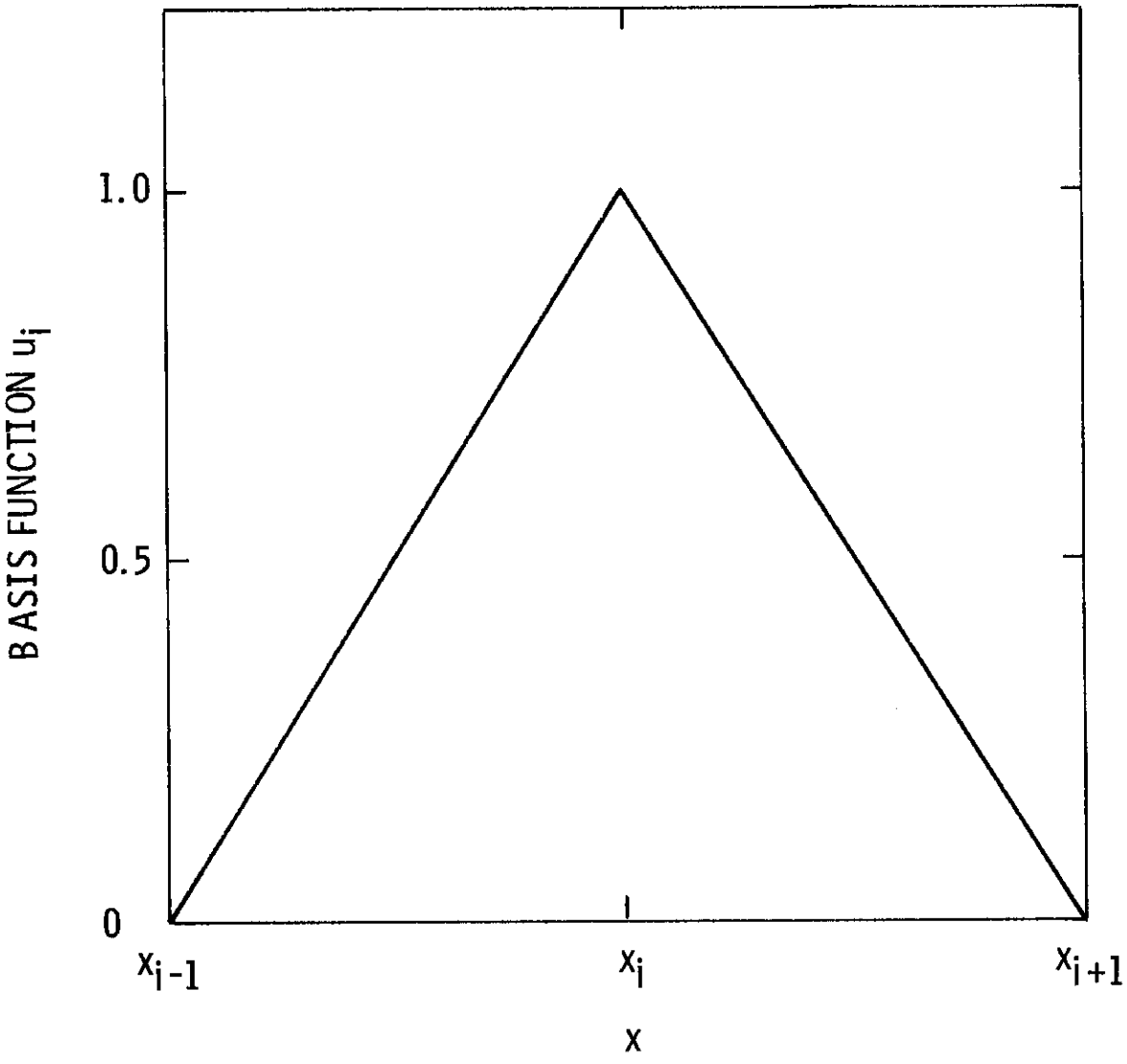

HERMITE CENPD-188	FINITE ELEMENT BASIS FUNCTION	Figure 2-1

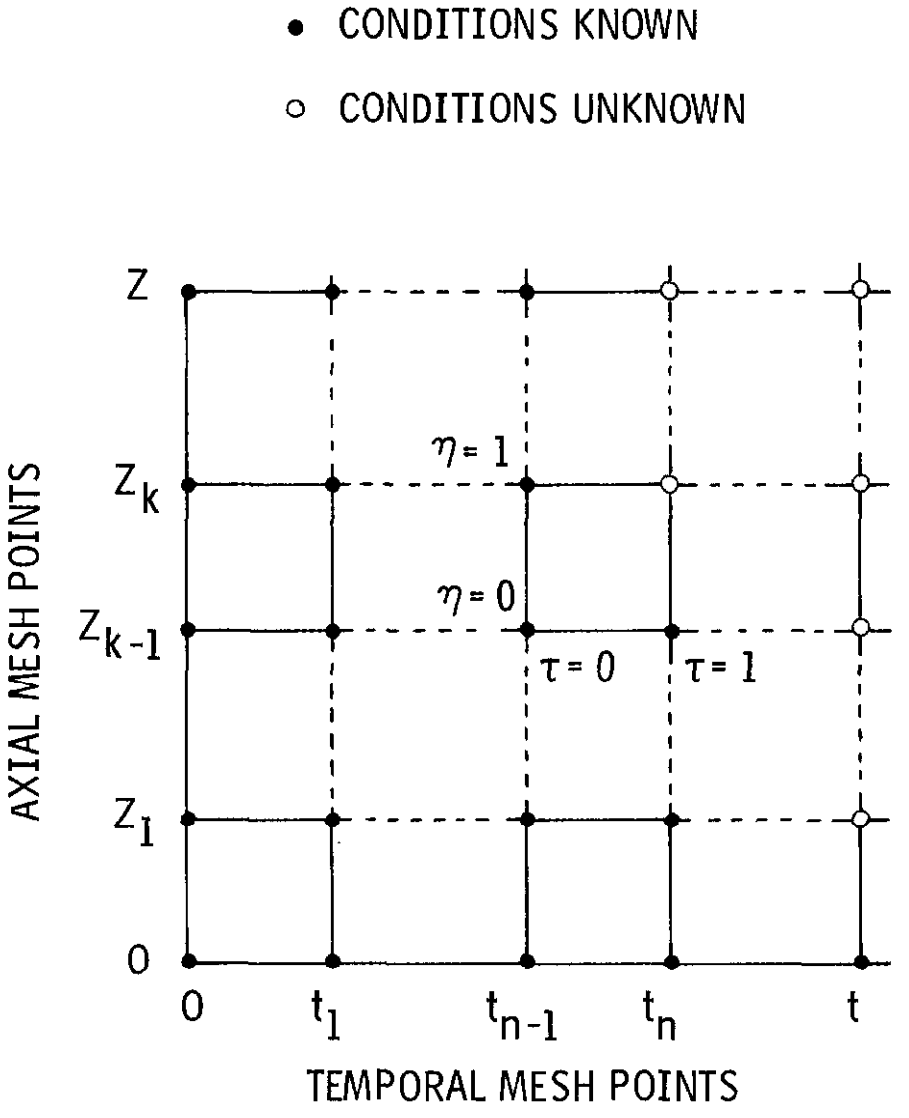

HERMITE CENPD-188	MESH STRUCTURE FOR A THERMAL-HYDRAULIC FLOW CHANNEL	Figure 2-2

3.0 THE HERMITE COMPUTER CODE

3.1 STRUCTURE OF THE HERMITE CODE

The HERMITE code is an overlayed program designed to run on a CDC-7600 computer. The code is written in FORTRAN and makes extensive use of MODEL, a Combustion Engineering - modified version of the Bettis Environmental Library (reference 3-1), for scratch disk I/O, dynamic memory allocation, and free-format input. The function and structure of the code's overlays are illustrated in Figure 3-1.

Execution begins with the processing of all input data in overlay (1,0). Control then passes to overlay (2,0). Based on user-supplied input, the code then performs a steady-state calculation, a transient calculation, or both. Transient calculations may start from the steady state (assumed to be time t=0) or at some point in a transient through input "restart" files.

The logic flow for a steady-state calculation is illustrated in Figure 3-2. The code first computes macroscopic cross sections for each of the problem's mesh rectangles. The finite element matrices are computed next, followed by calculation of an initial flux guess if this is the first pass. Otherwise, the previously computed flux is used as the flux guess for this pass. The inner and outer flux iterations described in Section 2.0 are performed next. For problems without thermal feedback, the spatial flux shape iterations continue until convergence is reached. For problems with thermal feedback, the number of flux iterations between feedback calculations is user-specified. After the specified number of iterations has been performed a thermal-hydraulic calculation is performed. If convergence of both the flux and thermal feedback variables has been reached, the problem is terminated after final editing. Otherwise, a new pass is initiated by updating the thermal feedback variables on the files used for cross section computation and then recomputing the macroscopic cross sections themselves.

Transient problems follow the same basic logic flow as steady-state problems-see Figure 3-3. There is, however, one notable exception. If there are no cross section changes from one time step to the next, the relatively costly computation of the finite element matrices can be bypassed. This feature can be used in problems where the neutronics time step size is much smaller than the thermal-hydraulic time step size and there is no significant control rod motion. In such cases, cross section changes for several neutronics time steps can be neglected without leading to significant errors.

3.2 FEATURES AND OPTIONS IN THE HERMITE CODE

Many of the important features and options in HERMITE have been mentioned in previous sections. Here all the major features will be summarized.

Neutronics

* From one to four neutron energy groups may be used.

* From zero to six delayed neutron precursor groups may be used.

* One-, two- and three-dimensional problems in rectangular geometry may be run. If thermal feedback is used, one-dimensional problems represent the core axially while two-dimensional problems represent the core radially.

* There are no fixed limits on problem size as a result of using dynamic storage allocation.

* Any number of full- and part-length control rods can be represented.

* Control rod movement is specified by user-supplied velocity versus time functions. Each control rod may move independently of all others.

* In a single run the code can perform a steady-state calculation, a transient calculation, or both.

* Steady-state results can be saved on restart files for later use as the initial conditions for transients.

* Transient results can be saved on disk or tape at specified time points for later use in restarting transients.

Cross Section Representation

The principal features of the cross section representation are:

* Any combination of macroscopic and microscopic cross sections may be used.

* Any number of nuclides may be used.

* Cross section variations for any combination of fuel temperature, moderator temperature and moderator density may be represented.

* A set of g-factors is provided for added flexibility.

* Microscopic cross sections, macroscopic cross sections, g-factors and thermal feedback variations may each be made a function of up to three independent variables which may be number densities or thermal feedback variables.

Thermal-Hydraulics

* Closed, parallel, vertical channels may be defined over arbitrary combinations of mesh rectangles in the x-y plane. Axial nodes correspond to one or more finite element mesh intervals.

* One-dimensional axial coolant continuity and energy conservation equations are solved for each channel.

* Homogeneous, two-phase slip flow is modeled.

* Inlet flow and temperature may be specified by channel. Core-wide ambient pressure is specified on input.

* Forced convection to subcooled water and nucleate boiling heat transfer regimes are modeled.

* The finite difference model of the fuel pin radial heat conduction equation allows an arbitrary number of nodes in pellet and clad.

3.3 REFERENCE FOR SECTION 3.0

3-1 R. S. Horeck, et al., "MODEL - Modified Environmental Library - CDC 6000 FORTRAN Programming Guide".

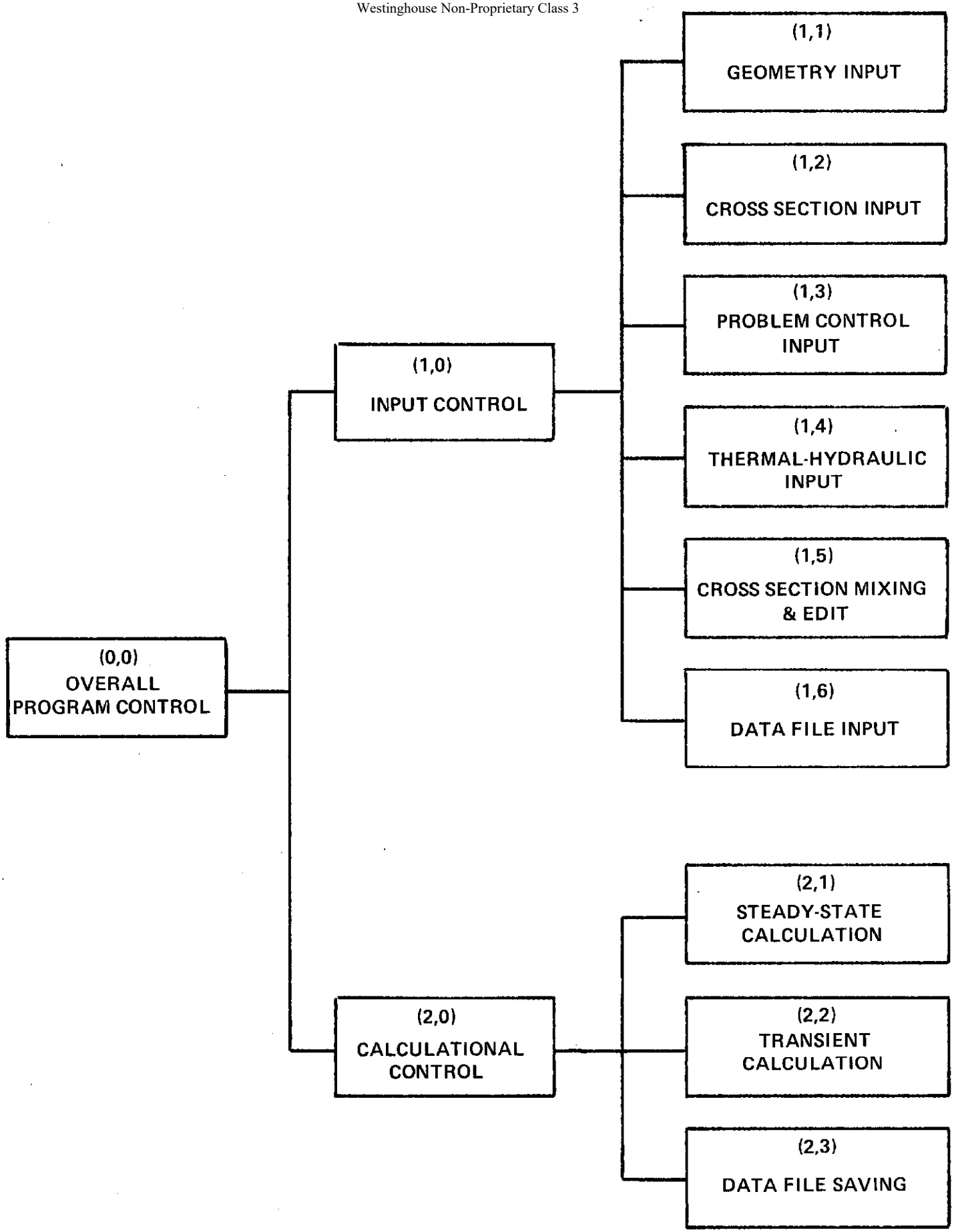

HERMITE CENPD-188	HERMITE OVERLAY STRUCTURE AND OVERLAY FUNCTIONS	Figure 3-1

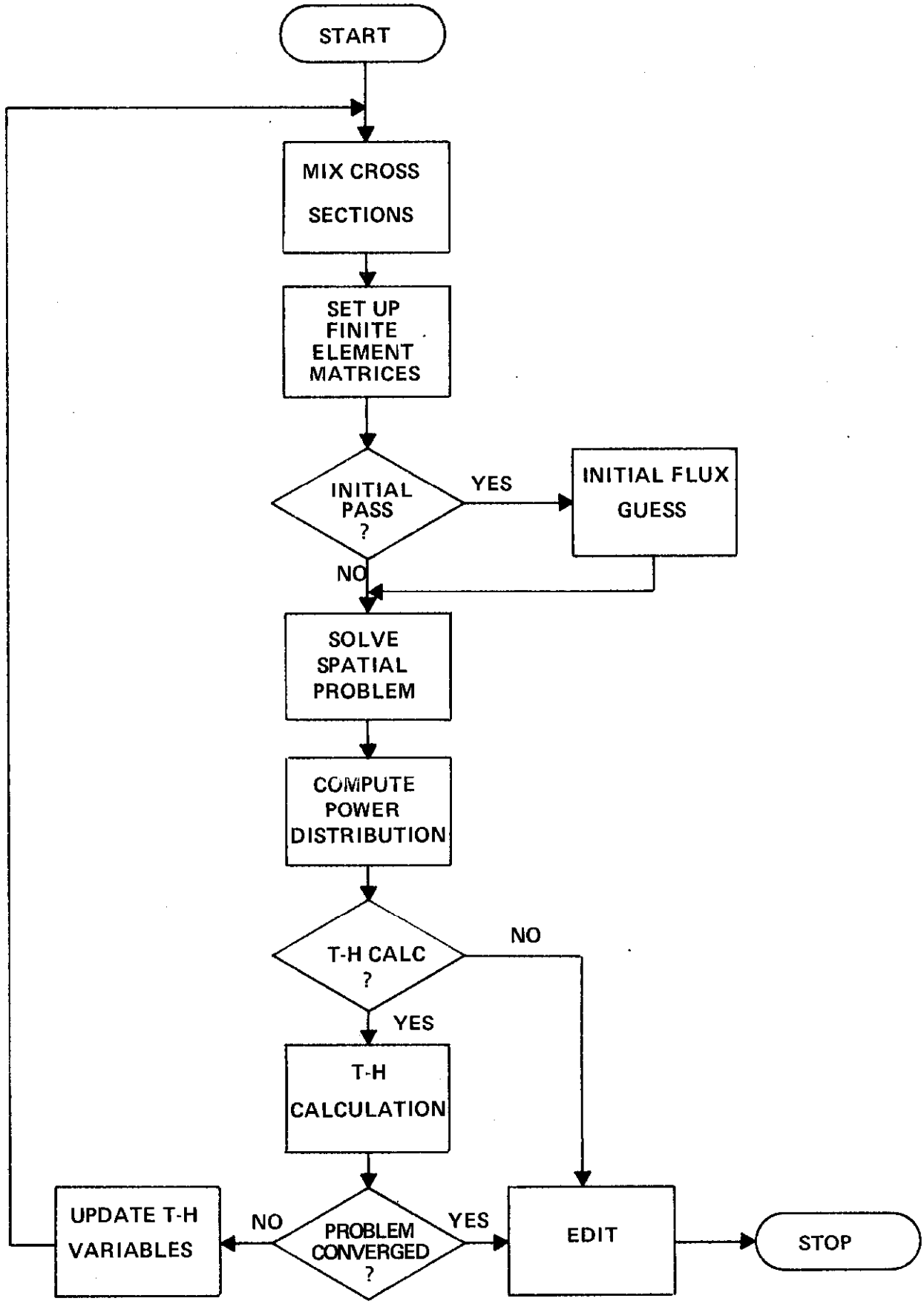

HERMITE CENPD-188	STEADY-STATE PROBLEM LOGIC DIAGRAM	Figure 3-2

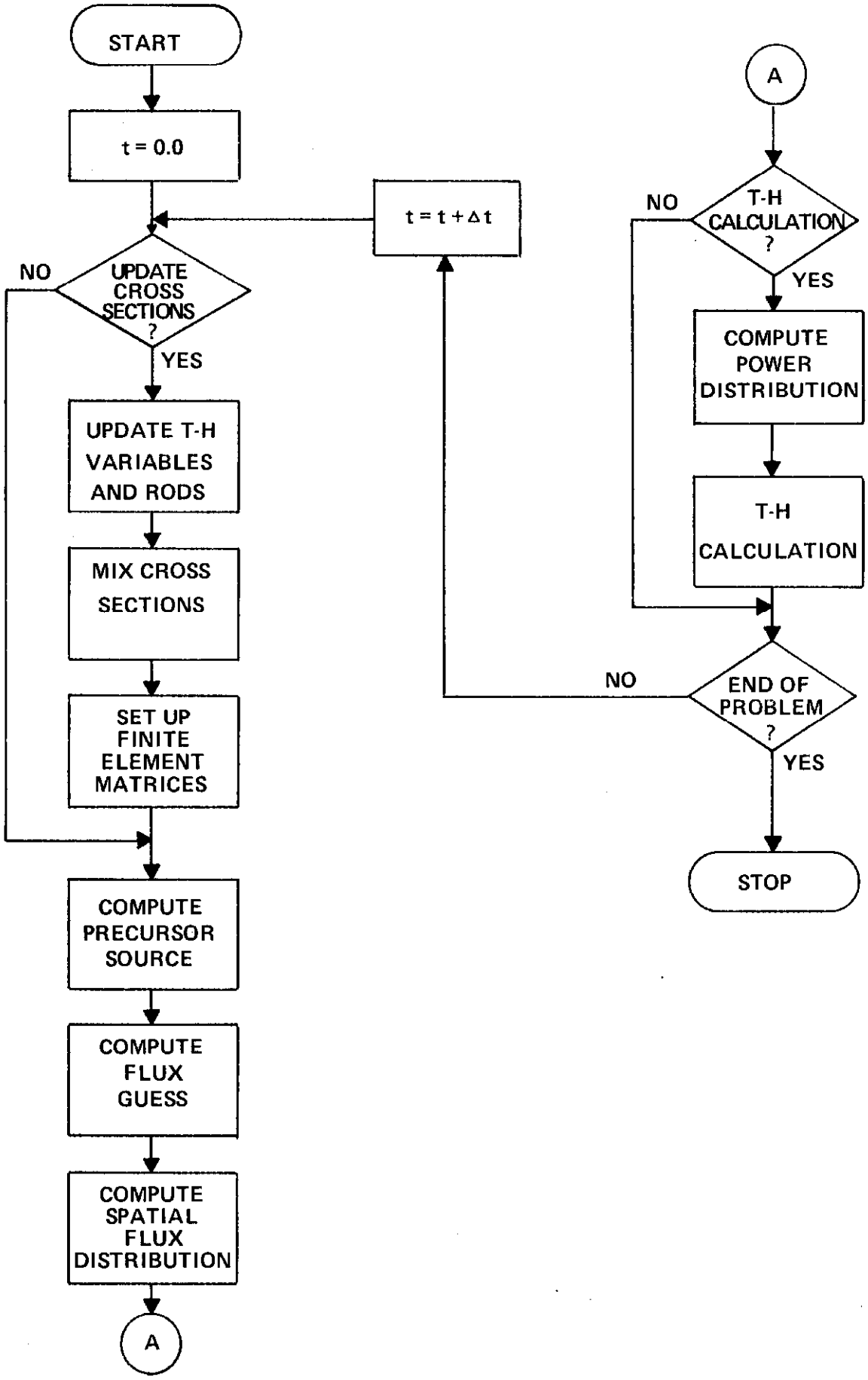

HERMITE CENPD-188	TRANSIENT PROBLEM LOGIC DIAGRAM	Figure 3-3

4.0 VERIFICATION OF THE HERMITE MODELS

The verification of the HERMITE code was accomplished by comparing numerical results from HERMITE to those from existing computer codes which utilize accepted calculational methodology. The first step was to verify HERMITE's neutronics model for test cases which did not include thermal-hydraulic feedback effects. The second step was to verify the thermal-hydraulic model independently of the neutronics calculation. Finally, HERMITE's combined neutronics and thermal-hydraulics results were verified.

4.1 VERIFICATION OF HERMITE'S NEUTRONICS MODEL WITHOUT THERMAL FEEDBACK

Verification of HERMITE's steady-state neutronics model was accomplished via comparison of eigenvalues and static power distributions from HERMITE and PDQ. Thermal-hydraulic feedback effects were not included. Similarly, HERMITE's transient neutronics calculations without feedback were verified by comparing HERMITE and TWIGL (reference 4-1) for a control element assembly ejection incident.

4.1.1 HERMITE and PDQ Eigenvalues and Static Power Distributions

Included in this section are results for three cases typical of Combustion Engineering PWR cores. The first case is a 217 fuel assembly core operating at full power conditions. The second is a 241 fuel assembly core operating at full power conditions, and the third case is the same 241 fuel assembly core operating at hot zero power conditions.

HERMITE eigenvalues and power distributions were compared to reference fine mesh PDQ cases. These reference PDQ cases are two-group, two-dimensional models of the x-y plane of the core with a 16 x 16 mesh per fuel assembly. Hereafter a reference PDQ calculation will be identified as a 16 x 16 PDQ.

HERMITE results for several coarse mesh structures are compared to the 16 x 16 PDQ cases. Some HERMITE cases use a 4 x 4 array of mesh intervals in each fuel assembly while others use a 2 x 2 array of mesh intervals. These

will be referred to as 4 x 4 or 2 x 2 HERMITE cases, as appropriate. To add perspective to these comparisons 4 x 4 PDQ and 2 x 2 PDQ results are also presented.

Fuel cross sections for the 4 x 4 and 2 x 2 mesh cases were obtained by flux and volume weighting the cross sections in each type of fuel assembly using fluxes from the appropriate 16 x 16 PDQ. Recent experience has shown that diffusion theory calculated power distributions in large PWR's are sensitive to the treatment of reflector and shroud cross sections (reference 4-2). Experience has shown that adjusting the fast group diffusion coefficients in the reflector and shroud regions improves the calculated power distributions. In Combustion Engineering cores, there is a 1.1 inch steel shroud immediately surrounding the outermost fuel assemblies. In the 4 x 4 PDQ and HERMITE cases this shroud must be represented by a 2.05 inch mesh, while in the 2 x 2 cases a 4.1 inch mesh is used. Shroud cross sections for the 4 x 4 and 2 x 2 cases were obtained by adjusting the 16 x 16 PDQ fast group diffusion coefficients.

The first case corresponds to a typical Combustion Engineering 217 fuel assembly core design operating at full power conditions. The control element assemblies shown to be fully inserted in Figure 4-1 were selected to increase the numerical difficulty of the power distribution calculation. A 4 x 4 mesh for each fuel assembly was used in the HERMITE calculation. A corresponding 4 x 4 PDQ calculation was performed in order to compare HERMITE and PDQ for equivalent mesh spacings.

The results of these comparisons are summarized in Figure 4-2. HERMITE shows good agreement with the 16 x 16 PDQ. HERMITE's eigenvalue is 0.15 percent larger than the 16 x 16 PDQ eigenvalue. The maximum percent difference in fuel assembly power is 1.83 percent, and the average absolute difference (average of the absolute values of all percent differences) is 0.757 percent. The 4 x 4 PDQ eigenvalue is 0.07 percent below the 16 x 16 PDQ eigenvalue which is more accurate than HERMITE's; however, the 4 x 4 PDQ power distribution results are less accurate than those from HERMITE since the maximum difference and average absolute difference are 3.56 percent and 1.04 percent, respectively.

In order to determine HERMITE's accuracy for a larger mesh spacing the 217 assembly test case was rerun with a 2 x 2 mesh per fuel assembly. The results are presented in Figure 4-3 along with those for the 4 x 4 mesh spacing. The 2 x 2 HERMITE eigenvalue is 0.33 percent larger than the 16 x 16 PDQ eigenvalue. The maximum difference in fuel assembly power for the 2 x 2 HERMITE case relative to the 16 x 16 PDQ is 6.54 percent, and the average absolute difference is 2.43 percent.

A comparison of HERMITE and a 16 x 16 PDQ for a 241 fuel assembly core design was performed using a 2 x 2 mesh per fuel assembly. Full power conditions were assumed for this case, and no control element assemblies were inserted into the core. The comparison of fuel assembly powers in Figure 4-4 shows a maximum difference of 4.06 percent, and an average absolute difference of 2.48 percent. The 2 x 2 HERMITE eigenvalue is 0.16 percent lower than the 16 x 16 PDQ eigenvalue. These results are similar to those for the 217 fuel assembly core design in Figure 4-3. The corresponding 2 x 2 PDQ results are presented along with those for HERMITE. The 2 x 2 PDQ eigenvalue is 0.32 percent lower than the 16 x 16 PDQ eigenvalue. The maximum assembly power difference and average absolute difference are 14.1 percent and 5.66 percent respectively. It can be seen that the 2 x 2 PDQ results are significantly less accurate than the corresponding HERMITE results.

The last case is a comparison of HERMITE and PDQ for a highly rodded 241 fuel assembly core at hot zero power conditions. A 2 x 2 mesh per fuel assembly was used. The control element assemblies, fully inserted as shown in Figure 4-5, provide a difficult numerical test of the 2 x 2 HERMITE neutronics calculation since the insertion of control element assemblies increases the radial power peaking in the core. The results in Figure 4-6 show that the 2 x 2 HERMITE eigenvalue is 0.32 percent lower than the 16 x 16 PDQ eigenvalue, and that the maximum difference and average absolute difference in fuel assembly power are 14.6 percent and 3.72 percent respectively. The 2 x 2 PDQ eigenvalue and power distribution are again less accurate than those from HERMITE. The 2 x 2 PDQ eigenvalue is 0.49 percent lower than the 16 x 16 PDQ eigenvalue. The maximum assembly power difference and average absolute difference are 17.5 percent and 5.94 percent respectively.

In conclusion, comparisons between PDQ and HERMITE show good agreement and indicate that a 2 x 2 mesh is appropriate for HERMITE space-time calculations.

4.1.2 HERMITE and PDQ Control Element Assembly Worths

As part of the HERMITE verification, control element assembly static worths were calculated. This was done by running two steady-state calculations; one with the control element assembly fully inserted, and one with the control element assembly fully withdrawn. If the eigenvalues for these cases are denoted by λ_0 and λ_1 respectively, then the worth (% $\Delta\rho$) is defined as:

$$\% \Delta\rho = \{(\lambda_1 - \lambda_0)/\lambda_1 \lambda_0\} \cdot 100\% . \qquad (4\text{-}1)$$

Some control element assembly worths presented in later sections also include equilibrium thermal-hydraulic feedback in the two static eigenvalue calculations for λ_1 and λ_0.

For the 241 assembly test problem described in Section 4.1.1, control element assembly worths are presented in Table 4-1. These were obtained from two-dimensional calculations without thermal-hydraulic feedback. The control element assembly patterns for these cases are shown in Figures 4-5 and 4-7. For comparison, 16 x 16 PDQ, 2 x 2 HERMITE and 2 x 2 PDQ worths are shown.

4.1.3 HERMITE and TWIGL Transient Neutronics

HERMITE was compared to TWIGL in order to show that HERMITE's finite element transient calculations compare well with those from an accepted finite difference neutronics code. The test problem was a two-dimensional (x-y plane), full power, central control element assembly ejection transient. Two prompt neutron energy groups and two delayed neutron precursor groups were used. The static worth of the central ejected control element was 0.16% $\Delta\rho$ (see Table 4-1) or \$0.22. A 2 x 2 mesh for each fuel assembly

was used in both HERMITE and TWIGL. Thermal-hydraulic feedback effects were not included in order to isolate the neutronics model. The central control element assembly was ejected from the core in fifty milliseconds.

A comparison of the resulting total core power levels, presented in Figure 4-8, indicates good agreement between HERMITE and TWIGL neutronics calculations without thermal-hydraulic feedback.

4.2 VERIFICATION OF HERMITE'S THERMAL-HYDRAULIC MODEL

Core thermal-hydraulic conditions can have a significant effect upon reactor behavior because cross sections are functions of fuel temperature, coolant temperature and coolant density. It is the function of the HERMITE thermal-hydraulic calculation to compute these three quantities. In this section the verification calculations for HERMITE's thermal-hydraulic model are described. This verification was performed by comparing HERMITE results to those from the STRIKIN-II computer code (reference 4-3). STRIKIN-II is a code which is used at Combustion Engineering to calculate the transient heat transfer behavior of a cylindrical geometry fuel pin. HERMITE's thermal-hydraulic subroutines were decoupled from the neutronics portion of the code so that HERMITE's thermal-hydraulic calculations could be forced with a pre-determined transient power level and a normalized axial power distribution which was constant during the transient. This modification was necessary to maintain consistency with STRIKIN-II. HERMITE and STRIKIN-II were compared for hypothetical full power and zero power control element assembly ejection incidents.

The core power forcing function for a hypothetical full power control element assembly ejection incident, Figure 4-9, was specified so as to give initial fuel temperatures and transient fuel temperatures which are higher than those predicted for a more typical full power control element assembly ejection incident. The results presented in Table 4-2 for a fuel pin with nineteen radial nodes show good agreement between HERMITE and STRIKIN-II. At the axial midpoint of the core the average fuel temperatures differ by approximately 4°F throughout the transient. This good agreement was expected

since the use of nineteen radial nodes enabled the accurate calculation of the radial fuel temperature profile (e.g., at t=0.0 seconds the centerline fuel temperature was 4293°F for HERMITE and 4289°F for STRIKIN-II). The coolant temperatures and densities predicted by both codes at the core midpoint and core exit show good agreement throughout the transient. To demonstrate that accurate results would be obtained with fewer radial nodes, the number of nodes in HERMITE was decreased from nineteen to nine. As shown in Table 4-3, accurate results were obtained with nine radial nodes.

A hypothetical zero power control element assembly ejection incident, characterized by rapid changes in fuel temperature, was simulated with the core power forcing function shown in Figure 4-10. The results presented in Table 4-4 for a fuel pin with nineteen radial nodes show good agreement between HERMITE and STRIKIN-II. At the axial midpoint of the core the average fuel temperatures differ by less than 4°F after a severe power excursion (Figure 4-10). The coolant temperatures and densities predicted by both codes at the core midpoint and core exit show good agreement throughout the transient. To demonstrate that accurate results would be obtained with fewer radial nodes, the number of nodes in HERMITE was decreased. Table 4-5 shows good agreement between results for cases with nineteen and nine radial nodes.

4.3 VERIFICATION OF HERMITE'S NEUTRONICS MODEL WITH THERMAL FEEDBACK

HERMITE results for transient neutronics calculations with thermal feedback were verified via comparison to the corresponding TWIGL calculations. The test problems were two-dimensional (x-y plane) central control element assembly ejection incidents for both zero and full power initial conditions. Only fuel temperature feedback effects were considered.

4.3.1 HERMITE and TWIGL Full Power Control Element Assembly Ejection Incidents

The test problem for this case is the same 241 fuel assembly core design described in Section 4.1.1 with a 2 x 2 mesh spacing for each fuel assembly. The central control element assembly in Figure 4-7 was ejected from the core in fifty milliseconds. The static worth of this control element was 0.13% $\Delta\rho$ or \$0.18 including thermal feedback effects. This worth is less than the 0.16% $\Delta\rho$ worth calculated in Section 4.1.2 without thermal feedback because the effect of fuel temperature feedback is to shift the core power distribution away from the center of the core and away from the ejected control element assembly.

TWIGL's fuel temperature model includes a single fuel node, a constant volumetric heat capacity, and a single overall pin-coolant heat transfer coefficient. For the analysis of a full power control element assembly ejection incident, which is characterized by small changes in fuel temperature, the clad was included in TWIGL's single fuel node in order to allow more accurate modeling of the pin-coolant heat transfer phenomena.

A comparison of the total core power transients is presented in Figure 4-11. HERMITE and TWIGL show excellent agreement while the control element is being ejected from the core ($t \leq 0.05$ seconds). The differences in asymptotic power after the control element assembly is ejected are small and the overall comparison of HERMITE and TWIGL is good.

4.3.2 HERMITE and TWIGL Zero Power Control Element Assembly Ejection Incidents

For this comparison the control element assembly was ejected from the center of a 241 fuel assembly core. The control elements for this case were arranged (see Figure 4-5) to give a high control element assembly static worth and a prompt critical power excursion. The static worth of the ejected control element was 1.19% $\Delta\rho$ or \$1.60. A 2 x 2 mesh per fuel assembly was used to model the core in the x-y plane.

TWIGL's fuel temperature model includes a single fuel node, a constant volumetric heat capacity, and a single overall pin-coolant heat transfer coefficient. Since the first second of zero power control element assembly ejection transients is characterized by large changes in fuel pellet temperature, only the fuel pellet was included in TWIGL's single fuel node.

The HERMITE and TWIGL core power transients for this case are compared in Figure 4-12. TWIGL's peak core power level is 4 percent larger than HERMITE's. Considering the severity of the power excursion for this incident and the differences between the fuel temperature models in HERMITE and TWIGL, the HERMITE and TWIGL numerical results show good agreement.

4.4 REFERENCES FOR SECTION 4.0

4-1 J. B. Yasinsky, et al., "TWIGL - A Program to Solve the Two-Dimensional, Two-Group, Space-Time Neutron Diffusion Equations with Temperature Feedback", WAPD-TM-743, February, 1968.

4-2 W. B. Terney, "Albedo - Adjusted Fast-Neutron Diffusion Coefficients in Reactor Reflectors", Nucl. Sci. and Eng., 57, 1975.

4-3 "STRIKIN-II, A Cylindrical Geometry Fuel Rod Heat Transfer Program", CENPD-135P, August, 1974.

Table 4-1

HERMITE and PDQ Control Element Assembly Worths (% $\Delta\rho$)

	16 x 16 PDQ	2 x 2 HERMITE	2 x 2 PDQ
Figure 4-5 Central Control Element Assembly Worth	1.1346	1.1930	1.1915
Figure 4-7 Total Control Element Assembly Bank Worth	0.7475	0.7705	0.7690
Figure 4-7 Central Control Element Assembly Worth	0.1580	0.1602	0.1614

Table 4-2

Thermal-Hydraulic Calculation for a Full Power Control Element Assembly Ejection Incident - A Comparison of HERMITE and STRIKIN-II Results*

At the Core Axial Midpoint

Time (Sec)	Average Fuel Temperature (°F)		Coolant Density (lbm/ft^3)		Coolant Temperature (°F)	
	HERMITE	STRIKIN-II	HERMITE	STRIKIN-II	HERMITE	STRIKIN-II
0.0	2930.7	2933.9	42.05	42.05	612.3	612.3
0.5	3083.6	3087.4	41.68	41.70	616.0	615.9
1.0	3154.0	3158.0	41.52	41.54	617.6	617.6
1.5	3145.6	3149.6	41.60	41.60	616.9	616.9
2.0	3066.7	3070.3	41.83	41.82	614.6	614.7

At the Core Exit

Time (Sec)	Coolant Density (lbm/ft^3)		Coolant Temperature (°F)	
	HERMITE	STRIKIN-II	HERMITE	STRIKIN-II
0.0	37.46	37.47	650.2	650.3
0.5	36.46	36.57	652.7	652.7
1.0	34.08	34.20	652.7	652.7
1.5	34.02	34.09	652.7	652.7
2.0	35.54	35.52	652.7	652.7

*Results are for a fuel pin with nineteen radial nodes.

Table 4-3

Thermal-Hydraulic Calculation for a Full Power Control Element Assembly Ejection Incident - A Comparison of HERMITE Results for Fuel Pins with Nineteen and Nine Radial Nodes

At the Core Axial Midpoint

Time (Sec)	Average Fuel Temperature (°F)		Coolant Density (lbm/ft^3)		Coolant Temperature (°F)	
	19 Nodes	9 Nodes	19 Nodes	9 Nodes	19 Nodes	9 Nodes
0.0	2930.7	2921.8	42.05	42.05	612.3	612.3
0.5	3083.6	3074.0	41.68	41.67	616.0	616.2
1.0	3154.0	3143.9	41.52	41.51	617.6	617.7
1.5	3145.6	3135.3	41.60	41.60	616.9	616.9
2.0	3066.7	3056.6	41.83	41.84	614.6	614.5

At the Core Exit

Time (Sec)	Coolant Density (lbm/ft^3)		Coolant Temperature (°F)	
	19 Nodes	9 Nodes	19 Nodes	9 Nodes
0.0	37.46	37.46	650.2	650.2
0.5	36.46	36.37	652.7	652.7
1.0	34.08	33.95	652.7	652.7
1.5	34.02	33.97	652.7	652.7
2.0	35.54	35.58	652.7	652.7

Table 4-4

Thermal-Hydraulic Calculation for a Zero Power Control Element Assembly Ejection Incident - A Comparison of HERMITE and STRIKIN-II Results*

At the Core Axial Midpoint

Time (Sec)	Average Fuel Temperature (°F)		Coolant Density (lbm/ft^3)		Coolant Temperature (°F)	
	HERMITE	STRIKIN-II	HERMITE	STRIKIN-II	HERMITE	STRIKIN-II
0.0	565.3	565.3	45.86	45.86	565.0	565.0
.06	567.0	567.1	45.86	45.86	565.0	565.1
.08	719.5	733.9	45.72	45.70	567.1	567.3
.10	1147.3	1168.4	45.30	45.28	572.9	573.3
.12	1403.0	1406.1	45.03	45.03	576.7	576.7
.14	1410.2	1410.0	44.96	44.99	577.5	577.2
1.0	1319.6	1319.9	44.21	44.21	587.4	587.4
2.0	1215.7	1215.9	44.60	44.60	582.3	582.3

At the Core Exit

Time (Sec)	Coolant Density (lbm/ft^3)		Coolant Temperature (°F)	
	HERMITE	STRIKIN-II	HERMITE	STRIKIN-II
0.0	45.86	45.86	565.0	565.0
.06	45.86	45.86	565.0	565.1
.08	45.84	45.83	565.2	565.5
.10	45.77	45.73	566.3	566.9
.12	45.67	45.64	567.8	568.2
.14	45.58	45.57	569.0	569.2
1.0	42.30	42.34	609.6	609.3
2.0	43.15	43.15	600.1	600.2

*Results are for a fuel pin with nineteen radial nodes.

Table 4-5

Thermal-Hydraulic Calculation for a Zero Power Control Element Assembly Ejection Incident - A Comparison of HERMITE Results for Fuel Pins With Nineteen and Nine Radial Nodes

At the Core Axial Midpoint

Time (Sec)	Average Fuel Temperature (°F)		Coolant Density (lbm/ft^3)		Coolant Temperature (°F)	
	19 Nodes	9 Nodes	19 Nodes	9 Nodes	19 Nodes	9 Nodes
0.0	565.3	565.3	45.86	45.86	565.0	565.0
.06	567.0	567.0	45.86	45.86	565.0	565.0
.08	719.5	719.5	45.72	45.72	567.1	567.1
.10	1147.3	1147.2	45.30	45.30	572.9	572.9
.12	1403.0	1402.7	45.03	45.03	576.7	576.7
.14	1410.2	1409.5	44.96	44.96	577.5	577.5
1.0	1319.6	1318.4	44.21	44.20	587.4	587.4
2.0	1215.7	1215.2	44.60	44.60	582.3	582.2

At the Core Exit

Time (Sec)	Coolant Density (lbm/ft^3)		Coolant Temperature (°F)	
	19 Nodes	9 Nodes	19 Nodes	9 Nodes
0.0	45.86	45.86	565.0	565.0
.06	45.86	45.86	565.0	565.0
.08	45.84	45.84	565.2	565.2
.10	45.77	45.77	566.3	566.3
.12	45.67	45.67	567.8	567.7
.14	45.58	45.58	569.0	569.0
1.0	42.30	42.26	609.6	610.0
2.0	43.15	43.16	600.1	600.0

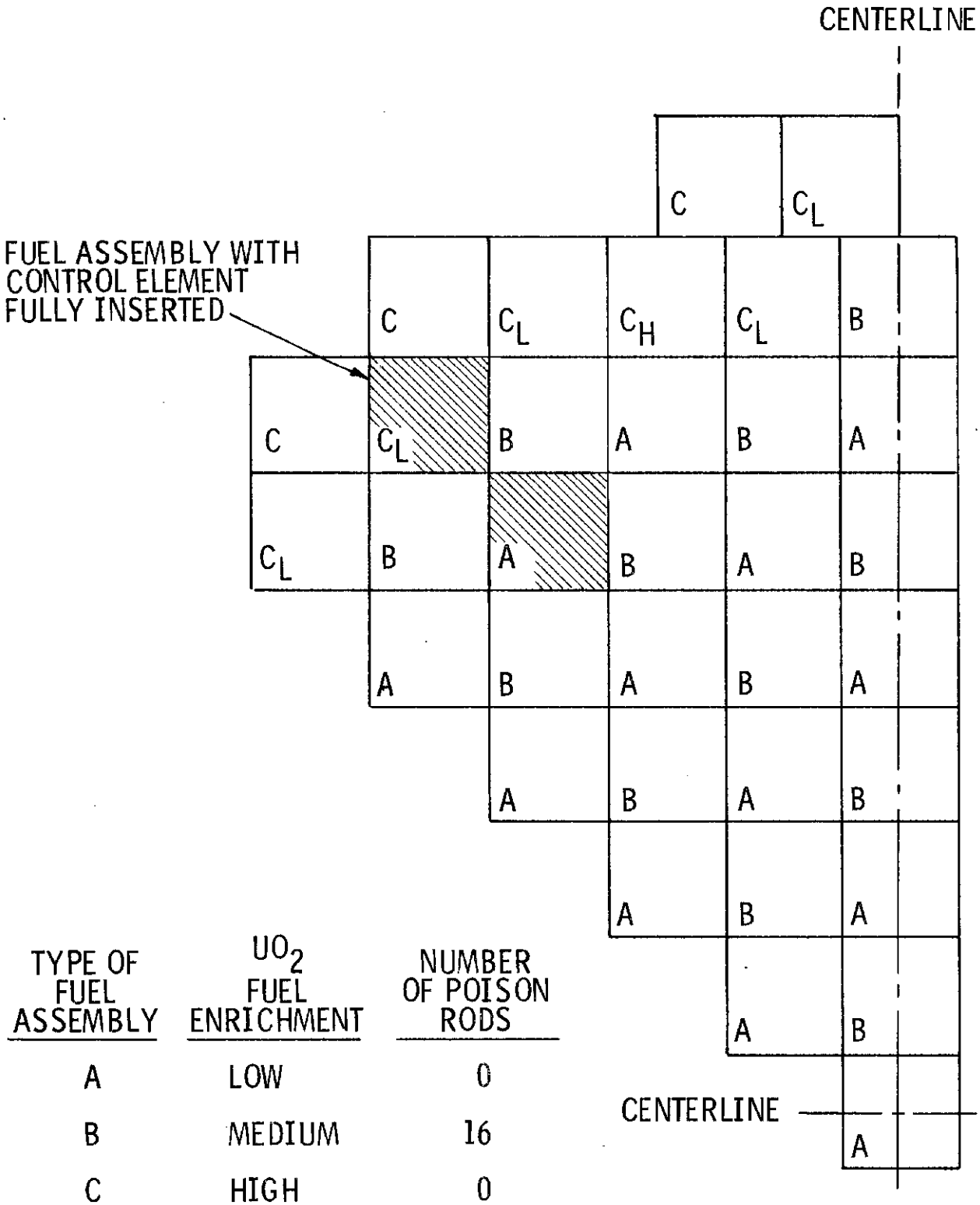

TYPE OF FUEL ASSEMBLY	UO_2 FUEL ENRICHMENT	NUMBER OF POISON RODS
A	LOW	0
B	MEDIUM	16
C	HIGH	0
C_L	HIGH	12
C_H	HIGH	16

HERMITE CENPD-188	217 FUEL ASSEMBLY CORE, FULL POWER CONTROL ELEMENT PATTERN FOR HERMITE VERIFICATION	Figure 4-1

PERCENT DIFFERENCE RELATIVE TO A 16 x 16 MESH PDQ

X.XX X.XX	4 x 4 HERMITE 4 x 4 PDQ

R	INDICATOR FOR A RODDED FUEL ASSEMBLY

				+0.75 +3.56	-0.54 +0.48
	+0.90 +1.85	-1.33 -0.12	-1.53 -0.34	-0.76 -0.45	-1.33 -1.48
+1.83 +3.00	R -0.75 -1.35	-1.33 -0.75	-0.56 -0.39	-1.00 -1.48	-0.37 +0.09
+1.51 +2.34	+0.23 +0.10	R -1.26 -1.99	-0.40 -0.86	+0.09 +0.51	-0.47 -1.20
	+1.02 +1.45	+0.11 -0.41	+0.66 +0.97	-0.06 -0.95	+0.47 +0.65
		+0.69 +1.06	+0.16 -0.78	+0.73 +0.74	+0.14 -0.91
			+0.79 +0.82	+0.25 -0.89	+0.83 +0.71
				+0.85 +0.74	+0.30 -0.91
					+0.88 +0.74

EIGENVALUES

16 x 16 PDQ	0.99926
4 x 4 HERMITE	1.0008
4 x 4 PDQ	0.99858

SUMMARY OF DIFFERENCE ANALYSIS

	HERMITE	4 x 4 PDQ
MAXIMUM DIFFERENCE	+1.83%	+3.56%
AVERAGE ABSOLUTE DIFFERENCE	0.757%	1.04%

HERMITE CENPD-188	HERMITE AND PDQ POWER DISTRIBUTION DIFFERENCES FOR A 4 x 4 MESH, 217 FUEL ASSEMBLY CORE AT FULL POWER	Figure 4-2

PERCENT DIFFERENCE RELATIVE TO A 16 x 16 MESH PDQ

X.XX	4 x 4 HERMITE
X.XX	2 x 2 HERMITE

R	INDICATOR FOR A RODDED FUEL ASSEMBLY

				+0.75 +6.16	-0.54 +2.09
	+0.90 +6.54	-1.33 +2.34	-1.53 +1.42	-0.76 +0.90	-1.33 -1.18
+1.83 +5.72	R -0.75 -1.82	-1.33 -0.35	-0.56 +2.46	-1.00 -2.11	-0.37 +1.66
+1.51 +3.69	+0.23 +0.48	R -1.26 -3.97	-0.40 -2.08	+0.09 +1.44	-0.47 -2.91
	+1.02 +2.90	+0.11 -2.13	+0.66 +1.66	-0.06 -2.94	+0.47 +1.15
		+0.69 +1.28	+0.16 -3.04	+0.73 +1.11	+0.14 -3.09
			+0.79 +1.05	+0.25 -3.19	+0.83 +0.94
				+0.85 +0.94	+0.30 -3.32
					+0.88 +0.91

EIGENVALUES

16 x 16 PDQ	0.99926
4 x 4 HERMITE	1.0008
2 x 2 HERMITE	1.00258

SUMMARY OF DIFFERENCE ANALYSIS

	2 x 2	4 x 4
MAXIMUM DIFFERENCE	+6.54%	+1.83%
AVERAGE ABSOLUTE DIFFERENCE	2.43%	0.757%

HERMITE CENPD-188	HERMITE POWER DISTRIBUTION DIFFERENCES FOR A 2 x 2 MESH, 217 FUEL ASSEMBLY CORE AT FULL POWER	Figure 4-3

PERCENT DIFFERENCE RELATIVE TO A 16 x 16 MESH PDQ

X.XX	2 x 2 HERMITE
X.XX	2 x 2 PDQ

			-1.18 -10.8	+0.33 -4.34	+0.01 -3.58	+0.31 -2.90
	-3.00 -13.3	-1.66 -7.31	+2.54 +3.01	+3.25 +4.84	+4.06 +8.12	+3.72 +6.15
-2.99 -14.1	+2.24 +1.61	-2.53 -5.91	+2.54 +4.81	-2.10 -3.41	+2.98 +6.72	-1.76 -2.54
	-3.07 -6.44	+2.18 +4.90	-2.85 -4.29	+2.94 +6.92	-2.64 -3.27	+3.07 +7.55
		-3.14 -4.68	+2.43 +6.09	-3.13 -4.16	+2.49 +6.68	-3.10 -3.85
			-3.31 -4.44	+2.20 +6.22	-3.41 -4.26	+2.16 +6.35
				-3.51 -4.41	+1.98 +6.14	-3.61 -4.41
					-3.67 -4.47	+1.85 +6.05
						-3.74 -4.51

EIGENVALUES

16 x 16 PDQ	0.99739
2 x 2 HERMITE	0.99584
2 x 2 PDQ	0.99421

SUMMARY OF DIFFERENCE ANALYSIS

	HERMITE	2 x 2 PDQ
MAXIMUM DIFFERENCE	+4.06%	-14.1%
AVERAGE ABSOLUTE DIFFERENCE	2.48%	5.66%

HERMITE CENPD-188	HERMITE AND PDQ POWER DISTRIBUTION DIFFERENCES FOR A 2 x 2 MESH, 241 FUEL ASSEMBLY CORE AT FULL POWER	Figure 4-4

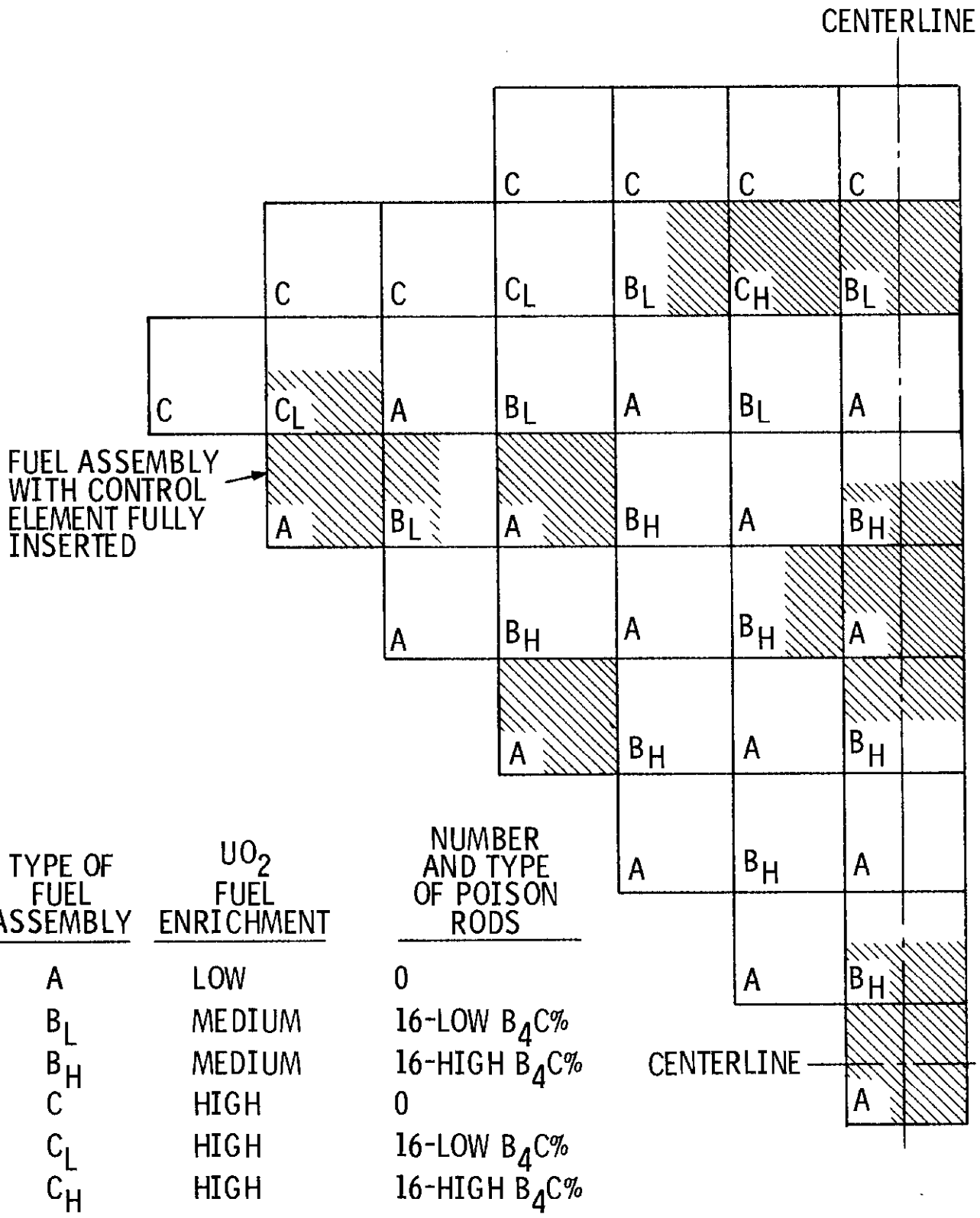

TYPE OF FUEL ASSEMBLY	UO_2 FUEL ENRICHMENT	NUMBER AND TYPE OF POISON RODS
A	LOW	0
B_L	MEDIUM	16-LOW B_4C%
B_H	MEDIUM	16-HIGH B_4C%
C	HIGH	0
C_L	HIGH	16-LOW B_4C%
C_H	HIGH	16-HIGH B_4C%

HERMITE CENPD-188	241 FUEL ASSEMBLY CORE, ZERO POWER CONTROL ELEMENT PATTERN FOR HERMITE VERIFICATION	Figure 4-5

PERCENT DIFFERENCE RELATIVE TO A 16 x 16 MESH PDQ

X.XX	2 x 2 HERMITE
X.XX	2 x 2 PDQ

R INDICATOR FOR A RODDED FUEL ASSEMBLY

			0.0 -1.61	-1.03 +1.83	-4.93 -0.75	-5.88 -1.05
	+0.53 -3.58	+1.48 +1.04	+6.17 +10.2	R +6.11 +11.8	R +14.6 +17.5	R +6.08 +13.0
-0.80 -9.37	R +9.22 +11.6	-0.13 -2.02	+4.34 +8.12	-3.18 -3.77	0.0 +3.26	-5.37 -7.56
	R +4.24 +5.05	R +4.63 +8.82	R +6.20 +8.24	+1.90 +4.71	-5.43 -8.09	R +2.34 +5.64
		-4.82 -6.63	+1.31 +2.99	-4.56 -8.06	R +2.00 +3.59	R -1.42 -2.06
			R +3.87 +4.12	+0.25 +0.88	-6.34 -11.4	R +1.31 +1.12
				-5.70 -9.41	+0.03 +0.07	-5.39 -11.3
					-6.85 -12.3	R +0.91 +0.58
						R -2.40 -4.53

EIGENVALUES

16 x 16 PDQ	0.96968
2 x 2 HERMITE	0.96661
2 x 2 PDQ	0.96494

SUMMARY OF DIFFERENCE ANALYSIS

	HERMITE	2 x 2 PDQ
MAXIMUM DIFFERENCE	+14.6%	+17.5%
AVERAGE ABSOLUTE DIFFERENCE	3.72%	5.94%

HERMITE CENPD-188	HERMITE AND PDQ POWER DISTRIBUTION DIFFERENCES FOR A 2 x 2 MESH, 241 FUEL ASSEMBLY CORE AT ZERO POWER	Figure 4-6

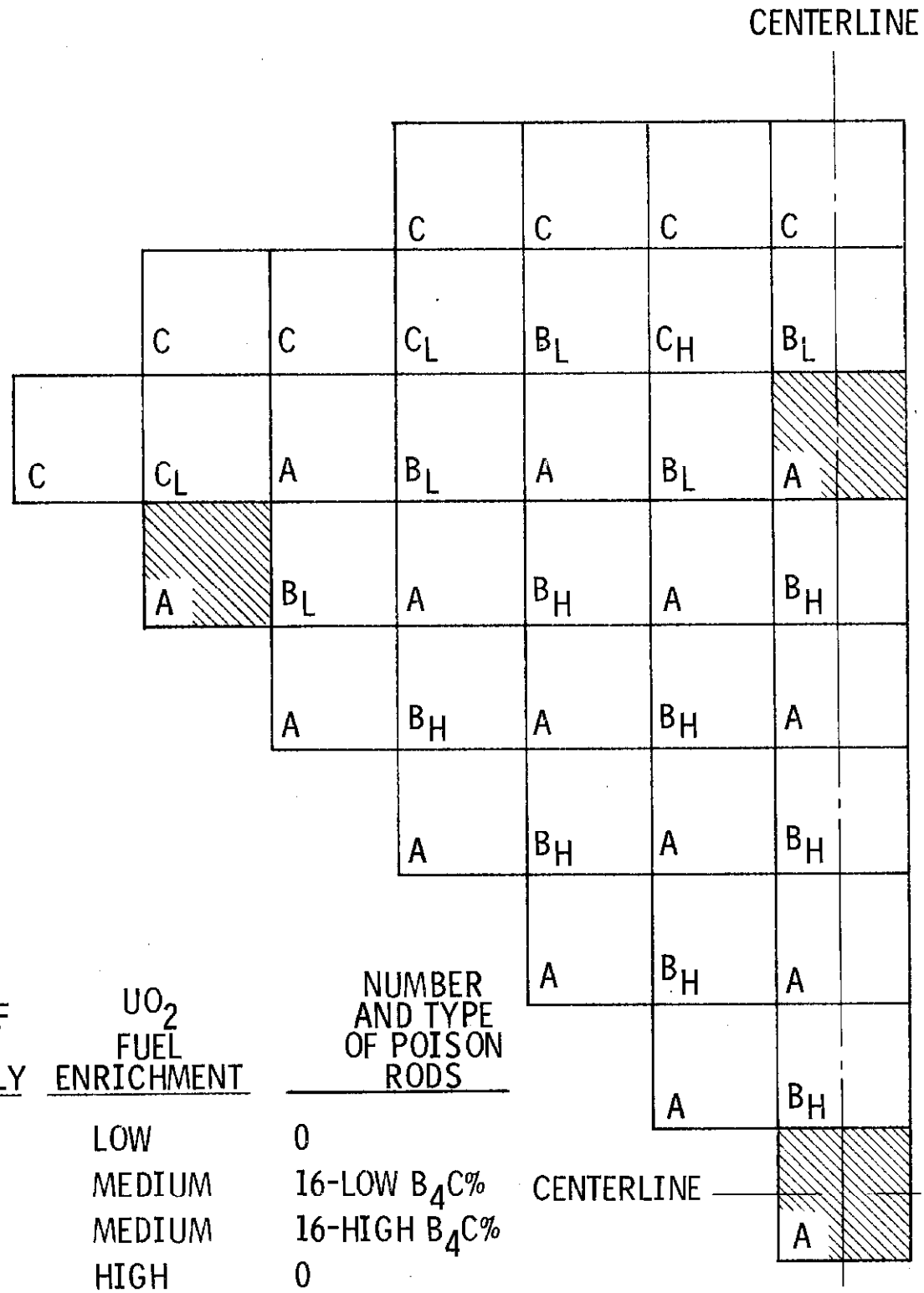

TYPE OF FUEL ASSEMBLY	UO_2 FUEL ENRICHMENT	NUMBER AND TYPE OF POISON RODS
A	LOW	0
B_L	MEDIUM	16-LOW B_4C%
B_H	MEDIUM	16-HIGH B_4C%
C	HIGH	0
C_L	HIGH	16-LOW B_4C%
C_H	HIGH	16-HIGH B_4C%

HERMITE CENPD-188	241 FUEL ASSEMBLY CORE, FULL POWER CONTROL ELEMENT PATTERN FOR HERMITE VERIFICATION	Figure 4-7

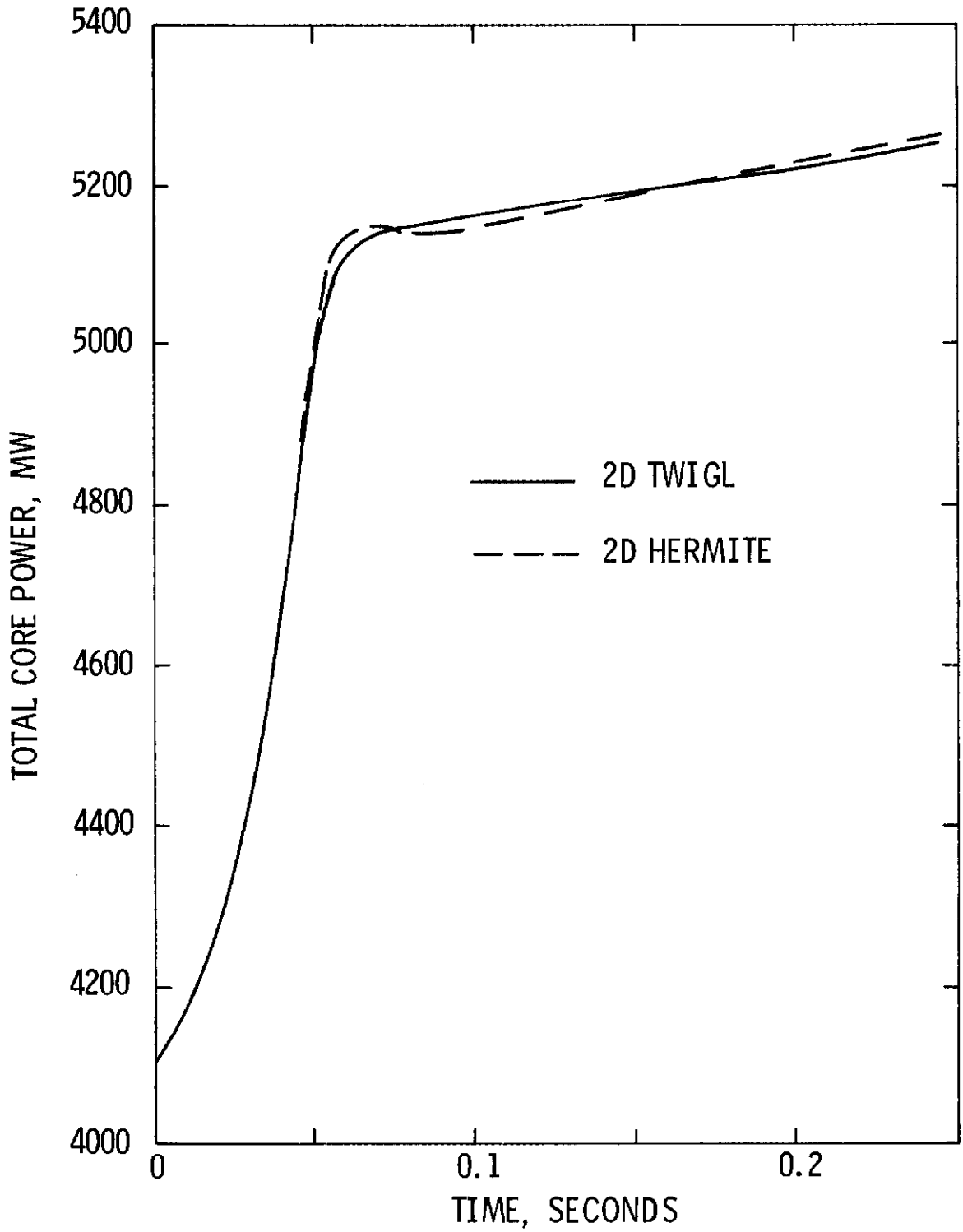

HERMITE CENPD-188	FULL POWER CEA EJECTION TRANSIENT, TOTAL CORE POWER WITHOUT FEEDBACK	Figure 4-8

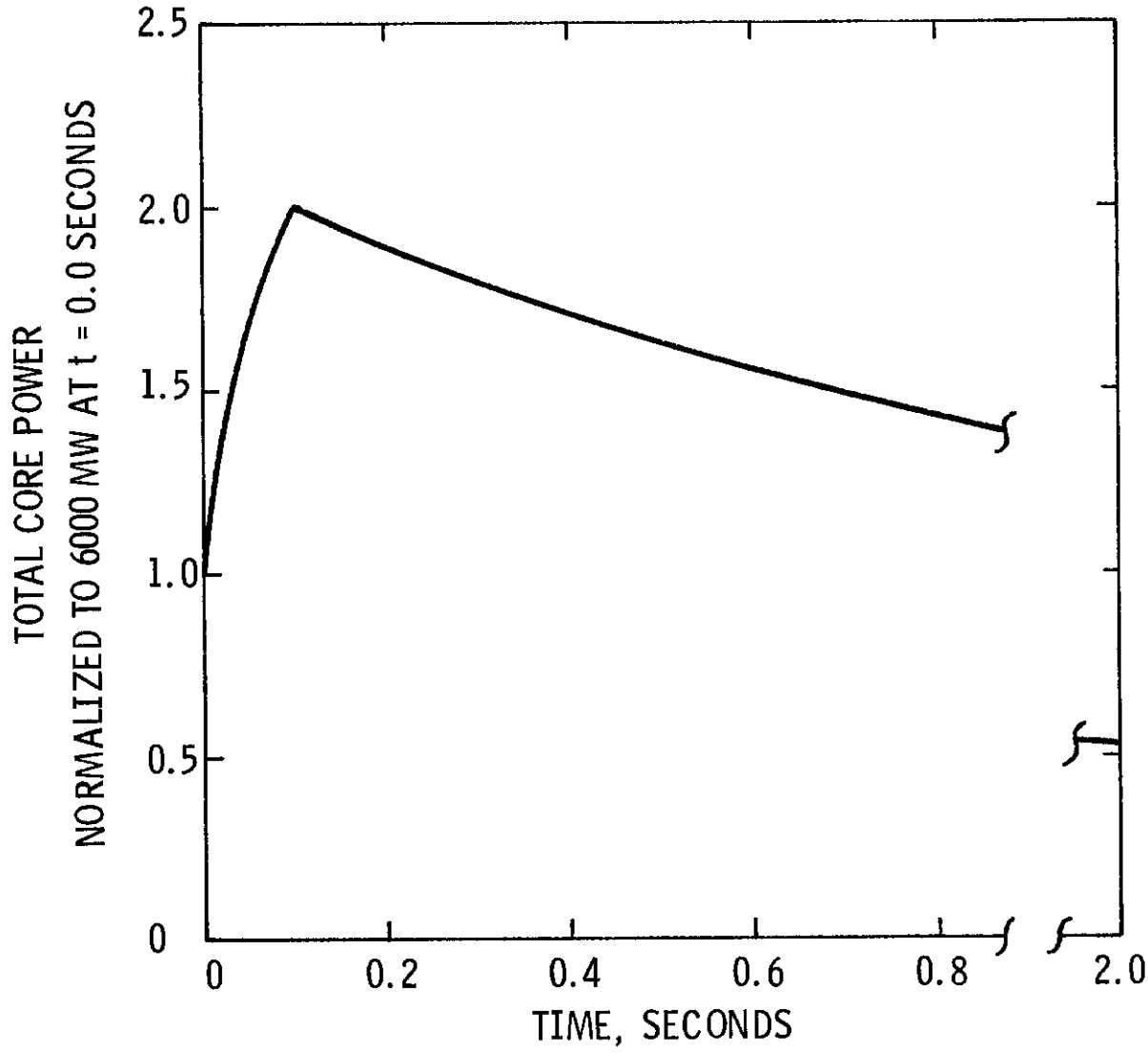

HERMITE CENPD-188	FULL POWER CEA EJECTION TRANSIENT, CORE POWER FORCING FUNCTION FOR THERMAL-HYDRAULIC MODEL VERIFICATION	Figure 4-9

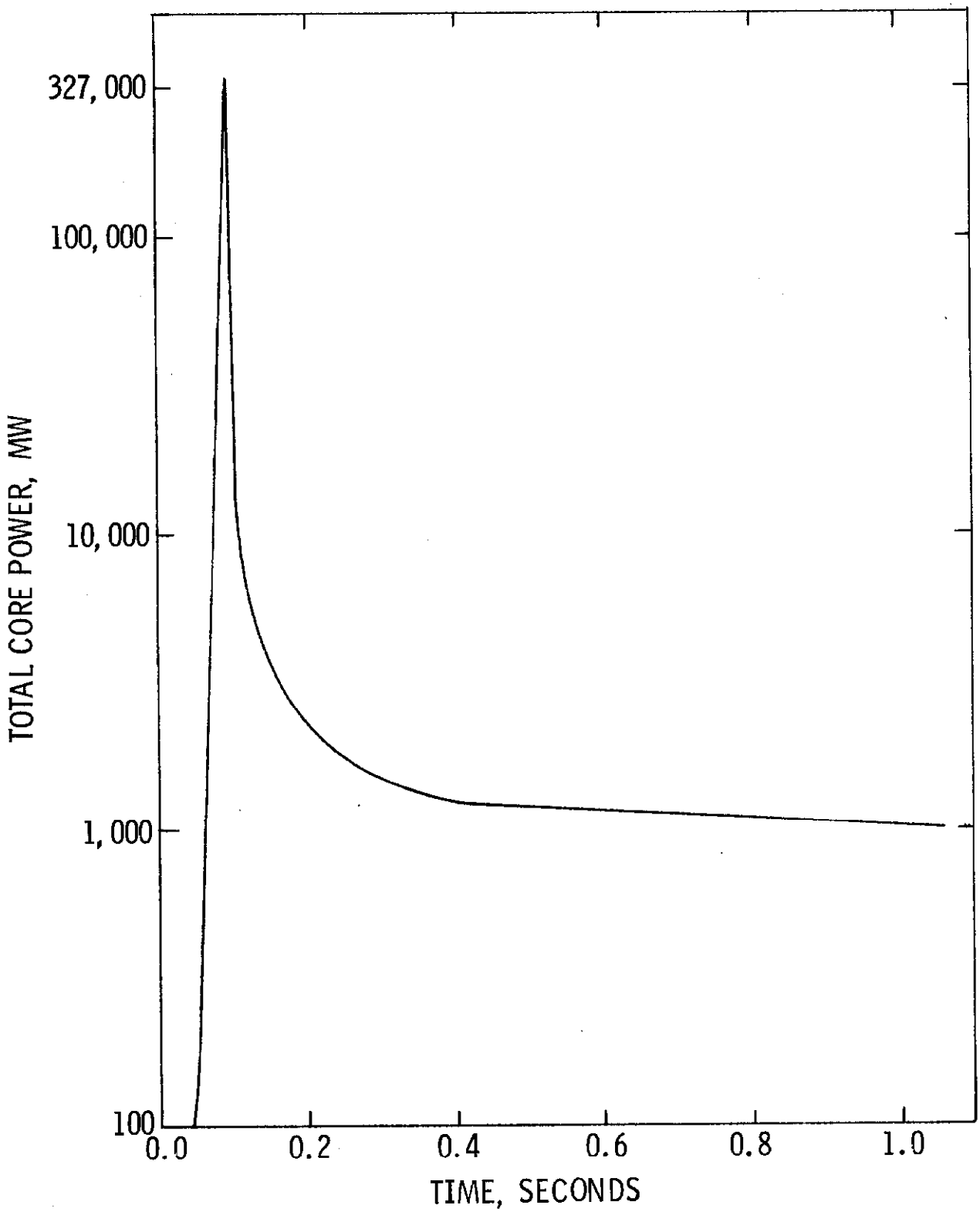

HERMITE CENPD-188	ZERO POWER CEA EJECTION TRANSIENT, CORE POWER FORCING FUNCTION FOR THERMAL-HYDRAULIC MODEL VERIFICATION	Figure 4-10

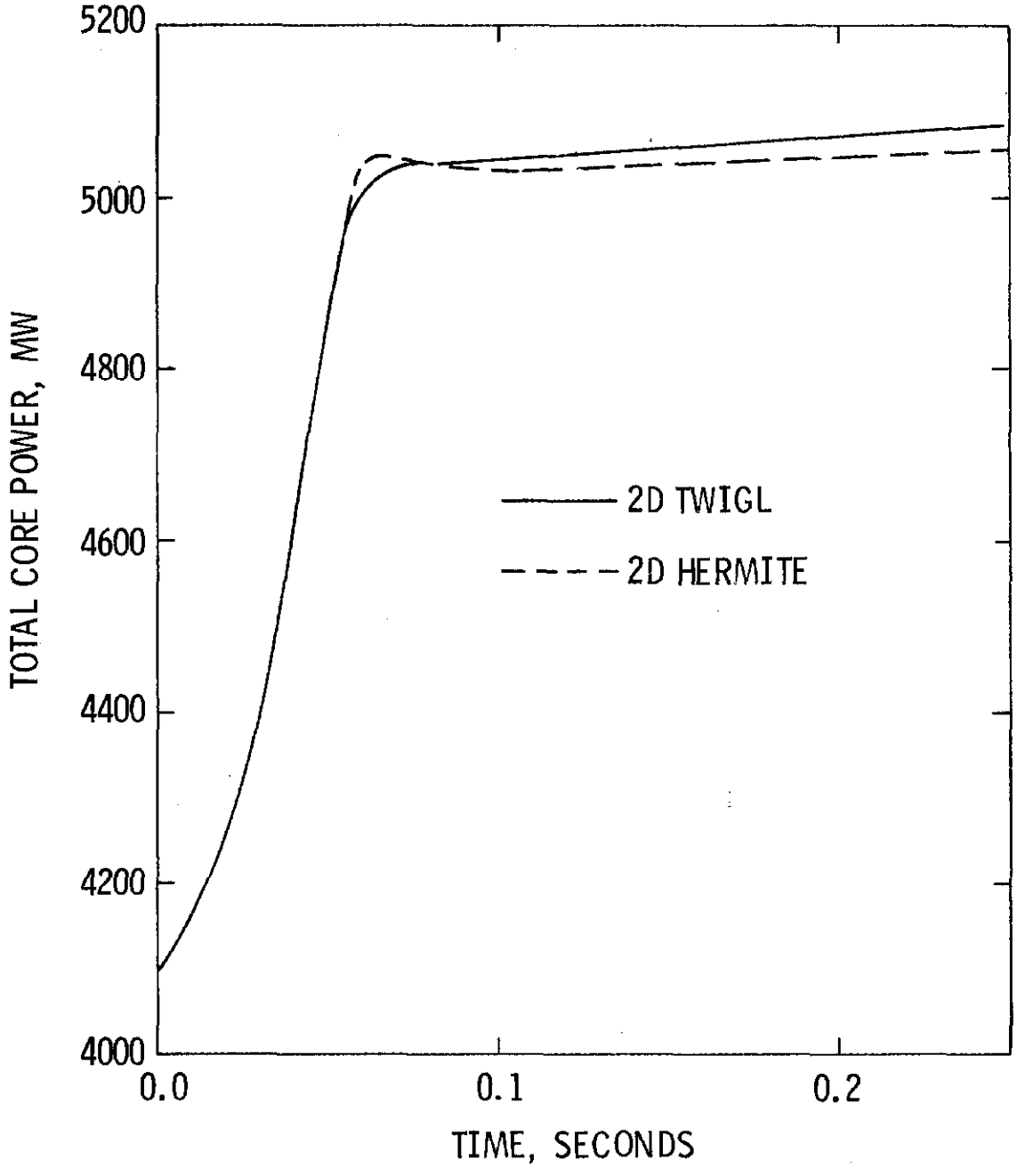

HERMITE CENPD-188	FULL POWER CEA EJECTION TRANSIENT, TOTAL CORE POWER WITH FEEDBACK	Figure 4-11

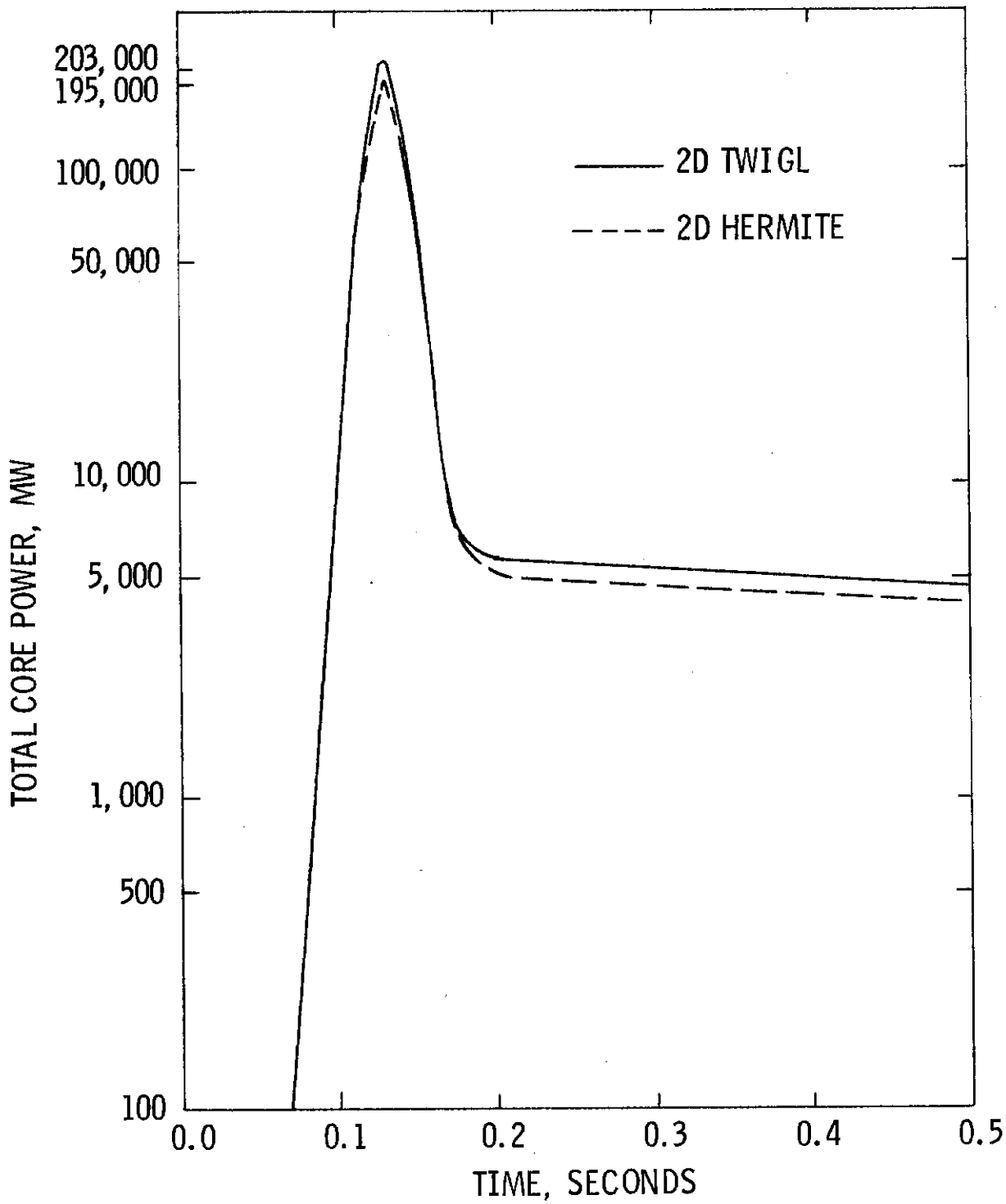

HERMITE CENPD-188	ZERO POWER CEA EJECTION TRANSIENT, TOTAL CORE POWER WITH FEEDBACK	Figure 4-12

5.0 THREE-DIMENSIONAL ANALYSIS OF THE CONTROL ELEMENT ASSEMBLY EJECTION INCIDENT

HERMITE was used for the three-dimensional analysis of the full power and zero power control element assembly ejection incidents. Results from the three-dimensional analyses of these incidents are compared to those from the corresponding two-dimensional analyses. For both the full power and zero power cases the core model is the 241 fuel assembly core described in Section 4.0. The full power and zero power control element assembly patterns are also the same as those described in Section 4.0, and in both cases the central control element assembly was ejected in fifty milliseconds (at a constant velocity). Each fuel assembly was partitioned into a 2 x 2 mesh array in the horizontal plane, as described in Section 4.0. For the three-dimensional analyses twelve axial mesh intervals were used, one for each of the top and bottom reflectors and ten for the active core region. One thermal-hydraulic channel was assigned to each fuel assembly. In this way, fuel temperature feedback was included on an assembly-by-assembly basis.

5.1 FULL POWER CONTROL ELEMENT ASSEMBLY EJECTION INCIDENT

For this case the initial core power was 4100 MW. As shown in Table 5-1, the static worth of the ejected central control element assembly was 0.132%$\Delta\rho$, or \$0.178, so that a delayed critical transient was induced.

The core power transient is shown in Figure 5-1 and the central fuel assembly power transient is shown in Figure 5-2. The differences between the two-dimensional and three-dimensional cases illustrate the axial spatial effects present in the three-dimensional case. These effects are caused primarily by changes in differential control element assembly worth as it moves out of the core. As is well known, when a control element tip is moving through regions near the bottom and top of a core, the reactivity inserted per unit distance traveled is smaller than when it is moving through the middle regions of the core. This is a consequence of the relatively lower neutron

flux and importance near the axial extremes of the core compared to the middle regions of the core. While this axial spatial effect is seen in three-dimensional calculations explicitly, it is not accounted for in the two-dimensional calculations.

As the control element assembly is ejected from the lower regions of the core the rate of reactivity addition and the rate of change in core power are lower for the three-dimensional case relative to the two-dimensional case, as can be seen in Figures 5-1 and 5-2 for $t \leq 0.01$ seconds. Then, as the tip of the control element assembly moves through the middle regions of the core the rate of reactivity addition and the rate of change in core power level for the three-dimensional case surpass those for the two-dimensional case. Finally, when the control element assembly is ejected from the upper regions of the core, the rate of reactivity addition and the rate of change in core power for the three-dimensional case decrease accordingly. The rapid rise in power ends when the control element assembly has been completely ejected from the core. Thereafter, the two-dimensional and three-dimensional power levels show good agreement. These transients were ended at 1.0 seconds, at which time the two-dimensional and three-dimensional core average energy depositions were 10.30 cal/gm and 10.26 cal/gm, respectively.

To illustrate axial power distribution changes during the transient, the central fuel assembly power distributions corresponding to several time points are shown in Figures 5-3 through 5-6. The axial power distribution shifts from a nearly symmetrical initial distribution (Figure 5-3) to a bottom peaked distribution (Figures 5-4 and 5-5), and then back to a nearly symmetrical distribution when the control element assembly is almost completely ejected (Figure 5-6).

To quantify axial flux distribution effects on the rate of reactivity addition during the ejection of the control element assembly from the core, cases were run where the control element assembly was ejected in one time step. As expected, the two-dimensional and three-dimensional core power transients, shown in Figure 5-7, show much closer agreement during the rapid power excursion.

Three-dimensional spatial effects on the thermal-hydraulic node with maximum power were also observed. Figure 5-8 shows the three-dimensional maximum node power relative to the core average node power as a function of time, and Figure 5-9 shows the location of the maximum power node during the transient. As the central control element assembly is ejected the three-dimensional power distribution shifts towards the center of the core and the maximum node power relative to the core average node power increases. When the control element assembly is approximately 56 percent ejected, t = 0.028 seconds, the axial power distribution is shifted towards the lower regions of the core (see Figure 5-5), and the location of the maximum power node is in the central fuel assembly. At this time the maximum node power relative to the core average node power is at its highest value as shown in Figure 5-8. As the ejection of the control element assembly continues the axial power distribution becomes more symmetrical, and as a result the maximum node power relative to the core average node power abruptly decreases. When the control element assembly is 96 percent ejected at t = 0.048 seconds, the location of the maximum node power moves to the fuel assembly adjacent to the central fuel assembly and remains there for the remainder of the transient.

In conclusion, the results from the three-dimensional analysis of this full power control element assembly ejection incident are consistent with those from the corresponding two-dimensional analysis.

5.2 ZERO POWER CONTROL ELEMENT ASSEMBLY EJECTION INCIDENT

For this case the initial core power was 1.0 MW. As discussed in Section 4.3.2, the control element assembly pattern was chosen to give a high central control element assembly static worth. As shown in Table 5-1, the static worth of the ejected central control element assembly was 1.19%$\Delta\rho$, or \$1.60, so that a prompt critical transient was induced.

The total core and central fuel assembly power transients are shown in Figures 5-10 and 5-11. Both the total core and central fuel assembly powers show similar behavior during the transient. Figures 5-10 and 5-11 show that the three-dimensional power excursion occurs at an earlier point in time relative to that for the two-dimensional case. This earlier power

excursion is the result of axial spatial effects on the rate of reactivity addition during the ejection of the control element assembly from the core. These effects were discussed in Section 5.1. The powers for the three-dimensional case are initially lower than those for the two-dimensional case. However, the three-dimensional rate of reactivity addition, and therefore core power, soon surpass those for the two-dimensional case. Due to this rapid increase in the rate of reactivity addition the prompt critical state is reached at an earlier time relative to the two-dimensional case, and the three-dimensional powers continue to rise ahead of the two-dimensional powers.

The increase in fuel temperatures, and the resulting increase in resonance absorption, is the most significant factor in terminating the prompt critical power excursion. The total core and central fuel assembly average fuel temperatures as a function of time are shown in Figures 5-12 and 5-13. The fuel temperatures begin to increase slowly after the control element assembly has been ejected from the core, and then rise very rapidly as a result of the energy deposited in the fuel during the prompt critical power excursion. The resonance absorption of neutrons increases and the power excursion is terminated. The two-dimensional peak power is 28 percent higher than that for the three-dimensional case since a given change in energy deposited in the fuel results in less negative reactivity from fuel temperature feedback for the two-dimensional case.

The fuel temperatures continue to increase in proportion to the energy being deposited in the fuel during the transient and consequently the core power level decreases. With the lower power levels both the rate of energy deposition and the rate of increase in fuel temperatures decrease. As a result, at about 0.12 seconds the fuel temperature rise begins to slow down. At about 0.17 seconds most of the energy generated during the power excursion has been deposited in the fuel and the rise in fuel temperature has slowed down significantly. Finally, since the rise in fuel temperatures has slowed down the rate of power decrease is reduced. This transient was ended at 1.0 seconds, at which time the two-dimensional core average energy deposition of 19.3 cal/gm is 25 percent larger than the value of 15.5 cal/gm for the three-dimensional case.

Changes in the axial power distribution, similar to those for the full power control element assembly ejection incident, were also observed for the zero power incident. Figures 5-14 through 5-17 show the central fuel assembly axial power distributions at several times during the transient. The axial power distribution shifts from a symmetrical initial distribution (Figure 5-14) to a bottom peaked distribution (Figures 5-15 and 5-16), and then back to a nearly symmetrical distribution (Figure 5-17).

Three-dimensional spatial effects on the maximum node power were also observed. Figure 5-18 shows the three-dimensional maximum node power relative to the core average node power as a function of time, and Figure 5-19 shows the location of the maximum power node during the transient. As the central control element assembly is ejected the three-dimensional power distribution shifts towards the lower and central regions of the core and the maximum node power relative to the core average node power increases. When the control element is approximately 40 percent ejected, t = 0.020 seconds, the axial power distribution has shifted towards the lower regions of the core (see Figures 5-15 and 5-16), and the location of the maximum power node is in the third axial node of the central fuel assembly as shown in Figure 5-19. At t = 0.036 seconds the maximum node power relative to the core average node power is at its highest value as shown in Figure 5-18, and is in the fifth axial node of the central fuel assembly. As the ejection of the control element assembly continues the axial power distribution becomes more symmetrical and the maximum node power relative to the core average node power abruptly decreases. After the control element assembly is fully ejected the location of the maximum node power is in the sixth axial node of the central fuel assembly where it remains for the remainder of the transient. At approximately 0.1 seconds the maximum node power relative to the core average node power decreases rapidly due to the effect of fuel temperature feedback and at approximately 0.17 seconds the maximum node power relative to the core average node power levels off somewhat.

In conclusion, differences between the corresponding two-dimensional and three-dimensional analyses of this control element assembly ejection incident are due to axial weighting effects on fuel temperature reactivity feedback.

Table 5-1

Central Control Element Assembly Static Worths (%Δρ)

Case	Two-Dimensional HERMITE	Three-Dimensional HERMITE
Full Power Without Thermal Feedback	0.1602	0.1596
Full Power With Thermal Feedback	0.1319	0.1322
Zero Power Without Thermal Feedback	1.1930	1.1897
Zero Power With Thermal Feedback	1.1927	1.1891

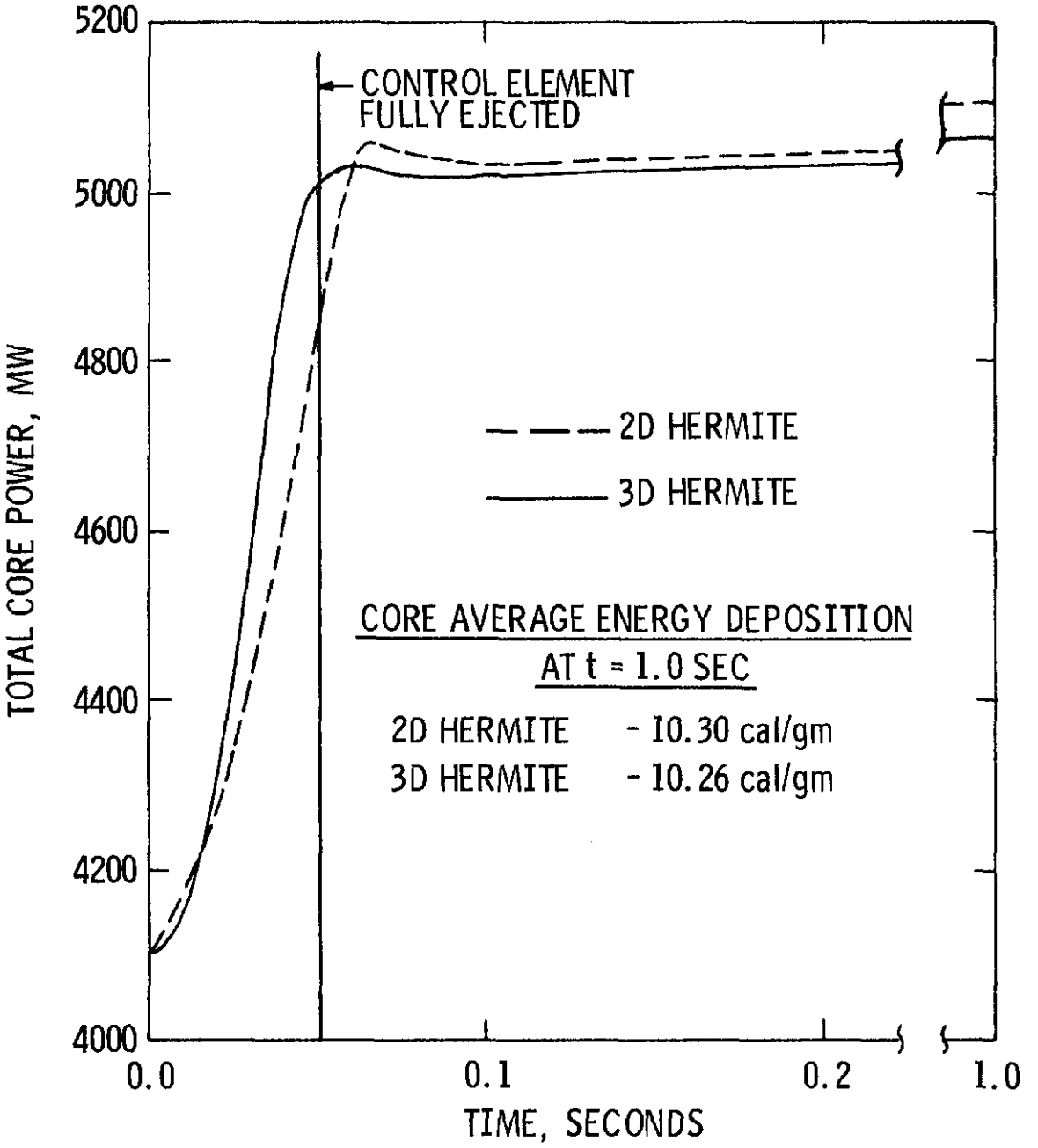

HERMITE CENPD-188	FULL POWER CEA EJECTION TRANSIENT, TOTAL CORE POWER	Figure 5-1

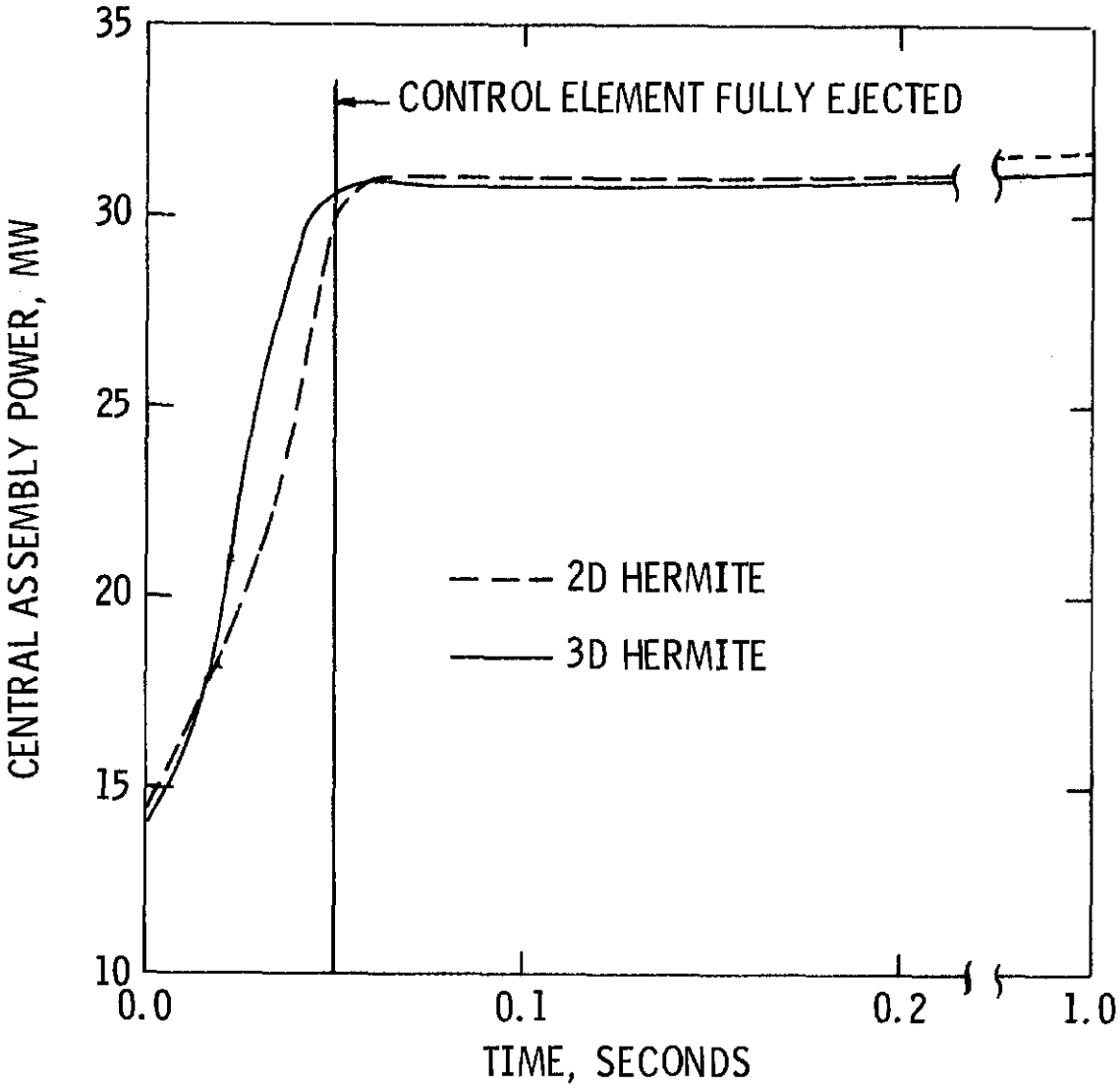

HERMITE CENPD-188	FULL POWER CEA EJECTION TRANSIENT, CENTRAL ASSEMBLY POWER	Figure 5-2

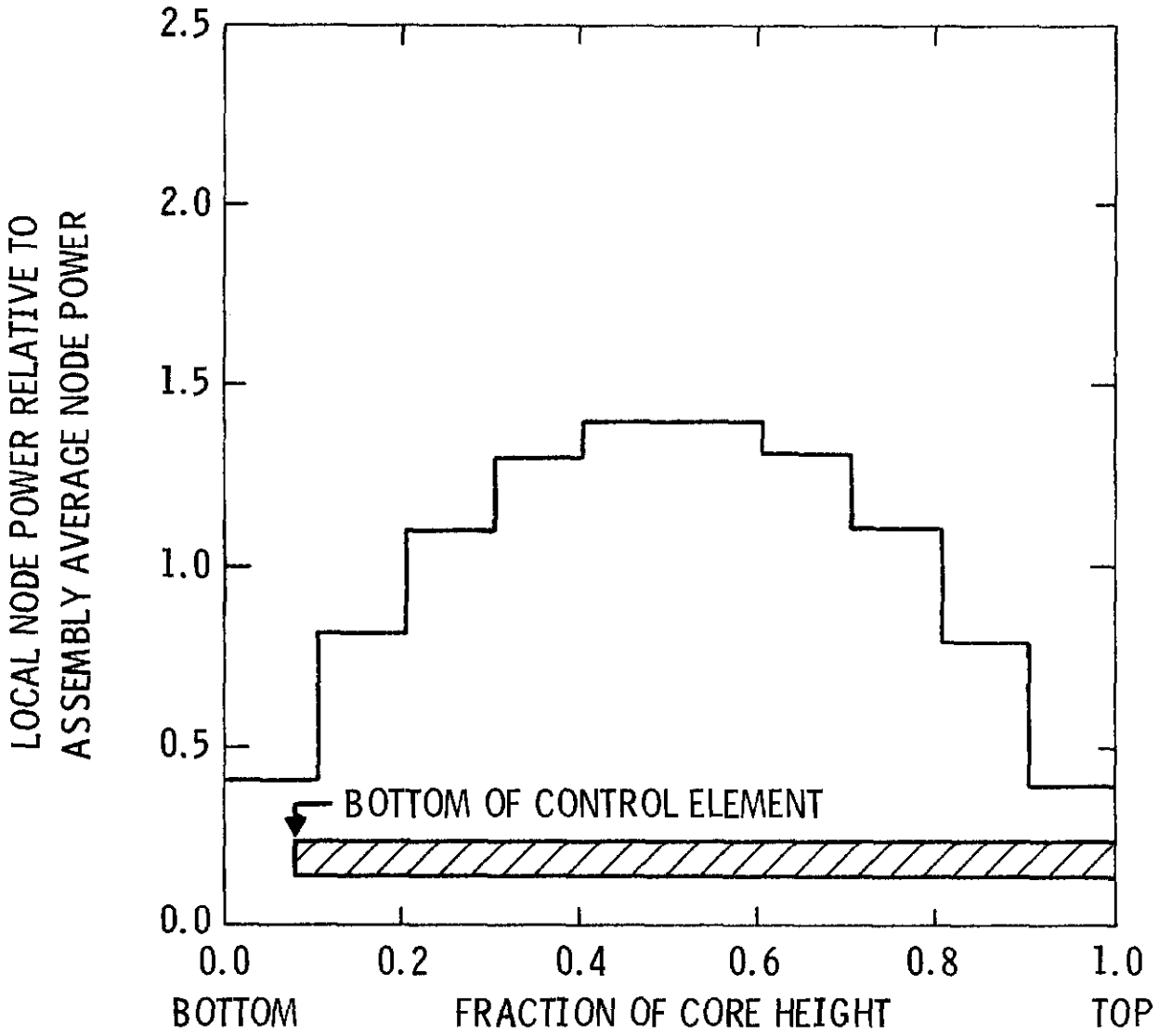

HERMITE CENPD-188	FULL POWER CEA EJECTION TRANSIENT, CENTRAL ASSEMBLY POWER DISTRIBUTION AT t = 0.004 SECONDS	Figure 5-3

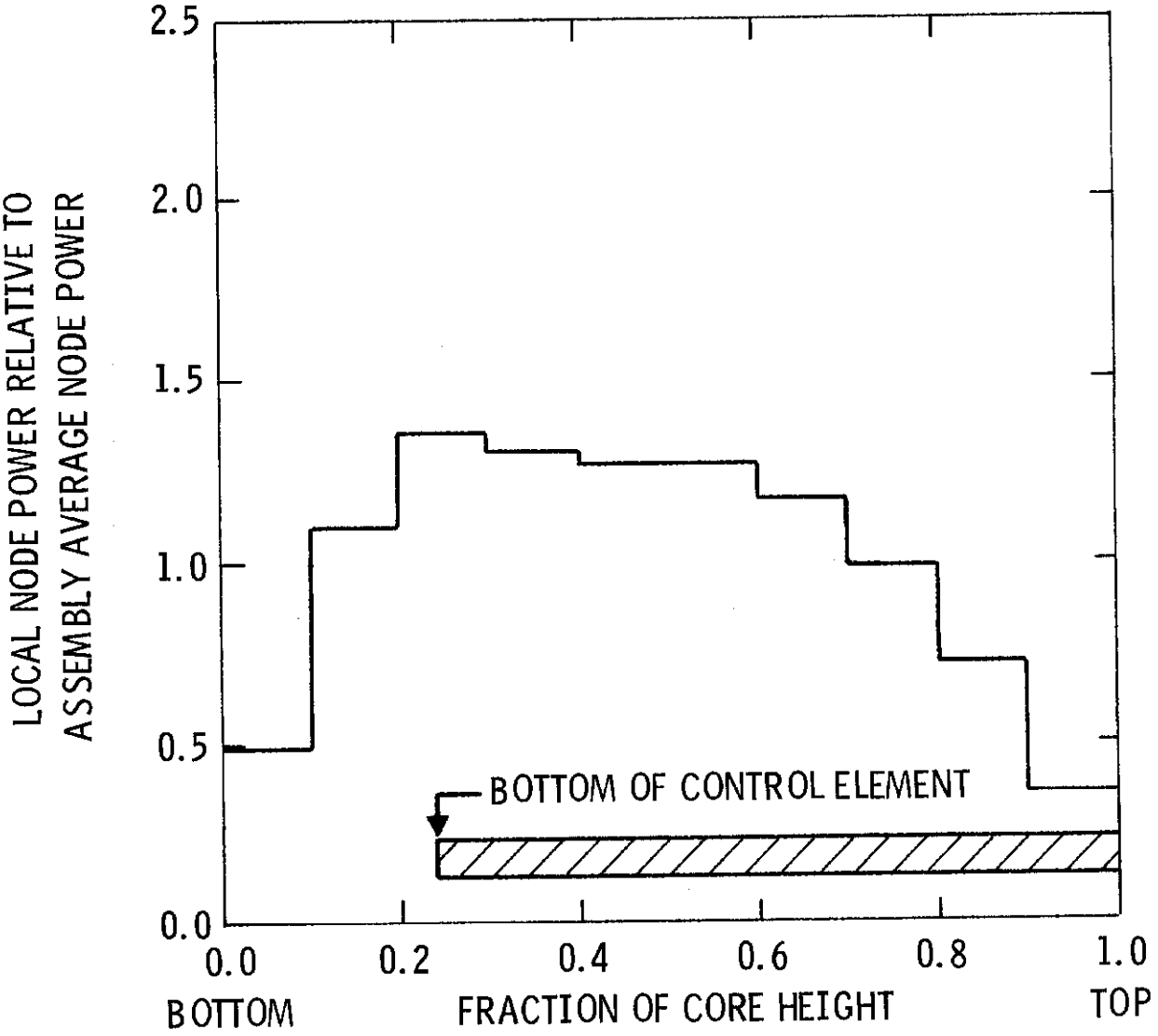

HERMITE CENPD-188	FULL POWER CEA EJECTION TRANSIENT, CENTRAL ASSEMBLY POWER DISTRIBUTION AT t = 0.012 SECONDS	Figure 5-4

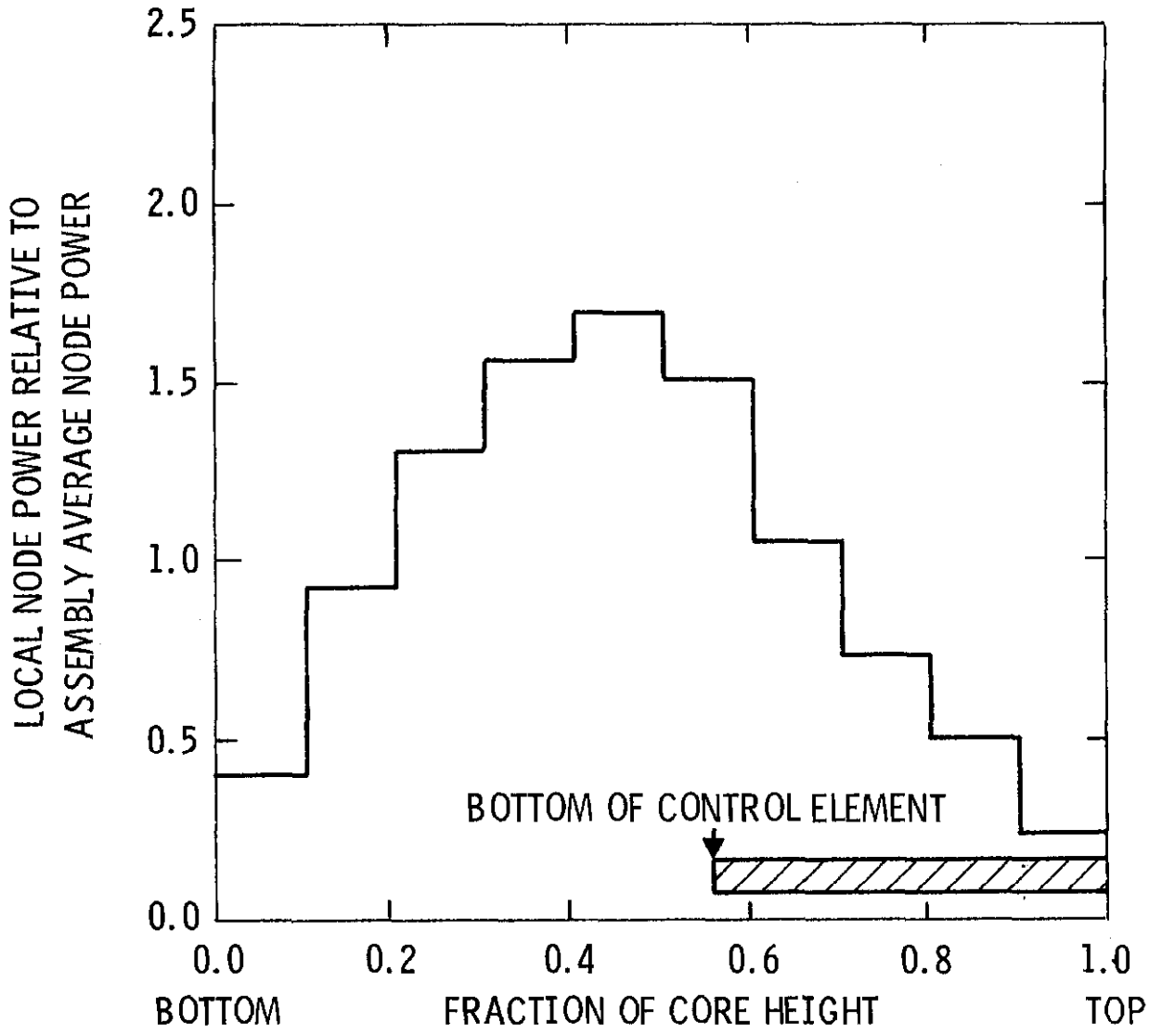

HERMITE CENPD-188	FULL POWER CEA EJECTION TRANSIENT, CENTRAL ASSEMBLY POWER DISTRIBUTION AT t = 0.028 SECONDS	Figure 5-5

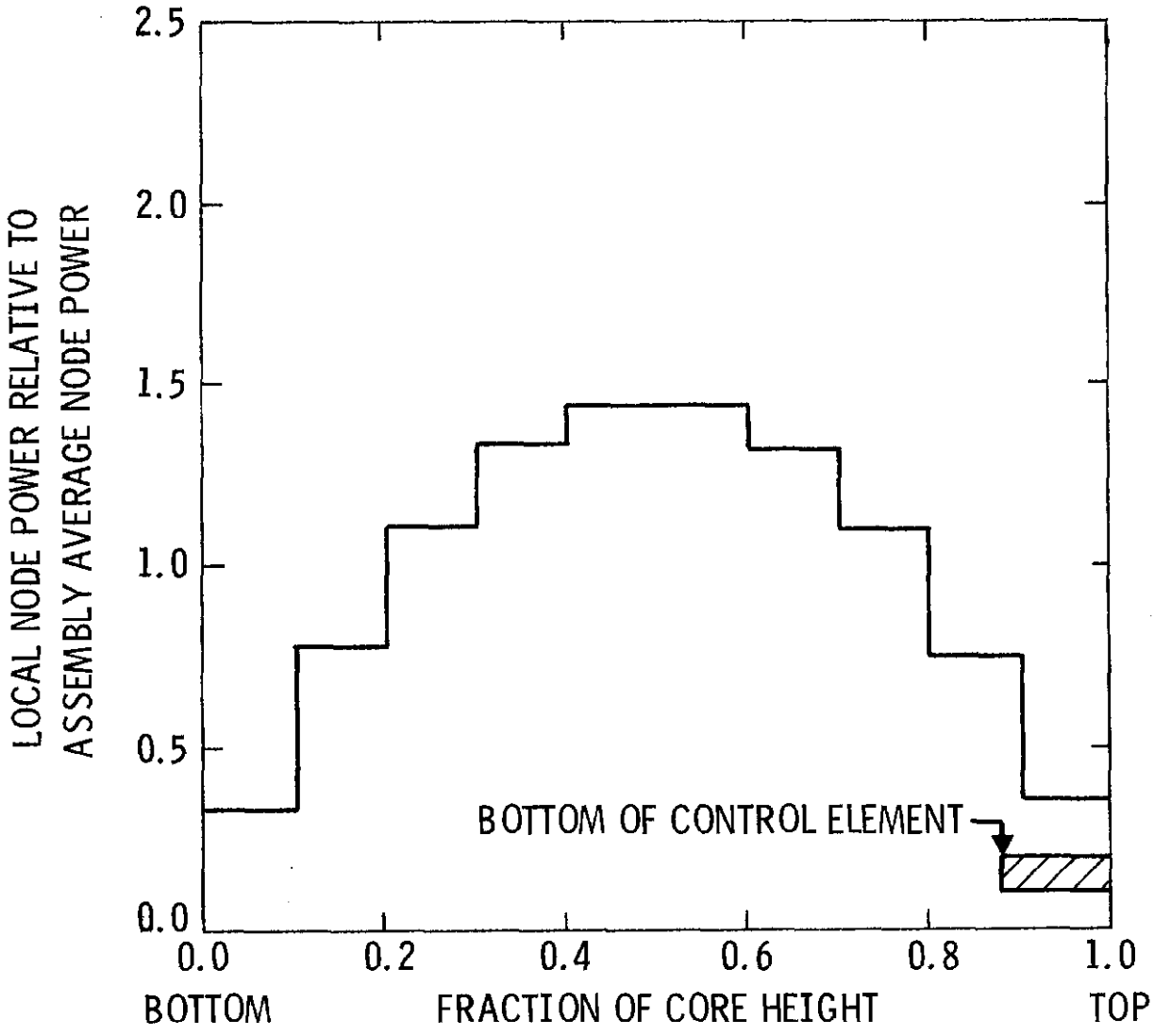

HERMITE CENPD-188	FULL POWER CEA EJECTION TRANSIENT, CENTRAL ASSEMBLY POWER DISTRIBUTION AT t = 0.044 SECONDS	Figure 5-6

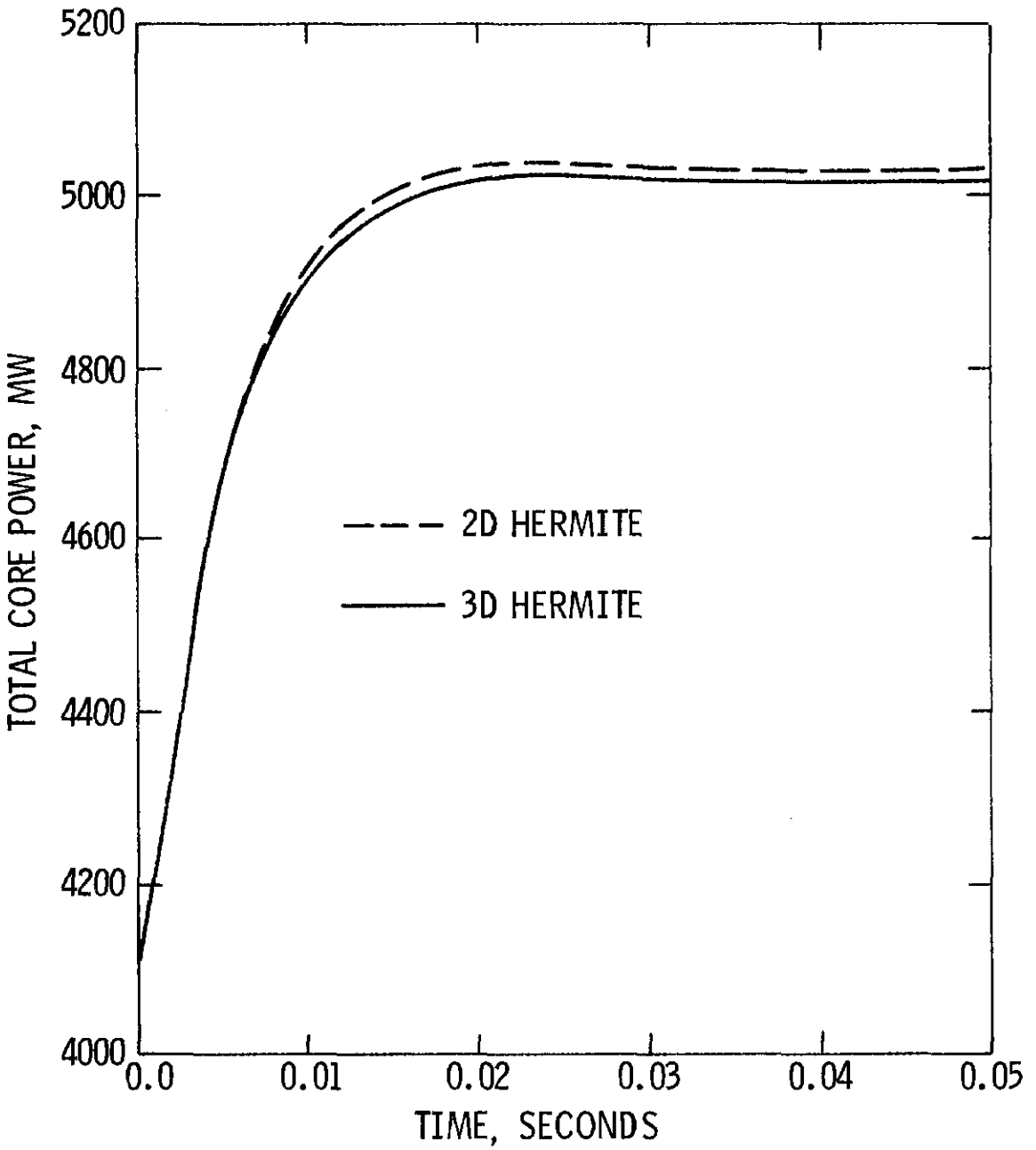

HERMITE CENPD-188	FULL POWER CEA EJECTION TRANSIENT, CORE POWER AFTER STEP EJECTION OF THE CEA	Figure 5-7

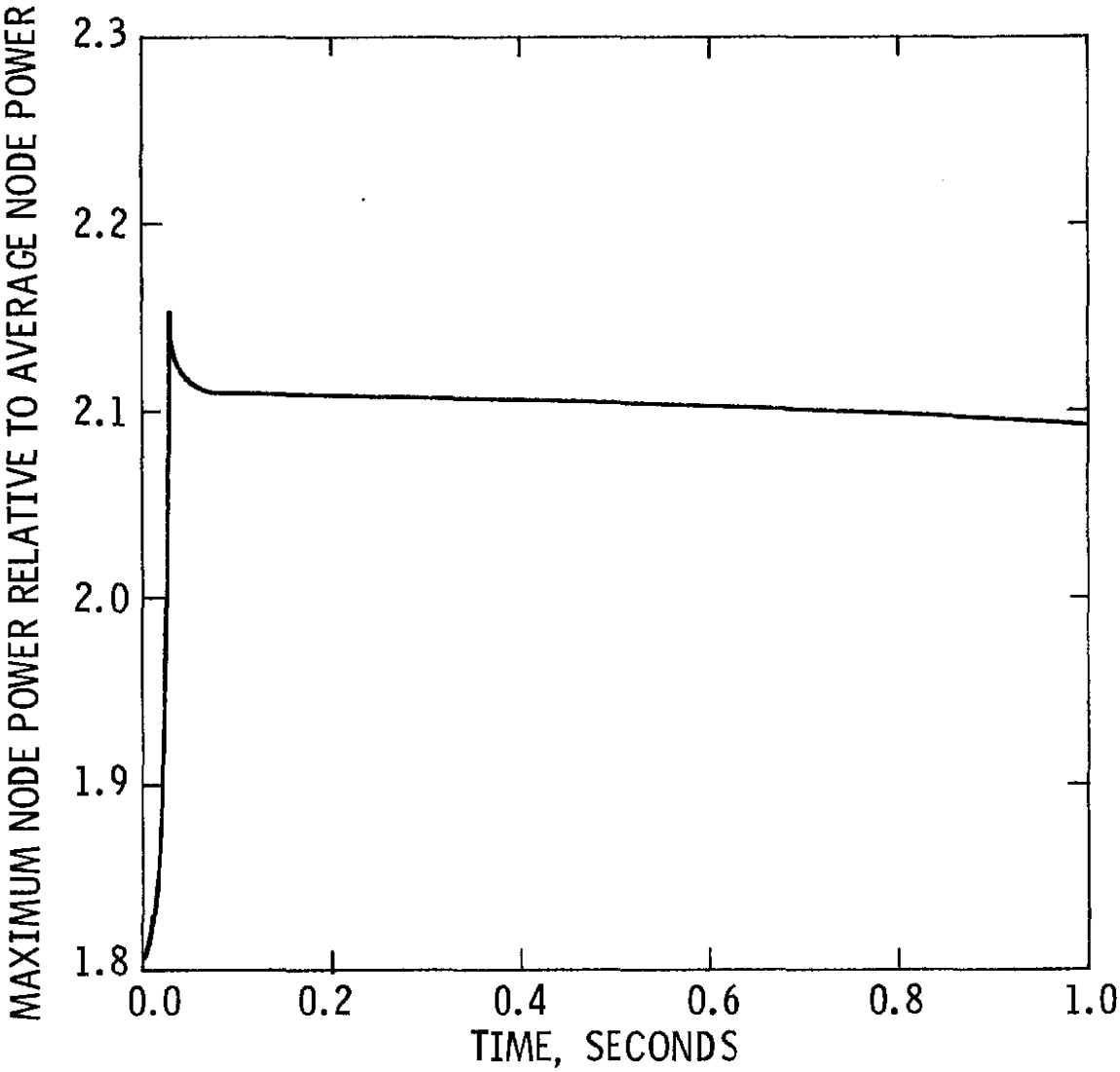

HERMITE CENPD-188	3D FULL POWER CEA EJECTION TRANSIENT, MAXIMUM NODE POWER RELATIVE TO AVERAGE NODE POWER	Figure 5-8

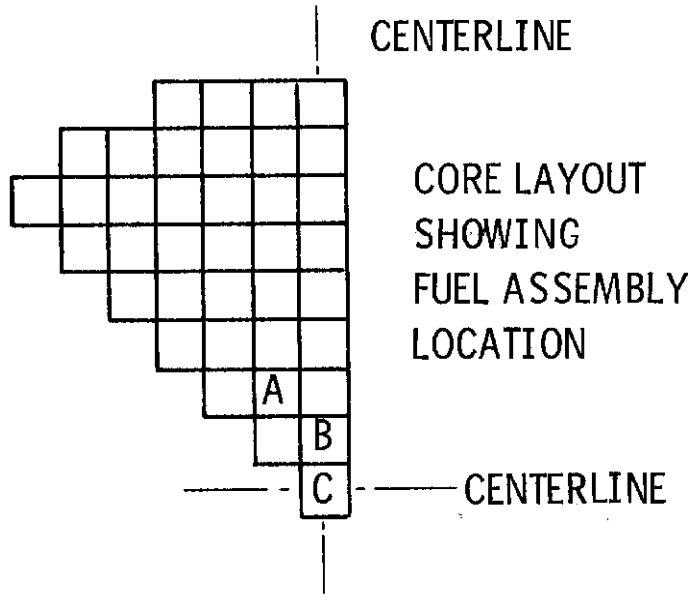

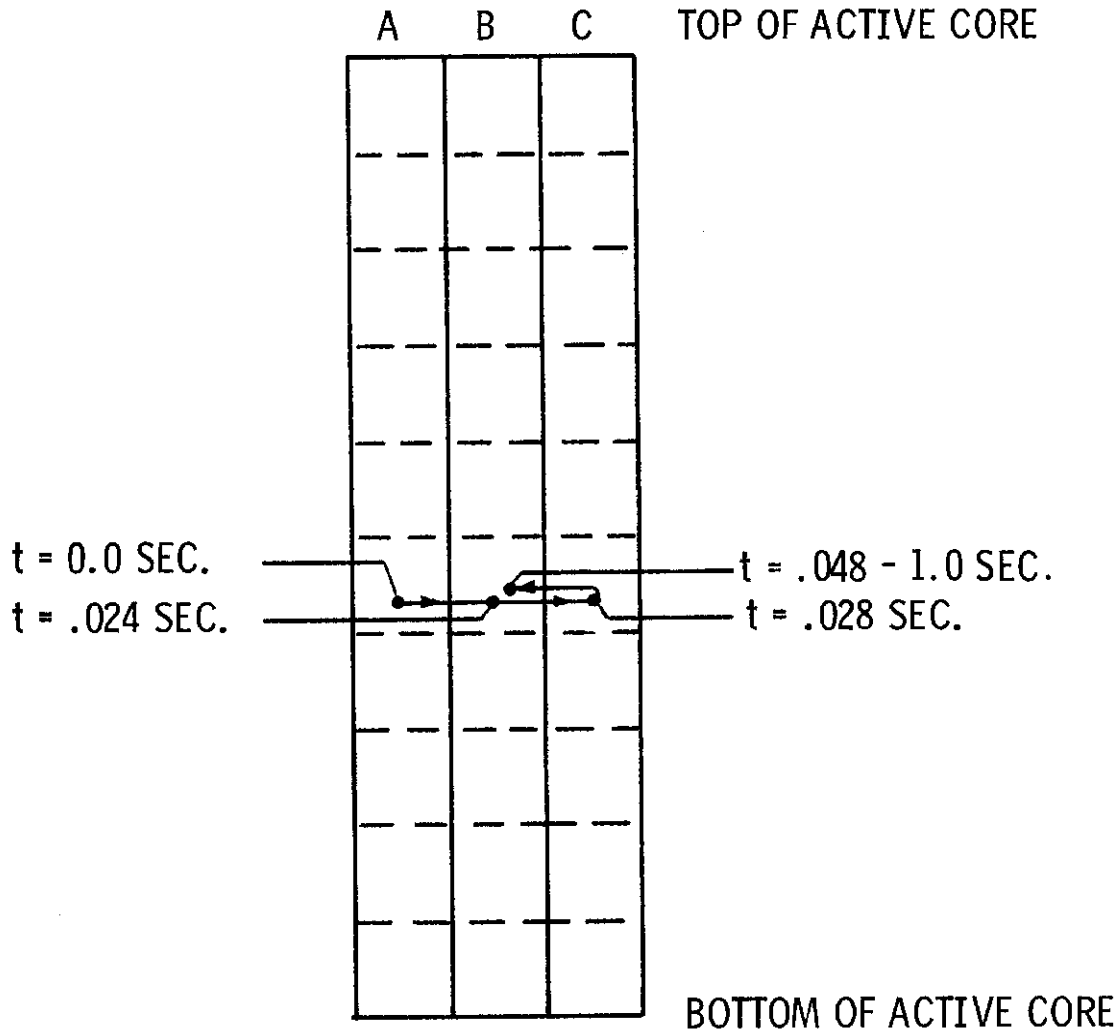

HERMITE CENPD-188	3D FULL POWER CEA EJECTION TRANSIENT, LOCATION OF MAXIMUM NODE POWER	Figure 5-9

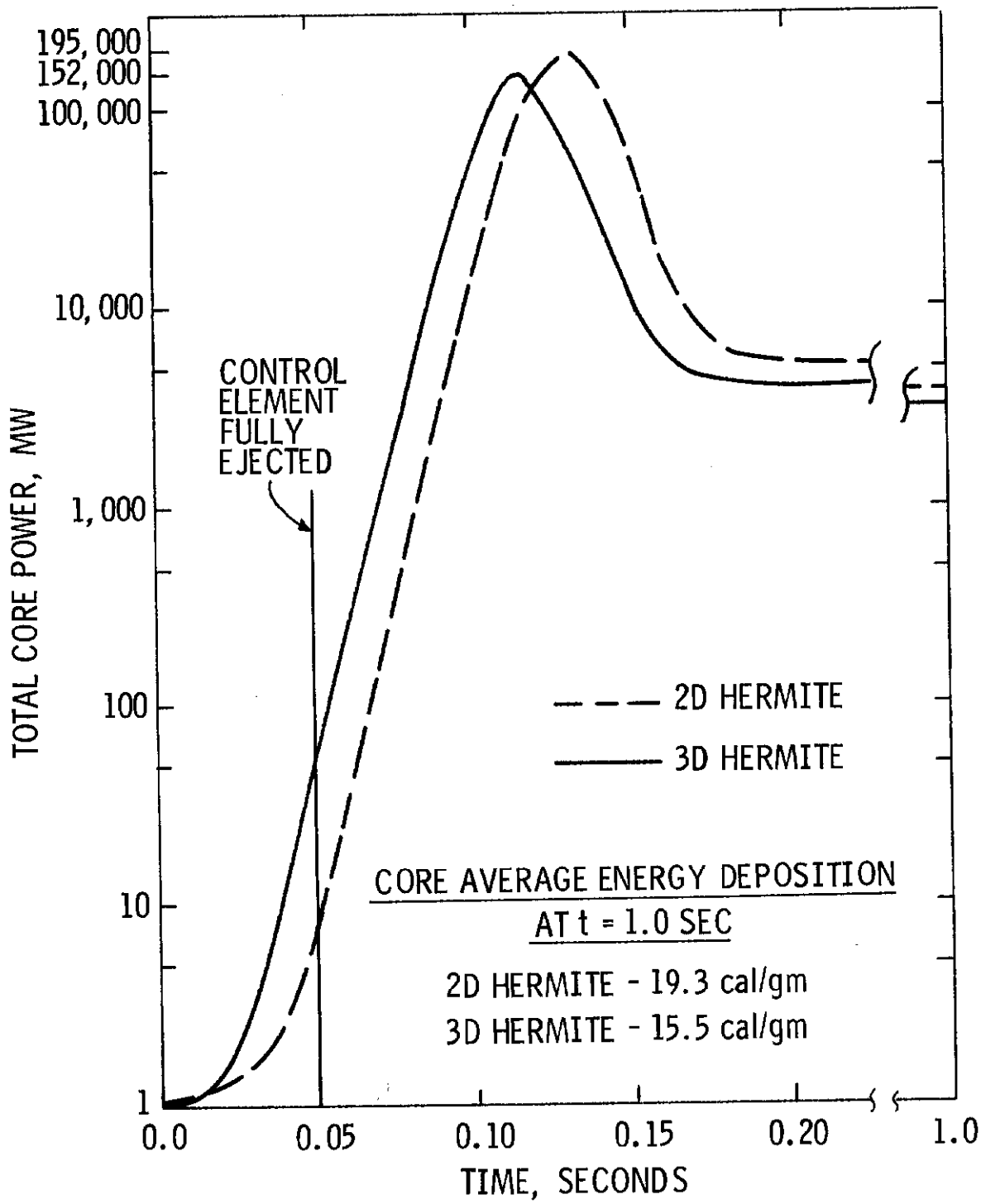

HERMITE CENPD- 188	ZERO POWER CEA EJECTION TRANSIENT, TOTAL CORE POWER	Figure 5-10

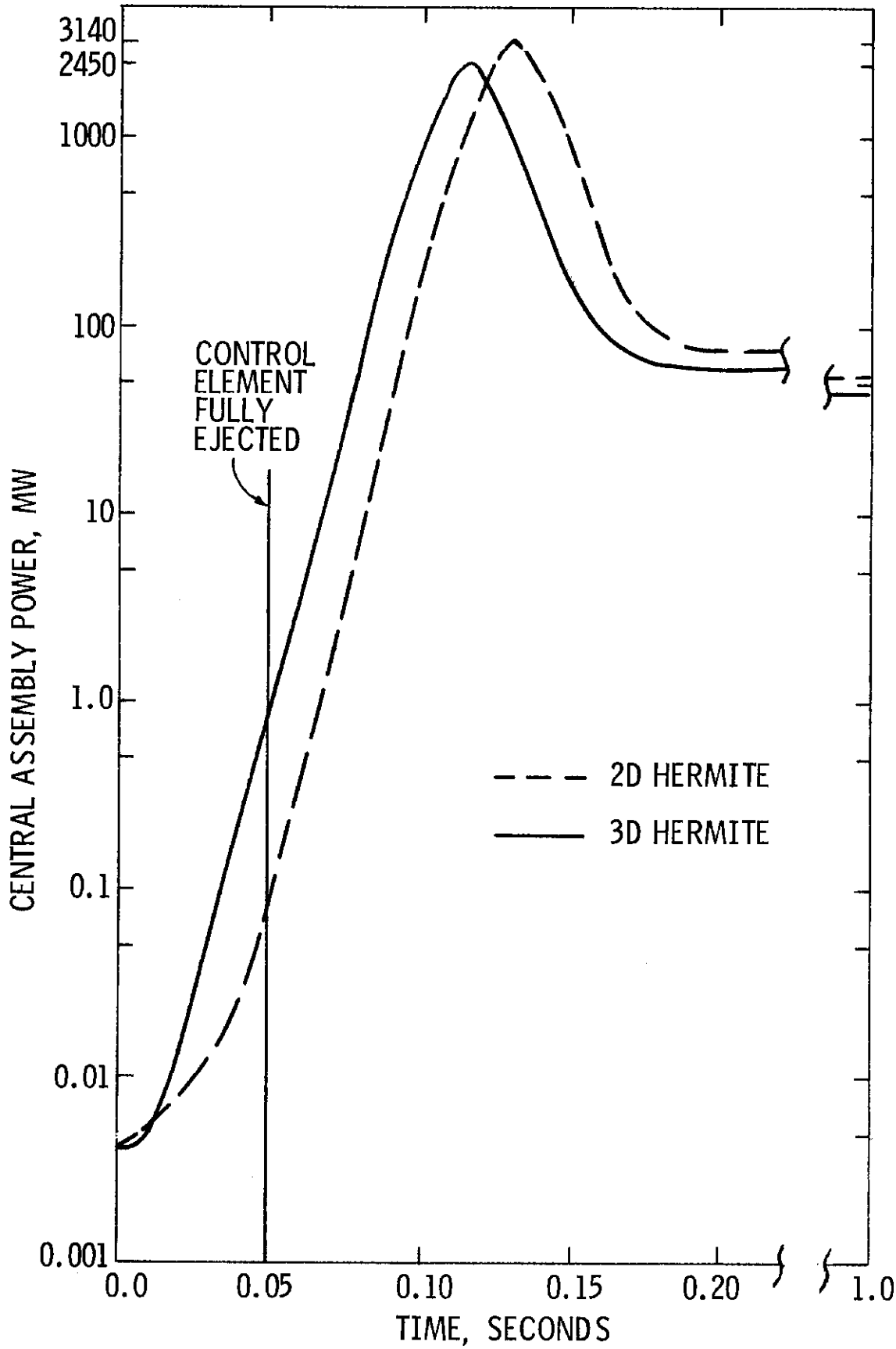

HERMITE CENPD-188	ZERO POWER CEA EJECTION TRANSIENT, CENTRAL ASSEMBLY POWER	Figure 5-11

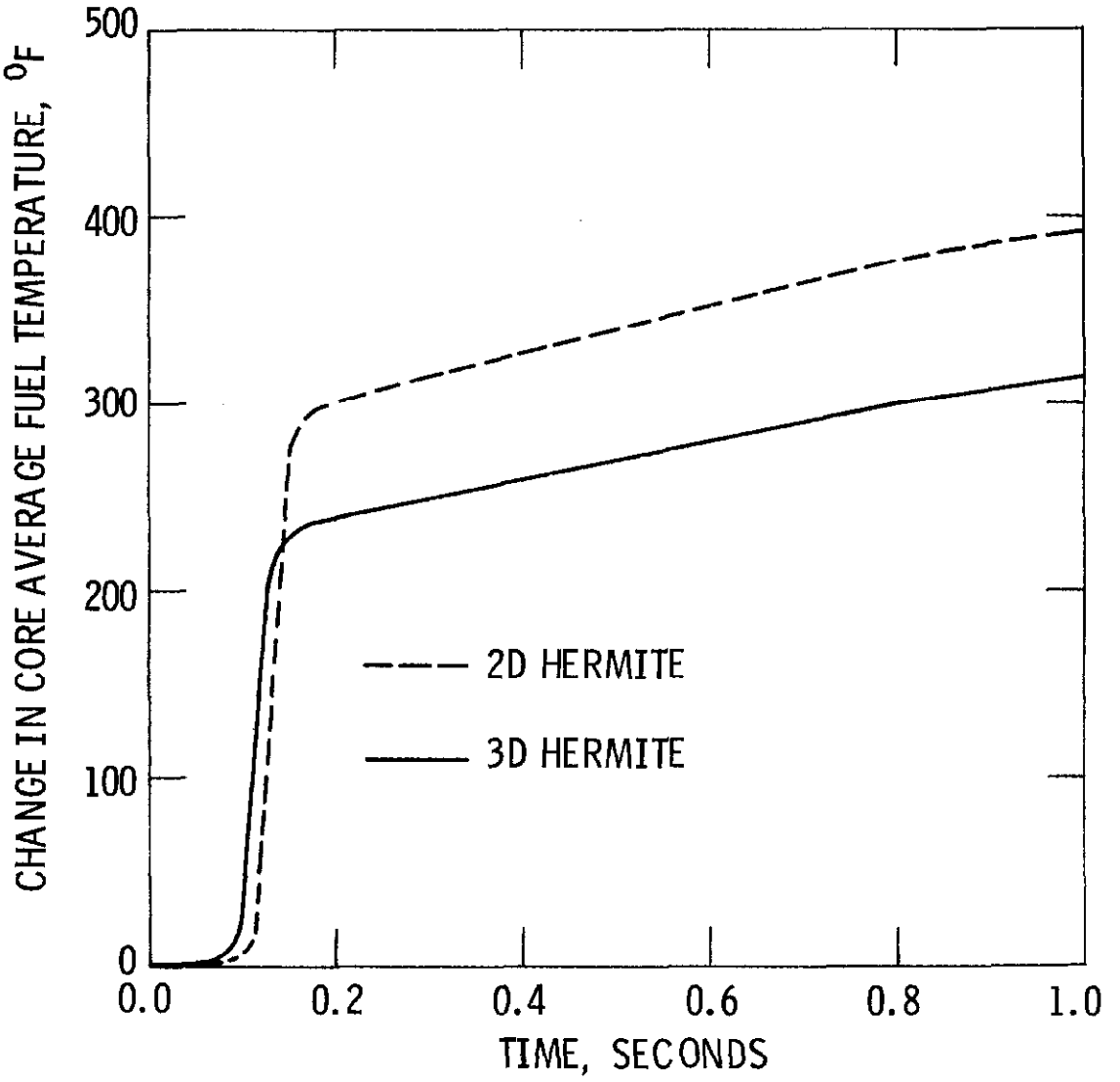

HERMITE CENPD-188	ZERO POWER CEA EJECTION TRANSIENT, CORE AVERAGE FUEL TEMPERATURE	Figure 5-12

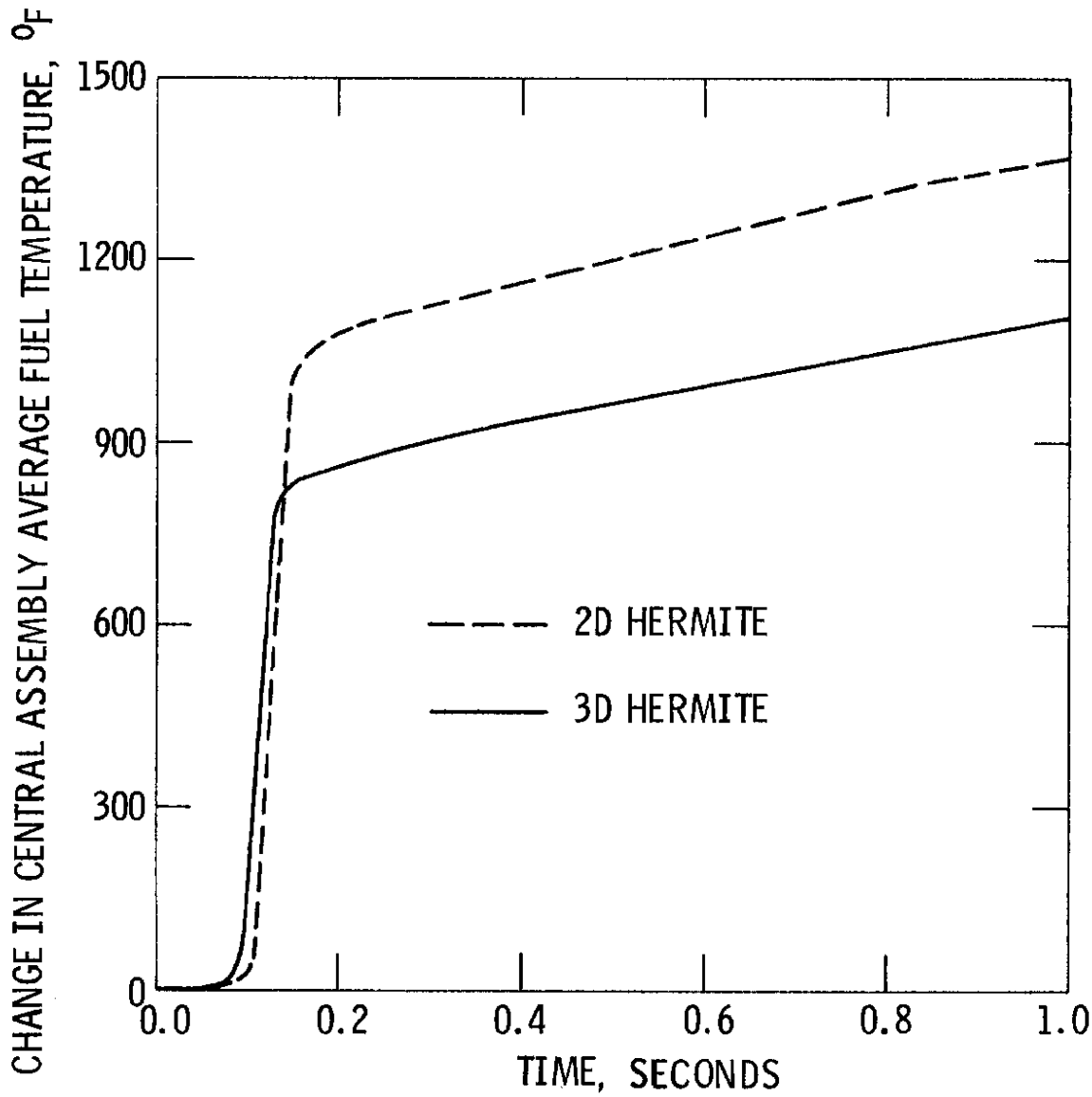

HERMITE CENPD-188	ZERO POWER CEA EJECTION TRANSIENT, CENTRAL ASSEMBLY AVERAGE FUEL TEMPERATURE	Figure 5-13

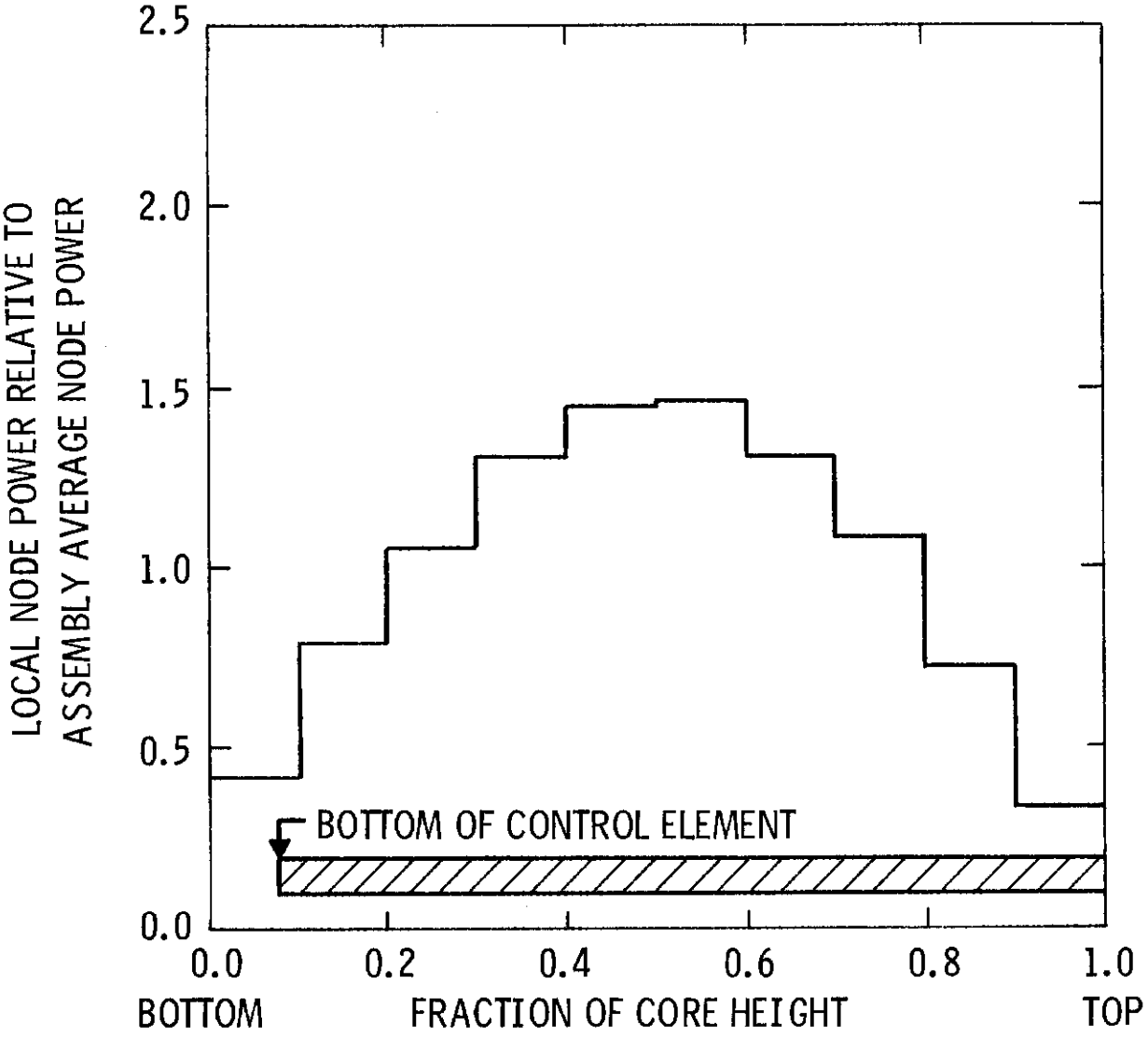

HERMITE CENPD-188	ZERO POWER CEA EJECTION TRANSIENT, CENTRAL ASSEMBLY POWER DISTRIBUTION AT t = 0.004 SECONDS	Figure 5-14

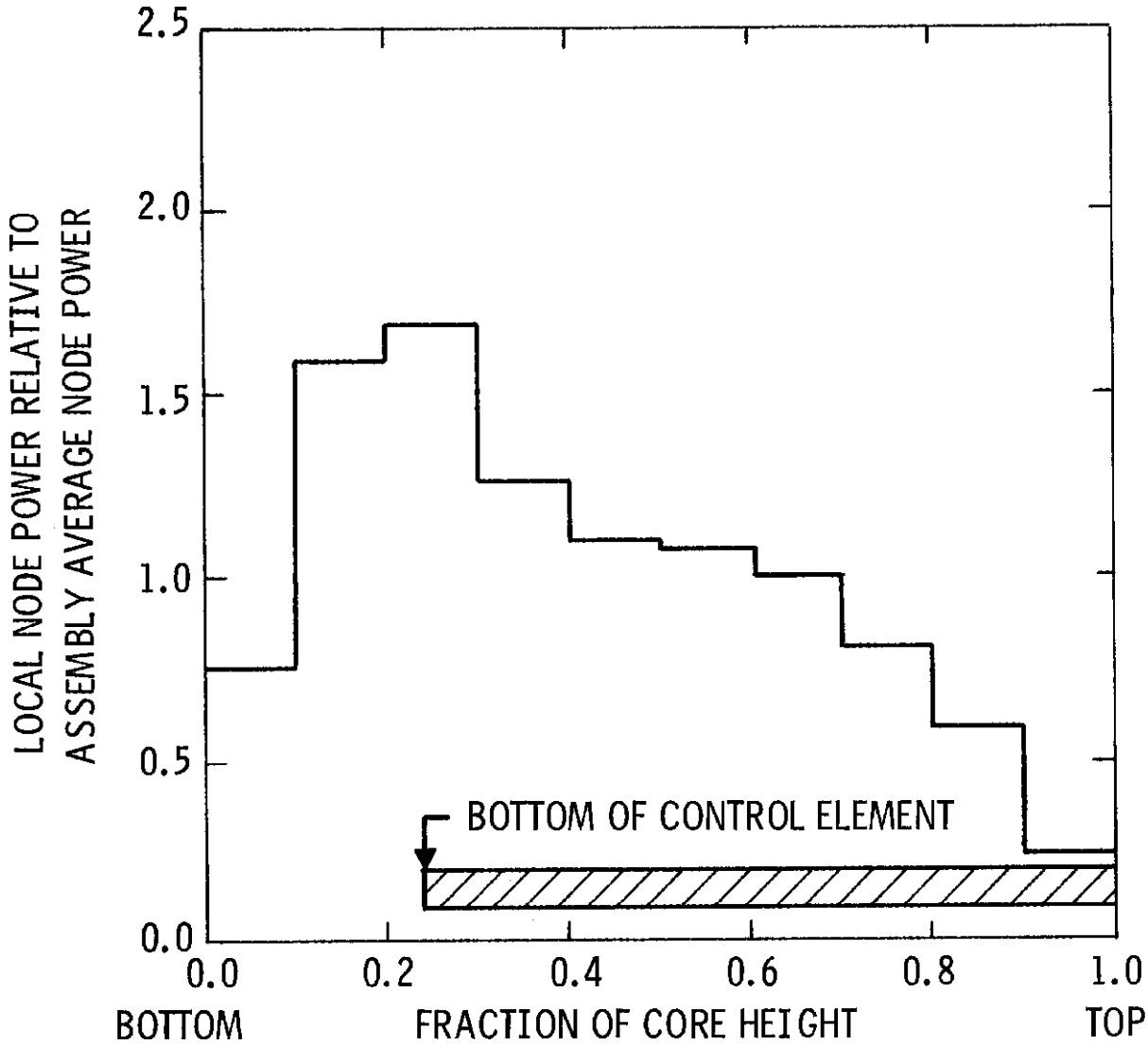

HERMITE CENPD-188	ZERO POWER CEA EJECTION TRANSIENT, CENTRAL ASSEMBLY POWER DISTRIBUTION AT t = 0.012 SECONDS	Figure 5-15

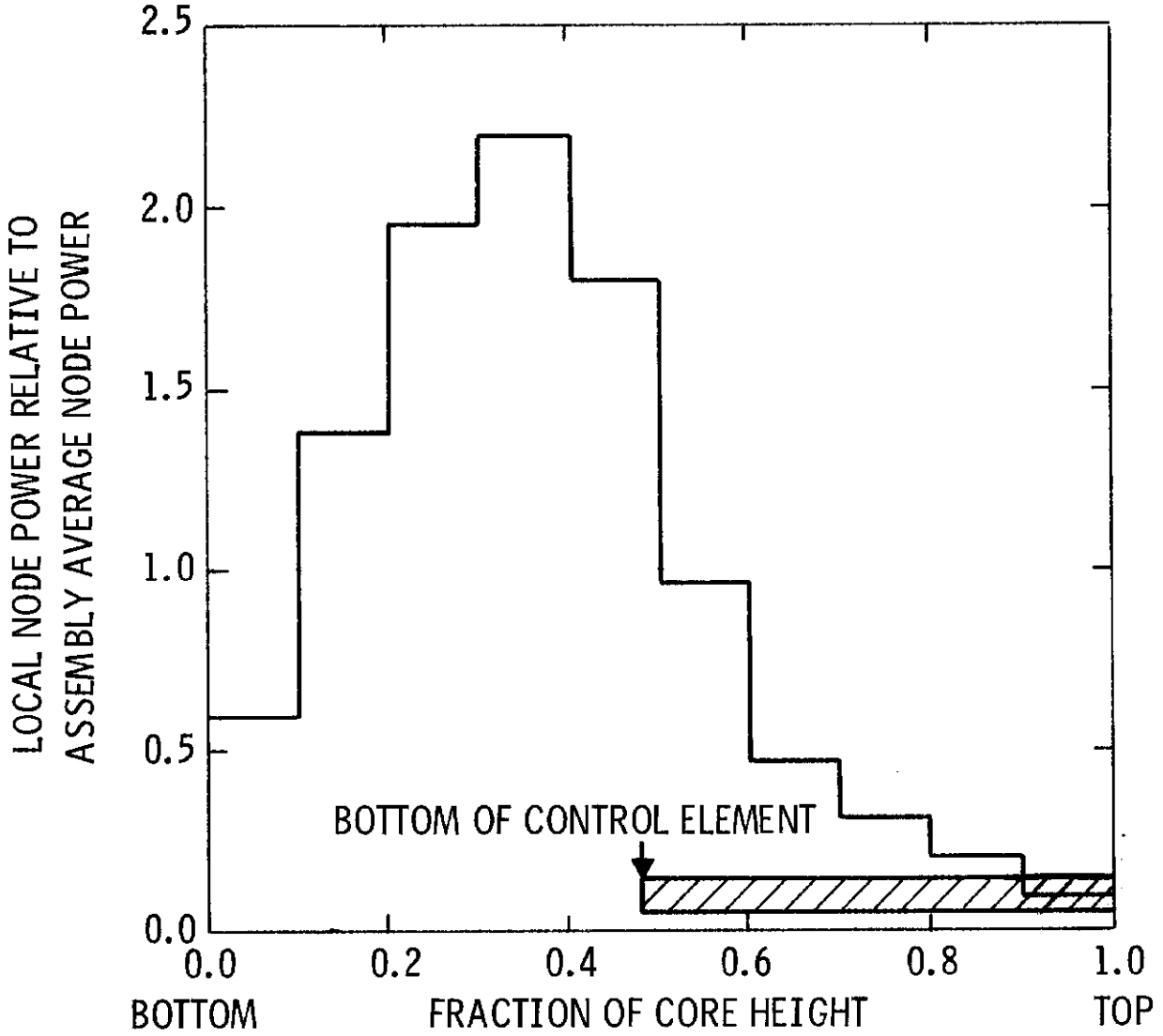

HERMITE CENPD-188	ZERO POWER CEA EJECTION TRANSIENT, CENTRAL ASSEMBLY POWER DISTRIBUTION AT t = 0.024 SECONDS	Figure 5-16

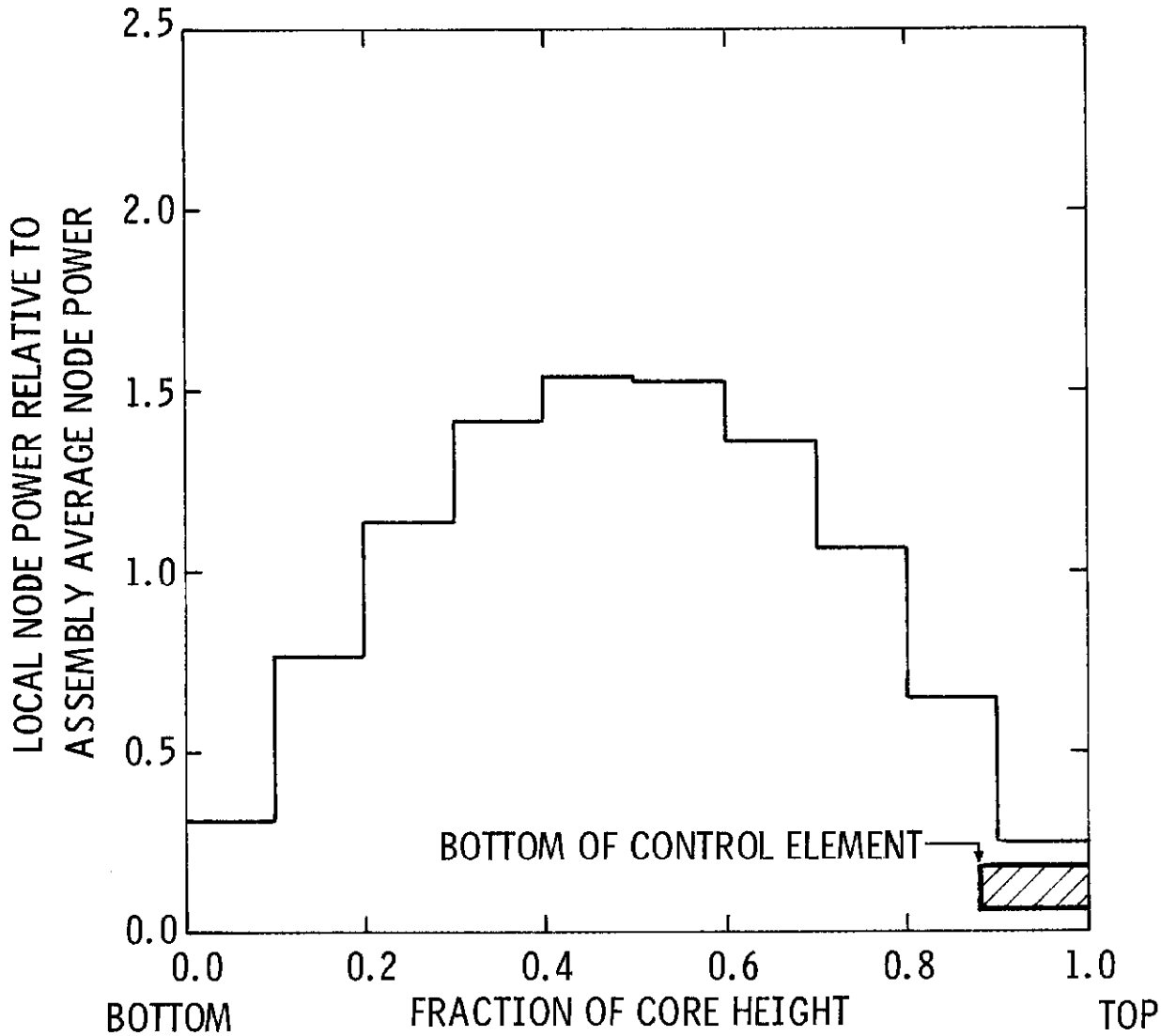

HERMITE CENPD-188	ZERO POWER CEA EJECTION TRANSIENT, CENTRAL ASSEMBLY POWER DISTRIBUTION AT t = 0.044 SECONDS	Figure 5-17

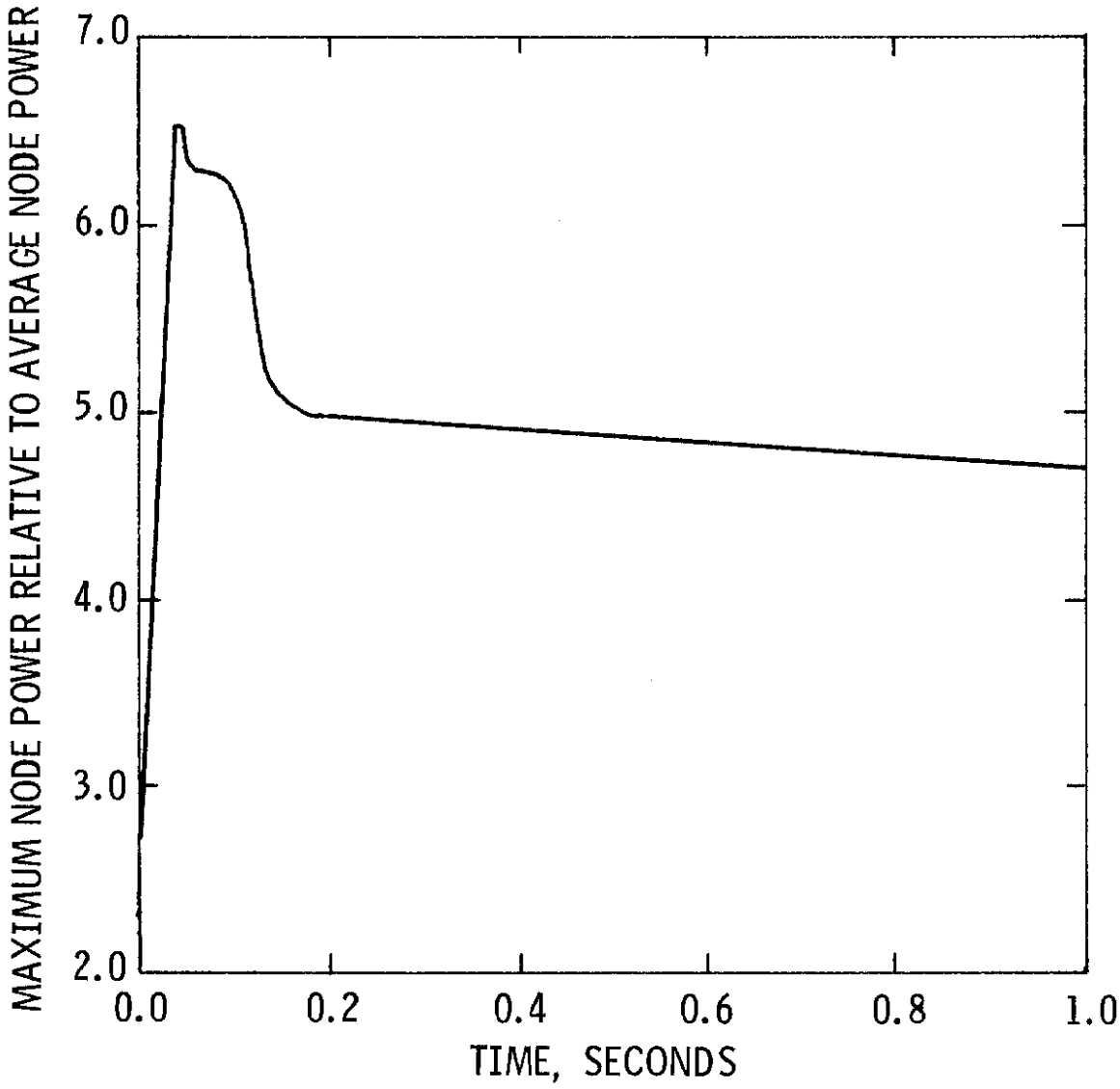

HERMITE CENPD-188	3D ZERO POWER CEA EJECTION TRANSIENT, MAXIMUM NODE POWER RELATIVE TO AVERAGE NODE POWER	Figure 5-18

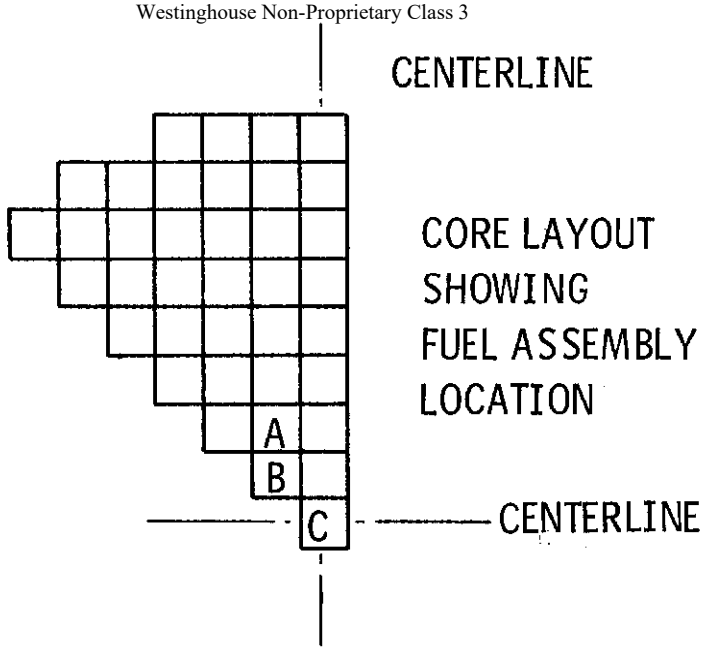

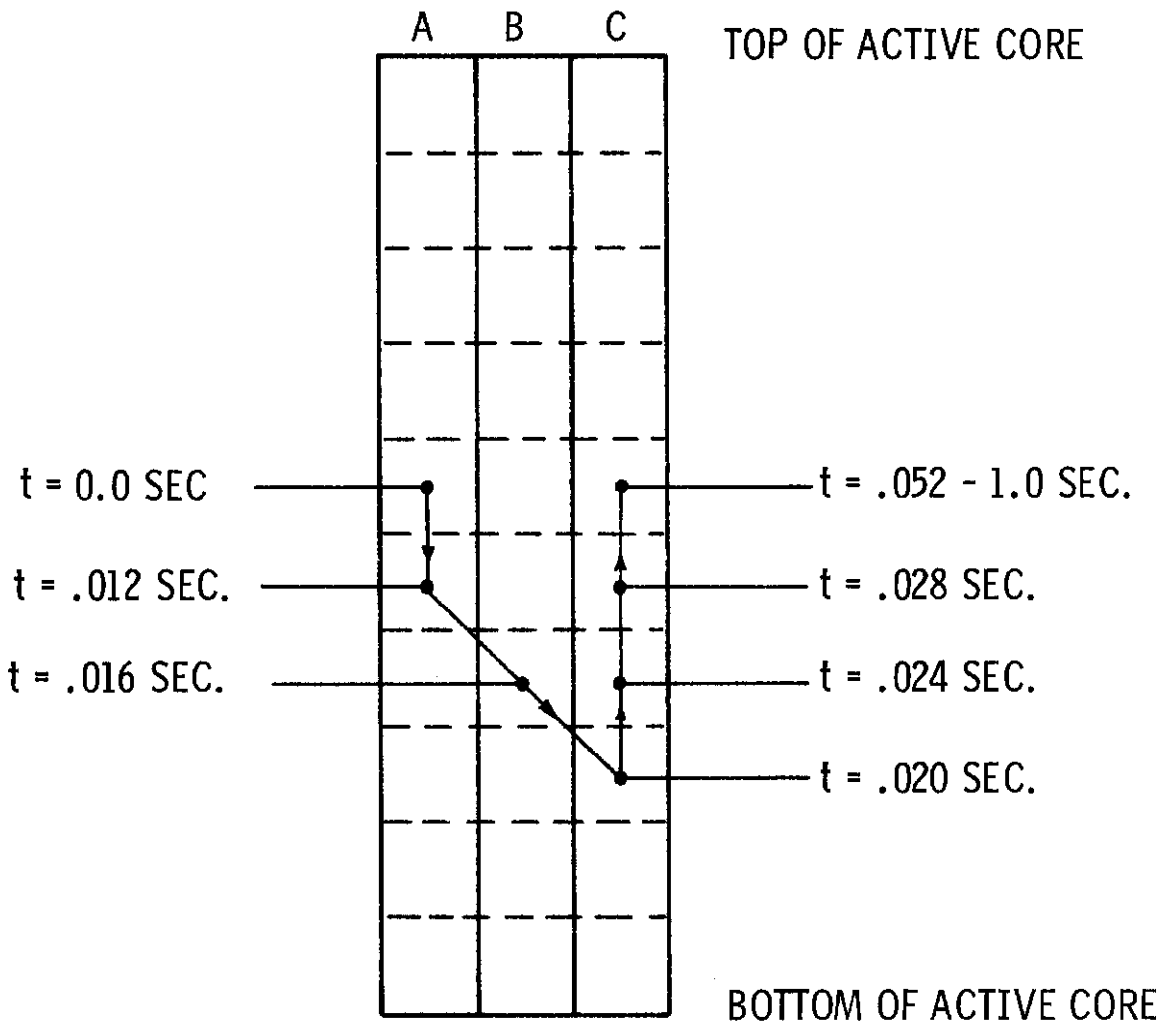

HERMITE CENPD-188	3D ZERO POWER CEA EJECTION TRANSIENT, LOCATION OF MAXIMUM NODE POWER	Figure 5-19

6.0 NOMENCLATURE

6.1 NEUTRONICS AND CROSS SECTION NOMENCLATURE FOR SECTIONS 2.1 AND 2.3

Symbol	Definition
A_g	Matrix solved by inner iterations
$\underline{C}_{n,o}$	Equilibrium delayed neutron precursor concentration (cm^{-3})
D_g	Diffusion coefficient for energy group g (cm)
$\mathcal{D}_g$	Tridiagonal submatrix of A_g
F	Transient fission matrix including inverse of steady state eigenvalue, λ
F_g	Group g submatrix of F
$\hat{F}$	Steady state fission matrix
$\hat{F}_g$	Group g submatrix of $\hat{F}$
g	Neutron energy group index
g_j	g - factor multiplier for σ_j
g_j^n	g - factor multiplier for $\delta\sigma_j^n$
G	Number of neutron energy groups
I	Number of mesh points in the x-direction
j	Isotopic species index
J	Number of mesh points in the y-direction
$\underline{k}_g$	Right hand side of equation solved by inner iterations
K	Number of mesh points in the z-direction
ℓ	Inner iteration index
L	Number of inner iterations (superscript)
L	Diffusion coefficient and total cross section matrix
L_g	Group g submatrix of L
$\mathcal{L}_g$	Lower triangular submatrix of A_g
m	Outer iteration index (superscript)

Symbol	Definition
m	Spatial basis function index (supscript)
M	Number of outer iterations (superscript)
M	Number of spatial basis functions (subscript)
n	Delayed neutron precursor group index
N	Number of delayed neutron precursor groups
N_j	Number density for isotopic species j (atoms/barn-cm)
p	Time step index
$\underline{r}$	Position vector in a rectangular coordinate system
$\underline{r}_I$	Position vector denoting interface points in the region of solution
$\underline{r}_s$	Position vector denoting surface points on the region of solution
R	Region of solution
S	Removal cross section matrix
S_g	Submatrix of S for removal from energy group g to energy group g + 1
$\underline{S}_{p,n}$	Effective initial delayed neutron precursor concentration vector for precursor group n at time t_p
t	Time (sec)
t_p	Time point p (sec)
u_i	x-direction spatial basis function
u_j	y-direction spatial basis function
u_k	z-direction spatial basis function
u_m	Spatial basis function, $u_m = u_i \cdot u_j \cdot u_k$
u_p	Temporal basis function
v	Test function for weak form of diffusion equation
v_g	Neutron velocity for energy group g (cm/sec)
V	Inverse neutron velocity matrix
U_g	Upper triangular submatrix of A_g

Symbol	Definition
X_n	One of the parameters (fuel temperature, moderator temperature, moderator density) used to modify cross sections
$X_{n,ref}$	Reference value of X_n
α_p	Coefficient of $F(t_p)\underline{\Psi}(t_p)$ in discrete diffusion equations
β	Total delayed neutron fraction
β_n	Delayed neutron fraction for precursor group n
γ_p	Coefficient of $F(t_p)\underline{\Psi}(t_{p+1})$ in discrete diffusion equation
$\delta\sigma_j^n$	Coefficient of ΔX_n in adjusting σ_j for feedback variable X_n
ΔX_n	Deviation of feedback variable X_n from input reference value $= X_n - X_{n,ref}$
$\varepsilon_{p,n}$	Coefficient of $F(t_{p-1})\underline{\Psi}(t_p)$ contribution to $\underline{S}_{p,n}$
κ_g	Average energy released per fission for neutron energy group g (watt-sec)
λ	Steady state eigenvalue
λ_n	Decay constant for delayed neutron precursor group n (sec^{-1})
$\mu_{p,n}$	Coefficient of $F(t_{p-1})\underline{\Psi}(t_{p-1})$ contribution to $\underline{S}_{p,n}$
ν_g	Average number of neutrons released per fission caused by neutrons in energy group g
σ_j	Microscopic cross section for isotope j (barns)
Σ	$\Sigma^f, \Sigma^r, \Sigma^T$ or Σ^{tr}-- general macroscopic cross section
Σ_g^f	Macroscopic fission cross section (cm^{-1}) for group g
Σ_g^r	Macroscopic removal cross section from group g to group g + 1 (cm^{-1})
Σ_g^T	Macroscopic total cross section (cm^{-1})
Σ_g^{tr}	Macroscopic transport cross section (cm^{-1}) = $1/(3D_g)$
χ_g	Fraction of neutrons released by fission and precursor decay into group g

Symbol	Definition
Ψ_g	Group g neutron flux ($cm^{-2}sec^{-1}$)
$\Psi_{g,m}$	Group g neutron flux at point m ($cm^{-2}sec^{-1}$)
$\underline{\Psi}$	Flux vector made up of all $\Psi_{g,m}$'s
$\underline{\Psi}_g$	Group g component of $\underline{\Psi}$
ω	Successive over-relaxation parameter

6.2 THERMAL-HYDRAULIC NOMENCLATURE FOR SECTION 2.2

Symbol	Definition
A	Flow area of a thermal-hydraulic channel (ft^2)
a_1, a_2	Coefficients in linear equation relating q''_w to T_w for fuel pin during transient
C_p	Specific heat capacity (Btu/lbm-°F)
$C_{p,UO2}$	Fuel pellet specific heat capacity (Btu/lbm-°F)
$C_{p,Zr}$	Clad specific heat capacity (Btu/lbm-°F)
$C_1,\ldots,C_4$	Coefficients for fuel temperature correlations
D	Hydraulic diameter (ft)
FS	Denotes fuel pellet outside surface (may be substituted for j where j is used as a subscript)
G	Mass velocity ($lbm/hr\text{-}ft^2$)
G_{inlet}	Inlet mass velocity ($lbm/hr\text{-}ft^2$)
h	Specific enthalpy (Btu/lbm)
h_B	Specific enthalpy of average or bulk coolant in a thermal hydraulic node (Btu/lbm)
h_{DB}	Dittus-Boelter heat transfer coefficient ($Btu/hr\text{-}ft^2\text{-}°F$)
h_f	Specific enthalpy of saturated liquid (Btu/lbm)
h_g	Specific enthalpy of saturated vapor (Btu/lbm)

Symbol	Definition
h_{gap}	Gap conductance (Btu/hr-ft^2-°F)
IC	Denotes inside clad surface (may be substituted for j where j is used as a subscript)
j	Index of radial mesh point in fuel pin
k	Fuel pin conductivity (Btu/hr-ft-°F)
k_B	Coolant conductivity at h_B (Btu/hr-ft-°F)
k_{j+}	Average conductivity between r_j and r_{j+1} (Btu/hr-ft-°F)
k_{j-}	Average conductivity between r_j and r_{j-1} (Btu/hr-ft-°F)
n	Time step index
N_{pins}	Number of fuel pins in a thermal-hydraulic channel
P	Pressure (psia)
Pr_B	Prandtl number at h_B
Q	Power generated in a thermal-hydraulic node (Btu/hr)
q'	Linear heat reate per fuel pin (Btu/hr-ft)
q"	Heat flux (Btu/hr-ft^2)
q''_{j-}	q" at r_{j-} (Btu/hr-ft^2)
q''_{j+}	q" at r_{j+} (Btu/hr-ft^2)
q'''	Volumetric heat generation rate in fuel pellet or coolant (Btu/hr-ft^3)
q'''_j	Average q''' for radial region j of fuel pin (Btu/hr-ft^3)
r	Radius from centerline of fuel pin (ft)
r_j	Radius of radial mesh point j in fuel pin (ft)
r_{j-},r_{j+}	Inner and outer radii of radial region j in fuel pin (ft)
R	Coolant mesh transport factor, $G\Delta t/(\rho\Delta z)$
R_c	Fraction of heat deposited directly in coolant

Symbol	Definition
Re_B	Reynolds number at h_B
t	Time (hr)
t_n	Time point n (hr)
T	Temperature (°F)
T_B	Temperature at h_B (°F)
T_{FUEL}	Average fuel temperature (°F)
T_j	Temperature at r_j in fuel pin (°F)
T_{sat}	Temperature of saturated water (°F)
v	Specific volume of coolant (ft^3/lbm)
v_g	Specific volume of saturated vapor (ft^3/lbm)
v_f	Specific volume of saturated liquid (ft^3/lbm)
V_j	Area of radial region j (ft^2)
V_{j-},V_{j+}	Area for region between r_{j-} or r_{j+} and r_j (ft^2)
w	Denotes clad-coolant surface or "wall" (may be substituted for j where j is used as a subscript)
α	Void fraction
γ	Slip ratio
Δt	Length of a time step, $t_n - t_{n-1}$ (hr)
Δz	Height of a thermal-hydraulic node, $z_k - z_{k-1}$ (ft)
ε_{TF}	Fuel temperature convergence criterion
η	$(z - z_{k-1})/\Delta z$
μ	Viscosity (lbm/ft-hr)
ρ	Density (ρ_c, ρ_{UO2}, or ρ_{Zr} depending on application)
ρ_B	Coolant density at h_B (lbm/ft^3)
ρ_c	Coolant density (lbm/ft^3)

Symbol	Definition
ρ_{UO2}	Fuel pellet stack height density (lbm/ft^3)
ρ_{Zr}	Cladding density (lbm/ft^3)
τ	$(t - t_{n-1})/\Delta t$

APPENDIX A

HERMITE Input Description

HERMITE INPUT DESCRIPTION

TABLE OF CONTENTS

Section		Title	Page
A1.0	INTRODUCTION		A1-1
A2.0	JOB CONTROL CARDS		A2-1
A3.0	GENERAL INFORMATION ON INPUT CARD FORMATS		A3-1
A4.0	BASIC CONTROL DATA		A4-1
A5.0	TRANSIENT DATA		A5-1
	A5.1	Basic Transient Data	A5-1
	A5.2	Transient Program Control	A5-2
	A5.3	Transient Iteration Control	A5-3
	A5.4	Feedback Override Cards	A5-3
A6.0	GEOMETRY DATA		A6-1
	A6.1	Regions of Solution	A6-1
	A6.2	Mesh Overlay Description	A6-2
	A6.3	Finite Element Mesh	A6-4
	A6.4	Geometry Example	A6-4
	A6.5	Basic Geometry Data	A6-5
	A6.6	Mesh Interval Data	A6-5
	A6.7	Overlay Data	A6-6
	A6.8	Composition Data	A6-8
	A6.9	Finite Element Boundaries	A6-9
A7.0	CROSS SECTION DATA		A7-1
	A7.1	Cross Section Model	A7-1
	A7.2	Nuclide Identification	A7-4
	A7.3	Table Sets and Compositions	A7-4
	A7.4	Cross Section Forms	A7-5

HERMITE INPUT DESCRIPTION
TABLE OF CONTENTS (Continued)

Section		Title	Page
	A7.5	Nuclide Identification Data	A7-6
	A7.6	Table Set (Composition) Identification Data	A7-7
	A7.7	Initial Number Densities	A7-8
	A7.8	Master Microscopic Tables	A7-9
	A7.9	Mask-Function Table Assignment	A7-9
	A7.10	Mask Description	A7-9
	A7.11	Function Tables	A7-11
A8.0	CONTROL ROD DATA		A8-1
	A8.1	Basic Control Rod Data	A8-2
	A8.2	Control Rod Geometry Data	A8-4
A9.0	EDIT CONTROL DATA		A9-1
A10.0	THERMAL-HYDRAULIC DATA		A10-1
A11.0	INPUT AND OUTPUT FILES		A11-1
A12.0	PLOT FILE CONTROL DATA		A12-1
A13.0	RESTART CAPABILITIES		A13-1

LIST OF TABLES

Table	Title	Page
A2-1	SCOPE Control Statements for Running HERMITE	A2-3
A2-2	Account Card Description	A2-4
A3-1	Summary of Input Card Formats	A3-4
A5-1	Transient Program Control Cards	A5-5

LIST OF FIGURES

Figure	Title	Page
A6-1	Sample of Mesh and Region of Solution	A6-10
A6-2	Sample Basic Figure with Planar Region Overlay	A6-11
A6-3	Rotational Orientation of a Sample Basic Figure	A6-12
A6-4	Rotational Orientations of a Reflected Sample Basic Figure	A6-13
A6-5	Sample Core Layout for Geometry Example	A6-14
A6-6	Geometry Example with Mesh Points	A6-15
A6-7	Initial Figures Required for Geometry Example	A6-16

A1.0 INTRODUCTION

As the size of large power reactors increases, space-time effects during reactor transients become more important. In order not to penalize reactor performance unduly by overly conservative design methods, it is desirable to have the capability of performing detailed space-time neutronics calculations for both design and off-design transients.

The HERMITE computer code has been developed to meet this objective. It solves the few-group, space and time dependent neutron diffusion equation including the feedback effects of fuel temperature, coolant temperature, coolant density and control rod motion. The static and dynamic neutronics equations are solved by means of a finite element method. The fuel temperature model explicitly represents the pellet, gap and clad regions of the fuel pin and solves the governing heat conduction equations by a finite difference method. Continuity and energy conservation equations are solved in order to determine the coolant temperature and density.

This input description gives detailed input preparation instructions for the code.

A2.0 JOB CONTROL CARDS

Table A2-1 shows a typical setup for a HERMITE job run on the CDC 7600 under the SCOPE operating system. The first card is the job identification card. The time limit in octal seconds and the priority must be filled in by the user. In addition to the normal priorities (P40, daytime; P30, overnight; and P20, weekend), two special priorities are recognized. P00 causes the job to run under standalone conditions, i.e. no other jobs running. P10 causes the code to enter a monoprogramming mode after input processing. This mode is similar to standalone but allows additional storage in large core memory (LCM).

The ACCOUNT card is completed in accordance with Table A2-2.

The USER card is optional unless data files are being saved. Its use on all cases is highly recommended, however, because the user name, if supplied, is printed at the top of every page of output.

SWITCH cards are optional and are described in Table A2-1.

The RFL card specifies small core memory (SCM) octal field length and is required. If insufficient field length is specified, the code will abort with an error message of the form

```
***ERROR NUMBER XX FROM SUBROUTINE LOCATE
```

where XX is 21, 27, 30, 34, or 47. These messages indicate that the code cannot find room in SCM for one of its arrays or buffers.

The HERMITE card places HERMITE into execution. The following variations may be useful:

```
HERMITE(INFIL)
HERMITE(,FILMPR)
HERMITE(INFIL,FILMPL)
```

In the first case, input cards are read from a file named INFIL which has been attached or created earlier in the job. No input cards should appear in the deck. In the second case, output is written on microfilm. The comma shown is required. In the last case input is read from INFIL and output is written to microfiche.

If any further processing is required the following card should come after the HERMITE card:

```
REDUCE.
```

This card releases the SCM required to run HERMITE.

Table A2-1

SCOPE Control Statements For Running HERMITE

```
NUXXX,CP70,R76,T---,P---.
ACCOUNT(---)
ATTACH(HERMITE)   PERMANENT FILE CONTAINING HERMITE PROGRAM IN ABSOLUTE FORM
USER(---)         1 TO 7 CHARACTER USER NAME
SWITCH(2)         OPTIONAL--TERMINATION AFTER INPUT CHECK
SWITCH(4)         OPTIONAL--CAUSES DAYFILE MESSAGE WHEN OVERLAYS LOADED
SWITCH(6)         OPTIONAL--DESTROYS OUTPUT AFTER OK INPUT CHECK (DEBUGGING USE ONLY)
RFL(120000)       CORE STORAGE ALLOCATION NEEDED FOR SMALL (21X21) 2-D PROBLEM.
HERMITE.
7/8/9             END OF SECTION CARD (MULTIPUNCH 7,8,9, IN COLUMN 1)
Input Cards.
6/7/8/9           END OF INFORMATION CARD (MULTIPUNCH 6,7,8,9 IN COLUMN 1)
```

Table A2-2

Account Card Description

The Account Card for jobs running HERMITE on the 7600 should be prepared in the following manner:

Columns 1-9	ACCOUNT($
Columns 10-13	A valid division number;
Columns 14-17	Cost center; right-justified, zero-filled
Columns 18-19	Section; right-justified, zero-filled
Columns 20-21	00
Columns 22-29	Contract or project number; right-justified, zero-filled. (All zeroes for division 0009)
Columns 30-39	Task or component number; right-justified, zero-filled
Columns 40-41	00
Columns 42-48	Code name; left-justified: HERMITE
Columns 49-58	Requestor's name; left-justified
Columns 59-60	$)

A3.0 GENERAL INFORMATION ON INPUT CARD FORMATS

All input cards are listed in the printed output. Columns 1-8 of these cards are ignored and may be used for identification purposes. Additional comment information may follow the data on any card if a dollar sign ($) is punched between the last data item and the comment. An asterisk (*) in column 9 denotes a card containing only comments. An input deck should contain a title card denoted by an equal sign (=) in column 9. The information on this card is used to title each page of printed output. If more than one title card is present, the last such card is used. Blank cards in the input deck are ignored.

Columns 9-14 of data cards must contain a six-digit card number, followed by a comma in column 15. The card number consists of a series number (one or two digits), a subseries number (zero to four digits), and a sequence number (remaining digits). The series and subseries numbers identify the type of data on the card; the sequence number begins at 1 for each subseries.

Data cards are divided into fields of arbitrary length, with the fields separated by commas and a comma following the last field optional. Each field contains either an integer number, a floating-point number, or an alphanumeric item. Leading and trailing blanks are ignored in all fields, and imbedded blanks are ignored in numeric fields. Data cards may be continued by placing a plus sign (+) in column 9 of the continuation card(s) followed by a comma and the data fields.

The integer format is

$$\pm xx...xx$$

and the floating-point format is

$$\pm xx...xx\pm yy,$$

where the leading sign may be dropped if it is plus and where each x and y is a decimal digit (0-9) or a blank. In the floating-point format the decimal point is assumed to precede the fractional part or may be included anywhere in the

xx...xx field. The signed one- or two-digit exponent is required unless a decimal point is present. A field is alphanumeric if it contains at least one character which is not one of the following: +, -, ·, 0, 1, 2, 3, 4, 5, 6, 7, 8, 9 or blank. A field can be forced to be interpreted as alphanumeric by enclosing it with the begin- and end-hollerith indicators. These are the left and right parentheses, respectively. Note that all input described in this manual is integer unless floating-point or alphanumeric is explicitly indicated.

Several different types of input are specified in expansion format. This format consists of sets of data. Each set consists of a fixed number of floating-point numbers followed by an integer. The floating-point numbers are the parameters to be expanded and the integer is the termination point for the expansion. The expansion begins at the termination point of the previous set and continues to the termination point of the current set. These termination points are generally composition numbers or mesh point numbers and always form a strictly increasing sequence. Mesh intervals, for example, are specified in the form

$$M_1,p_1,M_2,p_2,\ldots .$$

Here M_1 is associated with each of the intervals between points 0 and p_1, and M_2 with each of the intervals between points p_1 and p_2.

Any field may be repeated by having as the first non-blank part of the character string in a field the sequence: (1) left-repeat indicator, which is a slash (/), (2) integer equal to the number of repeats, and (3) right-repeat indicator, which is a second slash (/). If the integer is negative or zero, an error message is printed. The "field" to be repeated is the remainder of the field past the right-repeat indicator. For example,

```
701071,/3/1.0,2.0
```

is equivalent to

```
701071,1.0,1.0,1.0,2.0
```

The number of data fields may vary from card to card in any series or subseries. If the data consists of sets of numbers, however, each card must contain an integral number of sets. In general, the input data cards may appear in any order. If two or more cards have the same card number, however, only the last of these cards is retained. If this last card contains no data, it also is not retained, and the comma following the card number on such a card is optional. This has the effect of deleting that card from the deck.

Each job must be terminated by an end-of-input card. This card has a period in column 9.

Table A3-1 summarizes the above information.

TABLE A3-1

Summary of Input Card Formats

Item	Columns	Description
nnnnnn	9-14	Six digit data card number (followed by comma)
=	9	Title Card
*	9	Comment Card
+	9	Data card continuation
.	9	End of input data
,		Field separator
$		End of data fields, comments follow
±xx...xx		Integer field
±xx...xx±yy		Floating point field -Decimal point in xx...xx field, optional -±yy exponent, optional if decimal point present -Decimal point assumed before xx...xx field if missing
( )		Enclose alphanumeric field. Parentheses optional if field contains non-numeric information.
/nn...nn/		Precedes field to indicate repetition nn...nn times

A4.0 BASIC CONTROL DATA

010000,IC(1),IC(2),...,IC(11)

IC(I)	Value	Meaning
1	0/1/2/3	Steady-state only/steady-state and transient/ transient only/restart transient already in progress.
2	0	Not used.
3	0/1	Neutronics only/neutronics and thermal-hydraulics.
4	0	Not used.
5	--	Number of inner iterations per outer iteration.
6	--	Number of steady-state outer iterations (ignored if IC(3) = 1. Outer iterations are controlled by card 010030 and MXTHSS from card 010016).
7	--	Number of transient outer iterations before successive over-relaxation used on inner iterations.
8	0/1	No/Yes Volume weighted input cross section edit.
9	0	Not used.
10	0/1	No/Yes Steady-state power fraction edit.
11	--	Number of steady-state outer iterations before successive over-relaxation used on inner iterations.

Note: For "not used" items, be sure to input zero.

010002, boundary conditions

Two, four or six boundary conditions are input in the following order:

Column 0 then column boundary (all problems)
Row 0 then row boundary (2- or 3-D problems)
Plane 0 then plane boundary (3-D problems only).

A value of 0 denotes a zero-flux boundary condition, while a value of 1 denotes a zero-current boundary condition. Two values are required for 1-D problems, 4 values for 2-D problems and 6 values for 3-D problems.

010003,EPS(2),...,EPS(8) Floating Point

ESP(1) Convergence criteria used in steady-state spatial flux solution.
EPS(2) Not used. (Input 0.0).
EPS(3) Successive over-relaxation factor for inner iterations. (1.2-1.3 recommended).
EPS(4) User guess of critical eigenvalue.
EPS(5) Not used. (Input 0.0).
EPS(6) Not used. (Input 0.0).
ESP(7) Convergence criterion used in transient spatial flux solution.
EPS(8) Successive over-relaxation factor used in transient solution.

010004,CHI(1),...,CHI(NG) Floating Point

CHI(I) Normalized fission spectrum. As many values as there are neutron groups (NG from card 010010).

010005,POWER Floating Point

POWER Initial core power level (watts).

010010,NG,ND,NTZ,NPREC

NG	Number of neutron groups (1, 2, 3 or 4).
ND	Number of dimensions (1, 2 or 3).
NTZ	Number of time zones.
NPREC	Number of precursor groups (0-6).

A5.0 TRANSIENT DATA

A5.1 BASIC TRANSIENT DATA

020001, VELOC(1),...,VELOC(NG) Floating Point

VELOC(I) Neutron velocity (cm/sec) for neutron group I. As many values as there are neutron groups (NG from card 010010).

020002,RLAM(1),...,RLAM(NPREC) Floating Point

RLAM(I) Precursor group decay constant (sec^{-1}) for precursor group I. As many values as there are precursor groups (NPREC from card 010010).

020003,BETA(1),...,BETA(NPREC) Floating Point

BETA(I) Precursor group delayed neutron fraction for group I. As many values as there are precursor groups (NPREC from card 010010).

020004,TZ(1),...,TZ(NTZ) Floating Point

TZ(I) Width of time zone I (sec). At least as many values as there are time zones (NTZ from card 010010). If there are more than NTZ values on this card, the extra values are ignored.

020005,DELT(1),...,DELT(NTZ) Floating Point

DELT(I) Time step size for time zone I (sec). At least as many values as there are time zones (NTZ from card 010010). If there are more than NTZ values, the extra values are ignored.

Note: If the number of time steps in time zone I, that is TZ(I)/DELT(I), is not an integer, the code will automatically round off TZ(I)/DELT(I) to the nearest whole number and recompute DELT(I) accordingly. If the change in DELT(I) is substantial, a warning message is printed. The number of time steps per time zone is printed after card 020005 is processed.

A5.2 TRANSIENT PROGRAM CONTROL

021OSS, J_1, J_2, ..., J_{NTZ} (All optional)

Cards 021OSS each control the frequency with which a specific program operation is to be performed. Table A5-1 indicates which operation is controlled by which 021OSS card. In general, the operation is performed after every $|J_i|$ th time step during time zone i. If J_i is positive the operation is also performed at the end of the time zone. If J_i is zero the operation is not performed during or immediately after the time zone. (The effect of a positive value of J larger than the number of time steps in the time zone is to cause the operation to occur immediately after the time zone is completed.) If J_i is less than zero the operation is performed after every $|J_i|$th time step; but not at the end of time zone i, unless the number of time steps in time zone i is an integer multiple of $|J_i|$.

All 021OSS cards are optional and, if missing, result in default values of J_i which are either 0 or 1. See Table A5-1. If there are more than NTZ numbers on the cards, then the extra numbers are ignored. If there are fewer than NTZ numbers on the card, then a default of either 0, 1, or the last value on the card is supplied to generate the missing values. See Table A5-1.

The user may optionally specify that any 021OSS card be equivalent to any other 021OSS card as read and/or defaulted by placing the negative of the equivalent card number in place of J_1. The equivalent card must be either lower in card number or not itself equivalenced to another card.

A5.3 TRANSIENT ITERATION CONTROL

Optional card series 0211 provides user control over iteration limits during transients. There is one data field for each time zone. If one of the cards is missing, default values are supplied. If the card has too few items (<NTZ), the last value is used for the remaining time zones. If too many items (>NTZ) are found, the unneeded items are ignored.

021101,n_1,n_2,...

n_I Number of inner iterations per outer iteration for time zone I. (Default 4 or last value supplied).

021102,n_1,n_2...

n_I Maximum number of outer (source) iterations per time step for time zone I. (Default 100 or last value supplied).

A5.4 FEEDBACK OVERRIDE CARDS

022002, CHGTF, CHGTC, CHGRHO (Optional)
022004, CHGROD (Optional)

Values default to 0.0 if the card is missing or has fewer entries than illustrated.

Cards 021002 and 021004 each direct feedback calculations involving a recalculation of cross sections and a recomputation of neutronics matrix elements after the thermal-hydraulic and/or rod height calculations. Card series 0220 allows the user to require minimum cumulative changes in certain variables before the relatively expensive cross section and matrix recalculations are performed.

The code accumulates the maximum (for all thermal-hydraulic nodes) of the absolute value of the changes in TFUEL (average fuel temperature), TBULK (bulk coolant temperature), RHOBLK (bulk density), and rod height at each time step after each thermal-hydraulic or rod height calculation. The cumulative values are compared with the limits input by the user: CHGTF (°F), CHGTC (°F), CHGRHO (gm/cc), and CHGROD (cm) respectively.

If none of the cumulative changes exceeds its corresponding limit, then the cross section and matrix calculations are skipped and a message

****FEEDBACK OVERRIDE****

appears on the output file.

The effect of zero limits for CHGTF, CHGTC and CHGRHO is to require feedback calculations if any of the variables changes. On the other hand, a zero value of CHGROD will not by itself cause a feedback calculation unless actual rod motion takes place.

In certain situations the code forces feedback calculations to take place regardless of the above considerations. These are a) at the end of a time zone when time step size is likely to change and b) whenever a rod stops moving (such as when it reaches the top or bottom of the core). The latter situation forces a feedback calculation so that a rod will not be left a small distance (less than CHGROD) from its final position for the duration of the transient.

An edit of the cumulative changes in the above variables is printed each time a rod height or thermal-hydraulic calculation is performed.

Non-zero values of the feedback override limits on this series will generally reduce the numerical accuracy of the calculations while saving computer time. The user must take responsibility for his choice of limits in making this trade-off.

TABLE A5-1

Transient Program Control Cards

Card Number	Program Operation Controlled by Card	Default if Card Missing	Default if Fewer than NTZ Entries	Notes
021001	Thermal-hydraulic feedback calculation	1	last entry	1, 5
021002	Thermal-hydraulic edit	1	last entry	1, 2
021003	Calculate rod positions and modify rod group cross sections	1	last entry	3, 5
021004	Power fraction edit	1	last entry	4
021005	T_1 schedule for writing transient plot records	0	0	6
021006	T_2 schedule for writing transient plot records	0	0	6

Notes

(1) Card not read and 0's provided if no T-H calculation is being performed (see card 010001)

(2) Warning issued at input processing time if edit does not coincide with T-H feedback calculation as extra T-H calculation(s) without feedback will be performed.

(3) Ignored if no rod groups (see card 700000).

(4) Card not read if no power fraction edits (see card 010001).

(5) Use of these cards will normally result in some loss of accuracy. The user takes responsibility for the trade-off against computer costs.

(6) See card 019P00, Section A12.0.

A6.0 GEOMETRY DATA

The flexible HERMITE geometry description is designed to minimize the volume of data needed to describe a complex 3-D reactor core. A thorough understanding of the geometric description is essential for understanding HERMITE's method for editing output data, defining thermal-hydraulic channels and locating control rods.

Basically there are two distinct mesh structures. The finer mesh is used to describe the geometric structure of the reactor core and to assign the material compositions to each mesh rectangle. Superimposed or overlayed on this fine mesh is a (possibly) coarser mesh which describes the finite element boundaries. The principal restriction on this latter mesh is that each coarse mesh line and point must be coincident with a fine mesh line or point.

As will be described in detail below, each fine mesh rectangle has associated with it two numbers, a planar region number and a final figure number. One of the two numbers specifies the material composition present in that area of the mesh. The two numbers together are used for editing purposes.

The fine mesh geometric description presented here is also used, with some minor changes, to describe the location of control rods in the core.

A6.1 REGIONS OF SOLUTION

The region of solution is a rectangle of the x-y plane. The axes of the coordinate system coincide with boundary lines of the rectangle. As shown in Figure A6-1 the origin is placed in the upper left corner. Column numbers increase to the right along the x-axis, and row numbers increase downward along the y-axis.

Zero-flux or zero-current boundary conditions may be applied along each boundary of the region of solution.

For geometry purposes, one-dimensional problems are treated as two-dimensional problems with only two rows, zero and one. Three-dimensional problems are oriented with plane numbers increasing upward along the z axis. The bottom plane is plane zero, the top plane is the plane boundary, and each has a zero-flux or zero-current boundary condition.

A6.2 MESH OVERLAY DESCRIPTION

The row and column intersections in Figure A6-1 are the mesh points. The figure also determines an array of mesh rectangles. The purpose of the mesh description is to specify the location of all mesh points and also the location of all internal boundaries, or interfaces. Note that interfaces are composed of line segments which are the boundaries of mesh rectangles. The goal of the geometry description is to assign a composition number to each mesh rectangle.

The fundamental entities of a mesh description are basic figures. Basic figures are rectangles oriented as in Figure A6-2. Note that each basic figure has its origin at row 0, column 0 and has its own row and column boundaries. A basic figure often represents a fraction of the core whose structure may be repeated several times in the problem being solved.

Details of a basic figure are described by giving a planar region overlay together with sequences of mesh intervals along both row 0 and column 0. The planar region overlay consists of a series of overlay sets, each of which superimposes a particular planar region number throughout a specified rectangle of the mesh. The sets are processed sequentially and any set may overlay areas of the mesh specified in previous sets. Every mesh rectangle must be included within at least one of the overlay sets, and for each mesh rectangle, the last overlay set which includes that rectangle determines its planar region number. As an example, Figure A6-2 may be described by overlaying region 1 on the entire mesh; region 3 between columns 1 and 3, rows 2 and 4; region 2 between columns 2 and 4, rows 0 and 3; and region 3 between columns 3 and 4, rows 0 and 1.

Basic figures are numbered sequentially from 01 to 99. An auxiliary figure is obtained by modifying the planar region overlay of a basic figure. If two or more rectangles have the same mesh but different overlays, the use of auxiliary figures makes it unnecessary to repeat the mesh interval specification. The auxiliary figures for a particular basic figure are numbered sequentially from 1 to 9; the basic figure itself is assigned auxiliary figure number 0. A basic figure number followed by an auxiliary figure number identifies an initial figure. Initial figure numbers thus range from 010 to 999.

The rectangular region of solution is described by means of a final figure overlay. This consists of a series of overlay sets, each of which superimposes a particular initial figure on the solution region. The initial figure is positioned by giving the row and column of the solution region at which the initial figure origin is to be placed and the angle through which the initial figure is to be clockwise rotated. The angle must be a multiple of 90°. The initial figure also may be reflected, which implies an interchange of rows and columns. The rotational orientations of an initial figure are shown in Figure A6-3, and the reflection of this figure is shown in Figure A6-4. In all cases the origins are at the center.

As with the planar region overlay, the final figure overlay is sequential and may overlay areas of the solution region which have been specified previously. Any portion of an initial figure which extends outside the solution boundaries is ignored, and initial figure origins may actually be located outside these boundries. No part of the solution region may remain unspecified when the overlay is complete.

A final figure number is associated with each placement of an initial figure in the final figure overlay of the solution region. This permits the various overlays by a particular initial figure to be distinguished for editing purposes. Final figure numbers may range from 001 to 512 but need not be sequential or distinct. Note that the final figure overlay actually assigns two numbers to each mesh rectangle--a final figure number and a planar region number.

The fundamental restriction on the final figure overlay is that the mesh in the initial figures must be so chosen that rows and columns in adjoining initial figures meet at common boundary points. (This need not be true at every stage

of the overlay but only when the overlay is complete.) The final figure overlay determines the spacing of the rows and columns in Figure A6-1. In addition, all interfaces coincide with these rows and columns.

In a three-dimensional problem, all planar interfaces are projected onto a single plane which is then described as specified above. The only other mesh information required is the sequence of mesh intervals along the z axis.

A6.3 FINITE ELEMENT MESH

The mesh used for defining finite element basis functions (coarse mesh) is a simple rectangular mesh whose mesh lines are a subset of the mesh described above. *The column, row, and plane origins and boundaries must be included in* the finite element mesh.

A6.4 GEOMETRY EXAMPLE

Figure A6-5 represents one-fourth of a rectangular array. Fine mesh points have been added in Figure A6-6. Note that the rows and columns in adjoining figures all meet at common boundary points. As a result, some of the figures contain more rows and columns than are required to describe their interfaces.

All of the initial figures required for the rectangular overlay are shown in Figure A6-7. Note that (b) and (d) are auxiliary figures of the same basic figure. The overlay may be accomplished in the following steps:

Initial Figure	Origin (Column, Row)	Rotation
a	0,0	0°
a	4,4	90°
a	4,4	270°
b	4,8	90°
b	8,4	270° Reflected
a	8,8	180°

Initial Figure	Origin (Column, Row)	Rotation
d	8,8	90°
d	8,4	0°
c	8,8	0°
e	0,11	0° Reflected
e	11,0	0°

A6.5 BASIC GEOMETRY DATA

01000l, ten integers listed below

1. Column boundary
2. Row boundary (use 1 for 1-D problems)
3. Plane boundary (use 1 for 1-D or 2-D problems)
4. Maximum final figure number
5. Maximum planar region number
6. Maximum composition number
7. Composition correspondence--1/2--by figure/by region (region recommended). A negative number denotes a 1 to 1 correspondence.
8. 0/1 -- mesh given in centimeters/inches
9. 0/1 -- No/Yes for a final figure picture
10. 0/1 -- No/Yes for a planar region picture

A6.6 MESH INTERVAL DATA

05IISS,H_1,P_1,H_2,P_2,... II=01,...,99
SS=01,...,99

Fine mesh interval data is specified in expansion format, each set consisting of a floating-point interval length followed by a mesh point number.

For planar mesh intervals, the series number is 05 and any of subseries II=01-99 may be used. Each such subseries specifies a sequence of intervals extending from point 0 to an arbitrary final termination point. The data might consist of the following cards, for example.

```
050101, 15+1,4
050201, 15+1,2,3+1,3
050301, 1+1,1,3+1,2
```

The use of this data is illustrated in Section A6.7.

07SSSS,M_1,P_1,M_2,P_2,... SSSS=0001,...

Axial mesh intervals are required in three-dimensional problems. The series number is 07, there is no subseries number, and the final termination point must be the plane boundary. Expansion format is used again.

A6.7 OVERLAY DATA

8bb000,COLBDY,ROWBDY,i_1,i_2,...,0,j_1,j_2,...

A control card is required for each basic figure containing the column boundary, the row boundary, a set of column interval subseries numbers, i, a zero, and a set of row interval subseries numbers, j. The series number for the control card is 8, the subseries number is the two-digit basic figure number, and the sequence number is 000. The control card for basic figure 02 might be

```
802000, 4, 3, 1, 0, 2
```

where the interval subseries numbers refer to the example in Section A6.6. This basic figure has a column boundary of 4 and a row boundary of 3; the column intervals consist of subseries 01 and the row intervals consist of subseries 02.

The advantage of multiple mesh interval card subseries is that repeating sequences of intervals need be specified only once. Note that the final termination points of the column subseries must exactly add to the

column boundary of the basic figure, and similarly for the row subseries. Note also that the column and row boundaries may be as small as 1 and as large as desired.

If a column interval subseries number, i, or a row interval subseries number, j, is negative the order of the mesh intervals for that subseries is reversed.

8bbaSS,n_1,n_2,n_3,n_4,n_5 SS=01,...

Planar region overlay data consists of five-word sets: planar region number, n_1; left column, n_2; right column, n_3; top row, n_4; and bottom row, n_5. More than one set may appear on a card. The column and row numbers must define a nondegenerate rectangle which does not extend outside the basic figure boundaries. The series number for this data is 8 and the subseries number, bba, is the initial figure number, consisting of a two-digit basic figure number bb followed by a one-digit auxiliary figure number a. A complete basic figure overlay is given using auxiliary figure number 0 and then modifications to this overlay are given for each auxiliary figure. The complete set of card numbers for basic figure 16 might be

816000
816001
816002
816101
816201
816202

The first card is the basic figure control card, the next two cards contain the basic figure overlay sets, the fourth card contains overlay sets which modify the basic figure to form auxiliary figure 1, and the last two cards modify the basic figure to form auxiliary figure 2. Note that the basic figures must be numbered sequentially from 01 and for each basic figure, the auxiliary figures must also be numbered sequentially from 1. It is not necessary, however, that every basic figure and auxiliary figure actually be used in the final figure overlay.

17SSSS,N_1,N_2,N_3,N_4,N_5,N_6 SSSS=0001,...

Final figure overlay data is specified using series number 17. This data consists of six-word sets as follows:

N_1 final figure number

N_2 initial figure number, bba

N_3 origin column

N_4 origin row

N_5 rotation number, $0 \leq N_5 \leq 3$

N_6 reflection indicator, 0 or 1

The final figure number may be any number between 01 and 1296. The initial figure number must be between 010 and 999 and designates the particular basic figure or auxiliary figure being overlaid on the region of solution. There is no limitation whatever on the origin column and row numbers (e.g. they may be negative). The rotation number is the multiple of 90° through which the initial figure is to be clockwise rotated and must lie between 0 and 3. The reflection indicator is 1 for reflection and 0 for no reflection. There may be more than one six-word set on a card.

A6.8 COMPOSITION DATA

03ppps,n_i,c_j,n_k

If the composition correspondence is not one-to-one (see card 010001 in Section A6.5), it must be specified using series number 03. The data consists of one or more triples of the form n_i, c_j, n_k which assign composition c_j to planar regions (or final figures) n_i through n_k. The triples are processed sequentially and any triple may change an assignment established by a previous triple. For example, the set of triples

2, 1, 5
1, 3, 1
3, 2, 4

assigns composition 2 to regions 3 and 4, composition 3 to region 1, and composition 1 to regions 2 and 5. Note that every planar region (or final figure) must be assigned a composition number by this process.

Subseries ppp=000 is used for the composition correspondence in two-dimensional problems and for the bottom plane of three-dimensional problems. An additional subseries is required for each plane at which the correspondence changes. The three-digit subseries number ppp is the plane number at which the change occurs, and the triples in such a subseries are used to modify the correspondence of the previous plane. The correspondence may be changed at any plane.

A6.9 FINITE ELEMENT BOUNDARIES

040NOS, finite element boundary points S=1,...,9

The finite element boundary points are column, row and plane mesh points depending on whether N is 1, 2, or 3. Column, row and plane 0 and the respective boundary points on card 010001 are required. For 1-D problems, a card series with N = 1 is required. For 2-D problems, card series with N = 1 and N = 2 are required, and for 3-D problems card series with N = 1, 2, and 3 are required.

A compressed format is available as illustrated by the following example:

040101,0,-3,4,6,-10

is equivalent to

040101,0,1,2,3,4,6,7,8,9,10

In thermal-hydraulic calculations, one finite element boundary each must correspond exactly to the bottom and top of the active core (there is no automatic checking for this requirement).

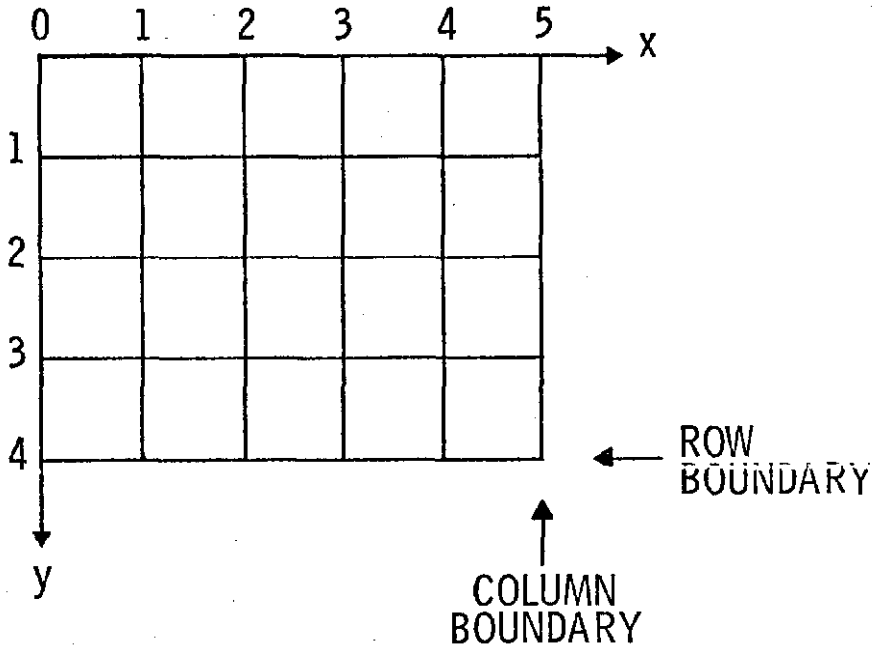

HERMITE CENPD-188	SAMPLE OF MESH AND REGION OF SOLUTION	Figure A6-1

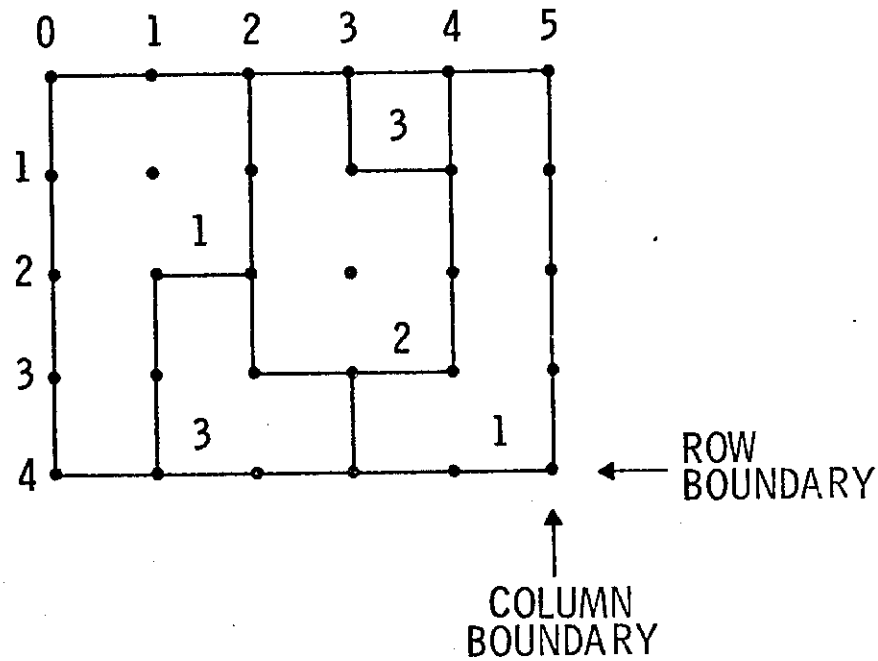

HERMITE CENPD-188	SAMPLE BASIC FIGURE WITH PLANAR REGION OVERLAY	Figure A6-2

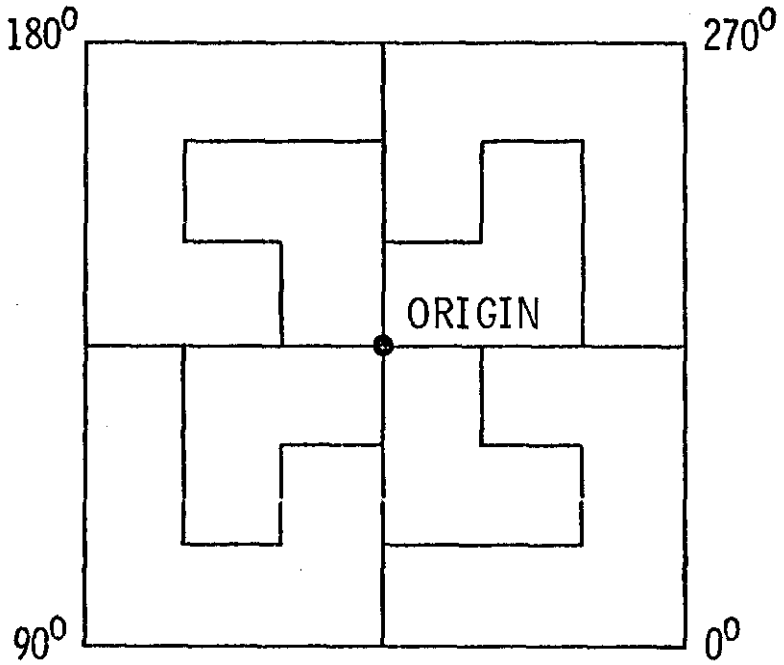

HERMITE CENPD-188	ROTATIONAL ORIENTATION OF A SAMPLE BASIC FIGURE	Figure A6-3

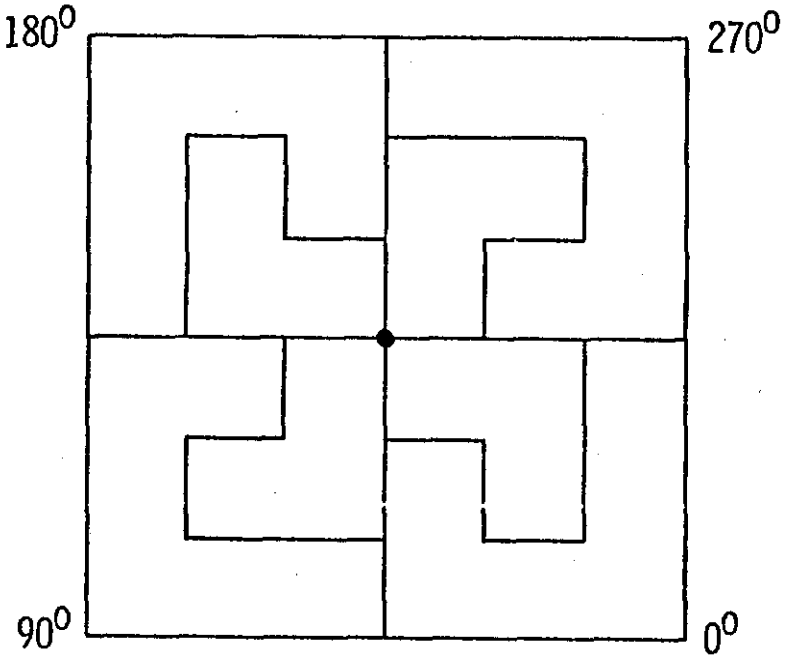

HERMITE CENPD-188	ROTATIONAL ORIENTATIONS OF A REFLECTED SAMPLE BASIC FIGURE	Figure A6-4

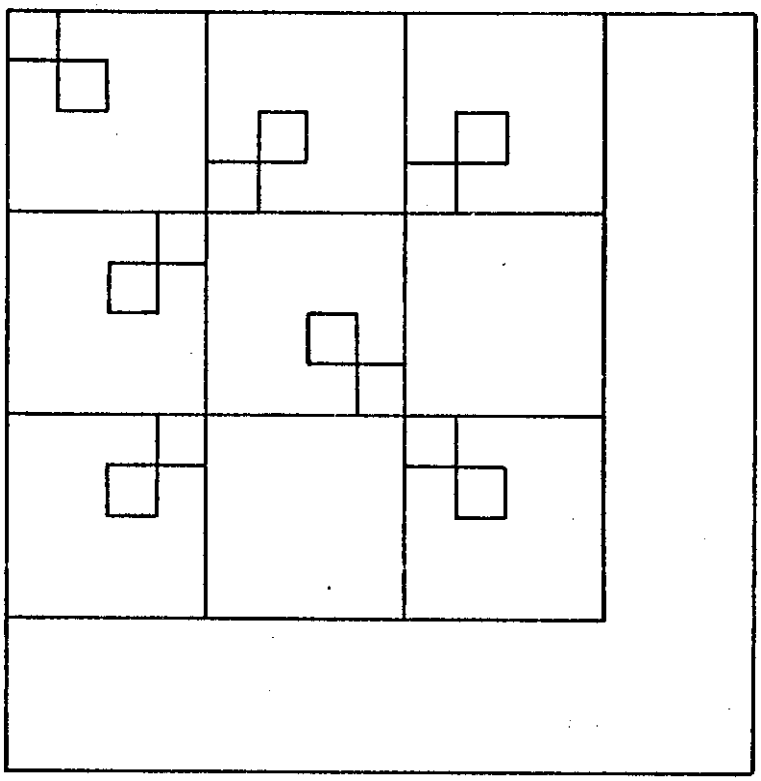

HERMITE CENPD-188	SAMPLE CORE LAYOUT FOR GEOMETRY EXAMPLE	Figure A6-5

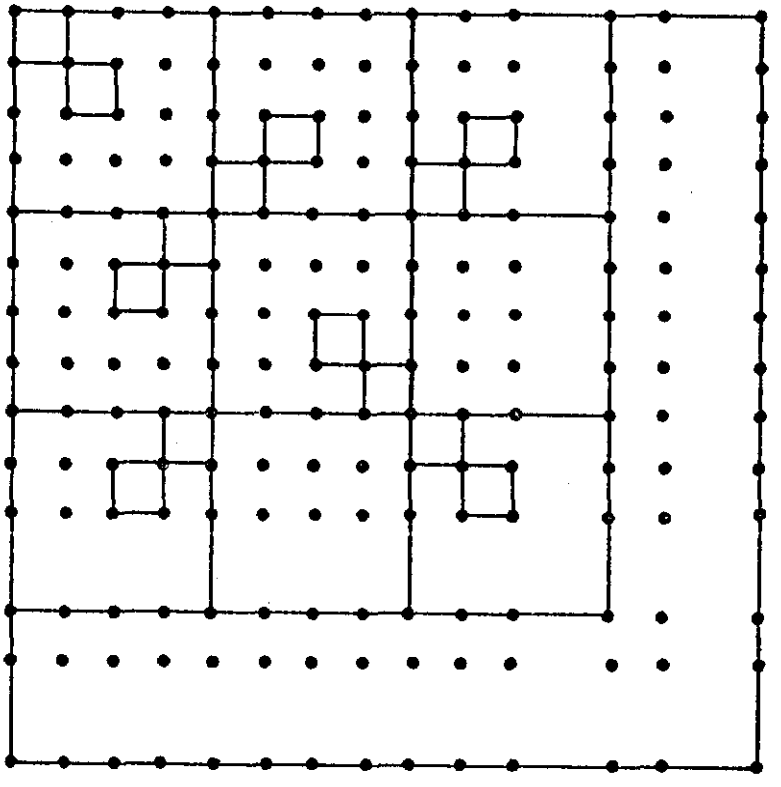

HERMITE CENPD-188	GEOMETRY EXAMPLE WITH MESH POINTS	Figure A6-6

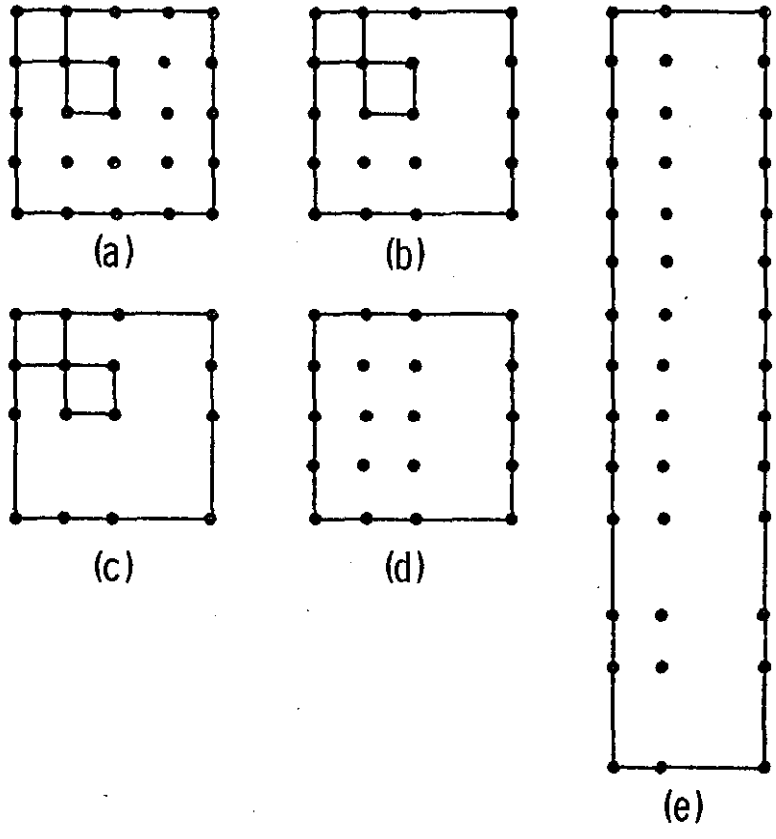

HERMITE CENPD-188	INITIAL FIGURES REQUIRED FOR GEOMETRY EXAMPLE	Figure A6-7

A7.0 CROSS SECTION DATA

A7.1 CROSS SECTION MODEL

Reactor core thermal-hydraulic conditions influence the neutronics calculations through changes in cross sections. In general, the cross sections need to be functions of fuel temperature, coolant temperature and coolant density. Because transients can involve large temperature and density changes, a flexible cross section representation is needed to account accurately for these variations.

In the most general case, the macroscopic constants used in the diffusion equation can be functions of a number of independent variables. The independent variables may be number densities of nuclides such as U-235, hydrogen, etc., or changes in fuel temperature, coolant temperature and coolant density.

The code computes macroscopic constants used in the diffusion equation from the following formula:

$$\Sigma = \sum_j N_j \{\sigma_j(N_1,N_2,N_3)\, g_j(N_4,N_5,N_6) + \sum_n \delta\sigma_j^n\,(N_7,N_8,N_9)\, g_j^n\,(N_{10},N_{11},N_{12})\, \Delta X_n\}, \qquad \text{(A7-1)}$$

where:

Σ macroscopic cross section (transport, absorption, removal, or fission) used in the neutron diffusion equation.

j index labeling nuclides such as U-235, hydrogen, etc.

n index over thermal-hydraulic quantities. Currently these may include fuel temperature, coolant temperature and coolant density.

N_j number density of nuclide j in atoms/barn-centimeter.

$\sigma_j(N_1,N_2,N_3)$ microscopic cross section in barns of nuclide j. σ_j may be a constant or a function of up to three of the number densities, N_j, or thermal-hydraulic variations, ΔX_n. This is indicated symbolically by the arguments N_1,N_2,N_3.

$g_j(N_4,N_5,N_6)$ this is called a g-factor multiplier on the microscopic cross section. It defaults to a value of 1.0 and is included in the representation for flexibility. g_j may be a function of up to any three of the number densities, N_j, or thermal-hydraulic variations, ΔX_n.

$\delta\sigma_j^n(N_7,N_8,N_9)$ this is the change in the microscopic cross section σ_j per unit change in the thermal-hydraulic variable X_n. $\delta\sigma_j^n$ may be a constant or a function of up to three of the number densities, N_j, or thermal-hydraulic variations, ΔX_n.

$g_j^n(N_{10},N_{11},N_{12})$ this is a g-factor multiplier on the change in microscopic cross section $\delta\sigma_j^n$. It defaults to 1.0 and is included in the representation for flexibility. g_j^n may be a function of up to three of the number densities, N_j, or thermal-hydraulic variations, ΔX_n.

ΔX_n is the variation in the thermal-hydraulic variable X_n from an input reference value,

$$\Delta X_n = X_n - X_{n,\,ref}$$

X_n fuel temperature, coolant temperature or coolant density. For fuel temperature, X_n is the square root of the fuel temperature in degrees Kelvin. For coolant temperature, X_n is in degrees Fahrenheit, and for coolant density it is in grams per cm^3. This is the density of pure water and is not, for example, the homogenized density of water in a fuel-water mixture.

Equation A7-1 is valid for transport, absorption, removal and fission cross sections. For $\nu\Sigma^f$ and $\kappa\Sigma^f$ a slightly different expression employing the product rule for derivatives is used. For $\nu\Sigma^f$ the expansion is

$$\nu\Sigma^f = \sum_j N_j \{\nu_j \sigma_j^f g_j^f + \sum_n [\nu_j \delta\sigma_j^{fn} + \sigma_j^f \delta\nu_j^n] \Delta X_n g_j^{fn}\}.$$

Each of the quantities ν_j, σ_j^f, g_j^f, g_j^{fn}, $\delta\sigma_j^{fn}$ and $\delta\nu_j^n$ may be a function of up to three of the number densities, N_j, or thermal-hydraulic variations, ΔX_n. A similar expression holds for $\kappa\Sigma^f$.

Often it is not necessary to use the cross section representation in its most general form. Usually g-factors are not used and the code defaults them to unity. Certain nuclides may be designated as being macroscopic quantities. For these nuclides the code automatically sets the number density to unity.

In practice, the concept of nuclides or isotopic species, with their associated number densities, is not restricted to the conventional meaning suggested by the notation. For example, a single nuclide may be defined to represent the homogenized macroscopic cross sections of a whole fuel assembly. As another example, a nuclide with zero microscopic cross sections may be defined so that its number density is equal to the system pressure and it may be used as an independent variable in the determination of other cross sections or g-factors.

A further example of this flexibility is provided by control rods. When control rods are present in the core, the user selects a specific nuclide to represent the rods' cross sections. The number density of this nuclide is given a value of 0.0 if the rod is not present in a mesh rectangle, a value of 1.0 if it is present, and a value between 0.0 and 1.0 if it is partially present in a mesh rectangle. Thus, the rod cross sections are, in effect, positive or negative changes in macroscopic quantities. Control rods may be assigned fission cross sections and thermal feedback variations if required to reflect spectral effects on macroscopic constants.

A7.2 NUCLIDE IDENTIFICATION

For input purposes, each element in the cross section representation is identified and distinguished from all others by a numeric nuclide ID. For example, for U-238, the base microscopic cross sections, $\sigma_{U\text{-}238}\ (N_1,N_2,N_3)$, might be assigned ID = 20. g-factors assigned to the base microscopic cross sections would also carry this same ID. An alphanumeric ID is also assigned to each nuclide.

The $\delta\sigma_j^n$'s are also assigned a unique ID. Using the same example, U-238, if cross section variations with respect to moderator density and fuel temperature are being considered, they might be assigned ID = 120 and ID = 220 respectively.

Hence, each nuclide will have assigned to it one or more ID's corresponding to the base cross sections, σ_j, and any defined $\delta\sigma_j^n$'s. Should a nuclide not have a particular $\delta\sigma_j^n$, no ID need be assigned.

The ID's for base cross sections, σ_j, are assigned on cards 300001-300499. The ID's for the $\delta\sigma_j^n$'s are assigned on cards 30n001-30n009.

The ΔX_n's are also assigned numeric ID's. This is done so that a cross section may be made a function of ΔX_n, to specify initial non-zero values for the ΔX_n, and to identify thermal feedback parameters.

A7.3 TABLE SETS AND COMPOSITIONS

HERMITE uses the table set concept. A table set is a collection of various cross section tables which together make up the cross sections for a given material or composition. There are two basic types of tables, master microscopic tables which contain fixed or constant cross sections, and function tables which contain cross sections or g-factors as a function of number densities and variations, ΔX_n.

In HERMITE, table sets and compositions are identical. Compositions or table sets are assigned to planar regions or final figures as described in Section A6.8.

A7.4 CROSS SECTION FORMS

a) Fixed or Constant Cross Section Data

Microscopic cross section data, σ_j or $\delta\sigma_j^n$, which is constant for the entire calculation is input on master microscopic table cards. These cards are numbered 4ttgss where tt is the table set number, g is the group and ss is the sequence number.

The cards each contain the ID number to identify the data and values for transport, absorption and removal cross sections. If applicable, fission cross sections, ν and κ are also included.

b) Cross Section Function Data

For those cross sections, σ_j or $\delta\sigma_j^n$, which are functions of number densities or ΔX_n's, and for all g-factors, function tables are used. Function tables are numbered 13fffs, where fff is the table number. Associated with each function table is a mask containing the tabulated values of the independent variables. Mask cards are numbered 12mm00 where mm is the mask number.

The function tables and masks are assigned to table sets on the 4ttuuu cards.

c) Macroscopic Data

The user may declare that any number of "isotopes" are to be treated as macroscopic data by using the card series 310001-310009. This has the effect of giving the isotope a number density of 1.0 for the entire calculation. All cross sections, both σ_j's and $\delta\sigma_j^n$'s, are treated as macroscopic data.

d) Initial Number Densities

At the beginning of a calculation, the user may preset the value of any number density or ΔX_n using the 100tts cards. Base ID's and the desired number densities are put on the card.

A7.5 NUCLIDE IDENTIFICATION DATA

300001-300499, $ID_1, ID_2, \ldots, ID_j, \ldots$

This card series is used to input the base cross section ID's associated with the σ_j's. ID's must be positive integers. This card series is required.

300501-300999, $\alpha_1, \alpha_2, \ldots, \alpha_j, \ldots$

This card series is used to input alphanumeric nuclide ID's. Each ID may be from 1 to 10 characters in length. The order of the ID's on this card must correspond to the order on card series 300001-300499. This card series is required.

30n001-30n009, $ID_1^n, ID_2^n, \ldots, ID_j^n, \ldots$

This card series is used to input ID's associated with $\delta\sigma_j^n$. The order of the ID's on this card must be the same as on card series 300001-300499. Thus, if U-238 has ID=20 on card 300001 and is the third ID on the card, then the third ID on card 30n001, say ID=120, is the identification of $\delta\sigma_{U\text{-}238}^n$. If a particular nuclide will have no $\delta\sigma_j^n$ cross sections, then ID=0 is used on the card. The ID's on this card series must be unique and not duplicate those on card series 300001-300499.

310001-310009, $ID_1, ID_2, \ldots$

This card series is used to designate the nuclides which are to be treated as macroscopic quantities. The ID's on this card series must also appear on card series 300001-300499--that is, they are base cross section ID's. The associated

$\delta\sigma_j^n$ cross section data, if any is input, will automatically be treated as macroscopic data. Thus, ID's appearing on cards 30n001-30n009 must not be used on this card series.

320001,ID^1,...,ID^n,...

This card is used to assign ID's to the ΔX_n's. There must be as many entries as there are values of n on series 30n001. These ID's must not duplicate any previously used ID on any other card series. This card is required. (See also card 4tt002 below and card 010016 under thermal-hydraulic input).

010016,,,,,,,(six other items)IDTMOD,IDDENS,IDTFUL

- Tells the thermal feedback subroutines which ID's to use for the three ΔX_n's.

- The following default values are used if the ID's are not specified on card 010016.

IDTMOD = 88	(Moderator temperature)
IDDENS = 89	(Moderator density)
IDTFUL = 98	(Fuel temperature)

- If any of these ID's are not listed on card 320001, then these variations are not fed back. A warning message is printed.

- A complete description of this card is given in Section A10.0.

A7.6 TABLE SET (COMPOSITION) IDENTIFICATION DATA

In the data card descriptions which follow, the composition or table set sequence number, tt, will appear often. The table set sequence number may range from 01 to 99. The table set sequence numbers need not be sequential or begin with 01.

4tt001,β

β Alphanumeric ID of the table set. Up to 40 characters may be input. These cards are required. They are used to determine which tt values are being used.

4tt002, ID^n,$X_{n,ref}$,...ID^n,$X_{n,ref}$,... (One card per table set)

- Assigns floating point reference values of the variables being used as ΔX_n's. $\Delta X_n = X_n - X_{n,ref}$ (in most cases. Exception: T_{FUEL}; $\Delta T_{FUEL} = T_{FUEL} - T_{FUEL,ref}$ where values are input in °F, converted to °K, and square rooted before ΔTFUEL is computed).
  Note: reference values are not to be confused with initial values which are set on card 100tts described in Section A7.7.

- Relationship to card 320001.

  - ID's on card 4tt002 need not be in the same order as ID's on card 320001.

  - If ID^n on 4tt002 is not on card 320001, then the reference value is ignored with a warning message. (Acceptable because the user may not be running a feedback problem or may not wish to feed back variable ID_j.)

  - If ID^n on 320001 is not on card 4tt002, then the reference value is assigned an arbitrary value of 0 with a warning message. (Acceptable if cross sections in a given table set do not vary with variable n or if the user desires to use the actual value of the variable as he might in a mask-function table set up.)

A7.7 INITIAL NUMBER DENSITIES

100tts,ID_1,N_1,ID_2,N_2,... s=1,2,...,9

This card series is used to initialize number densities and ΔX_n's for each table set. Any isotope or ΔX_n not mentioned on this card series is given a

number density of zero. ID is for a base cross section or a ΔX_n. It may not be the ID of a $\delta\sigma_j^n$. N is the associated floating point initial value. ID's placed on card series 310001-310009 for treatment as macroscopic cross sections must not be used on this card series.

A7.8 MASTER MICROSCOPIC TABLES

4ttgss, ID_j, σ_j^{tr}, σ_j^a, σ_j^r, σ_j^f, ν_j, κ_j ss=01,...,99

or

4ttgss, ID_j^n, $\delta\sigma_j^{tr,n}$, $\delta\sigma_j^{a,n}$, $\delta\sigma_j^{r,n}$, $\delta\sigma_j^{f,n}$, $\delta\nu_j^n$, $\delta\kappa_j^n$

For table set tt and group g, ID_j or ID_j^n is the numeric nuclide ID of the base cross section, σ_j, or the $\delta\sigma_j^n$ as appropriate. σ^{tr}, σ^a, σ^r and σ^f and the corresponding $\delta\sigma$'s refer to the transport, absorption, removal, and fission cross sections in barns. If σ_j^f or $\delta\sigma_j^{f,n}$ is zero then ν and κ or $\delta\nu_j^n$ and $\delta\kappa_j^n$ may be left out.

A7.9 MASK-FUNCTION TABLE ASSIGNMENT

4ttuuu,m_j,$f_{j,k}$ for k=1,2,... uuu=600+j, j=1,2,...

On one card, a mask m_j ($01 \le m_j \le 99$) is selected which is to be used with all function tables $f_{j,k}$ ($001 \le f_{j,k} \le 999$) listed after it on that card. The specification of the function table itself indicates the cross section which is to be interpolated in this table set.

A7.10 MASK DESCRIPTION

12mm00,DIM,ND,NOD mm=01,02,...

$1 \le DIM \le 3$, dimension of the table (the number of independent variables).
$1 \le ND$, number of diagonal entries.
$0 \le NOD$, number of off-diagonal entries.

12mmjs,ID,N/F,N_1,...,N_{ND} for each dimension j=1,2,...,ND

For each j, cards are sequenced s=1,2,... For $s \ge 2$, omit ID and N/F.

j=1,2,3 determines which independent variables are designated by ROW, COLUMN, and PLANE respectively on cards 12mm9s.

ID is the identification number of independent variable j. ID may be a base cross section ID in which case the N_ℓ are the corresponding isotope number densities, or, ID may refer to a ΔX_n, in which case N_ℓ is a value of ΔX_n.

N/F--not currently used, set to 0

N_ℓ is a concentration (floating point)

For each j, the entires must be in decreasing order, $N_\ell < N_{\ell-1} < N_{\ell-2} \cdots$.

12mm9s,(see below)

If NOD>0, give the off-diagonal positions. Visualize a two-dimensional mask as a matrix of elements with the diagonal of the mask appearing as the diagonal of the matrix with N_1 appearing as the row label and N_2 as the column label. Then off-diagonal entries can be located by giving the row number followed by the column number of the matrix position of the entry. Each off-diagonal entry will be described by a doublet if the table is two-dimensional or a triplet if the table is three-dimensional. For example,

$12mm9s, ROW_1, COL_1, ROW_2, COL_2, \ldots, ROW_{NOD}, COL_{NOD}$ (2-dimensional)

$12mm9s, ROW_1, COL_1, PLANE_1, \ldots, ROW_{NOD}, COL_{NOD}, PLANE_{NOD}$ (3-dimensional)

That is for the nth off-diagonal entry, give the location first for the j=1 variable, then the j=2 variable, then the j=3 variable. For j=1, the number must be non-decreasing, i.e., $ROW_k \geq ROW_{k-1}$, k=2,...,NOD. All the off-diagonal entries corresponding to the first value of the j=1 variable must be given first, then all the off-diagonal entires corresponding to the second value of the j=1 variable, etc. Take as an example the mask of figure shown below where the X's indicate entries.

		ID = 238 (j=2)			
		.04	.03	.02	.01
ID=235 (j=1)	.10	X			
	.09		X	X	X
	.08		X	X	X
	.07				X

Sample Mask

This sample mask may be specified as

```
12mm00,2,4,4
12mm11,235,0,1-1,9-2,8-2,7-2
12mm21,238,0,4-2,3-2,2-2,1-2
12mm91,2,3,2,4,3,2,3,4
```

For two- or three-dimensional function evaluation, the mask must contain one or more imbedded rectangles (2-D) or rectangular parallelopipeds (3-D) formed by four (2-D) or eight (3-D) neighboring points. All points to be interpolated must lie within the rectangle--the code will not extrapolate. In the example above, only points satisfying

$.03 > N_{238} > .01$,
$.09 > N_{235} > .08$

can be interpolated.

A7.11 FUNCTION TABLES

13fff0,k,ID,t,g,0,f,ID_ℓ,t_ℓ $\quad \ell=1,2,3,\ldots$

The function table numbers, fff, ($001 \leq fff \leq 999$) need not begin with 001 and need not be sequential. However, storage requirements will be minimized if they do begin with 001 and are sequential.

k -- Type of quantity represented.
= 4 for a microscopic cross section, σ_j, or variation cross section, $\delta\sigma_j^n$.
= 5 for a g-factor.

ID -- identification number of σ_j or $\delta\sigma_j^n$

t -- cross section type, see below

g -- group number

O -- order of interpolation for one-dimensional function tables only ($1 \le O \le 5$). Set to 1 for two- or three-dimensional functional tables.

f -- 0/1--function itself is to be interpolated/inverse of the function is to be interpolated.

When k=5 (g-factor function table), the function table can be used to represent the g-factor for several different ID,t combinations for the same group. Then the additional pairs of values of ID and type t are listed following f given above as ID_ℓ, t_ℓ.

The type identification (t) may be determined from the following table.

t	1	2	3	4	5	6
σ	σ^{tr}	σ^a	σ^r	σ^f	ν	κ

When t=4 for a g-factor, it is applied to σ_f, $\nu\sigma_f$ and $\kappa\sigma_f$. Thus t>4 is not permitted for k=5 (g-factors).

13fffs,f_i i=1,...,ND

Use s=1,2,...,S to give floating point function values for the diagonal of the table. Note that ND must match up with the mask given for the table and the function values must be input in the same order as the mask entries.

13fffs,f_j j=1,...,NOD

Continue the card sequence numbering, s=S+1,... to give the floating point off-diagonal function values (if any) in the order specified by the mask. Note that if f = 1 on 13fff0, all f_i and f_j must be non-zero. It is assumed that when the inverse of the cross section is interpolated, the cross sections, not the inverses, are available in the table.

A8.0 CONTROL ROD DATA

Any number of full and part length control rods may be used. These rods are divided into "rod groups" and each rod group moves independently of all other rod groups.

Control rod input consists of: 1) basic control rod data, 2) description of where the rods are located in the core, and 3) the control rod cross sections.

The location of control rod groups on the problem mesh is done by means of a geometry overlay system virtually identical with the problem's basic geometric description. The concepts of initial figures, final figures, planar region numbers, etc. are all used. The only concept not used is the actual mesh interval widths. The user generates initial figures using card series 9bb000 and 9bba01-9bba99. There are two differences in the use of these cards compared to the use of cards 8bb000 and 8bba01-8bba99 used in the basic problem geometric description. First, no mesh interval subseries numbers are used on cards 9bb000--hence these cards contain only two numbers, the column and row boundaries of the basic rod figure. Secondly, planar region number 0 is used in the planar region overlay to indicate unrodded regions of the basic figure.

With the initial rod figures, a final rod figure overlay is constructed using card series 180001-180999 in a manner analogous to using card series 170001-170999 to construct the problem's basic geometric overlay. There is one difference in the process when constructing the final rod figure overlay--not all regions of the problem need be covered. Only those regions which are to be rodded need be specified. The code automatically places final rod figure number zero in other locations.

The basic control rod data consists of the maximum rod final figure and planar region numbers used in constructing the overlay, the number of rod groups being defined and how the rod groups are assigned to the overlay. This may be done by assigning rod groups to rod planar region numbers or to rod final figure numbers. Pictures of the two rod overlays may be requested as part of the basic control data.

The mechanism for assigning cross sections to control rods is to designate one numeric nuclide ID for control rods. If a rod is fully inserted in a mesh rectangle, the number density of this nuclide is set to 1.0. If the rod is fully withdrawn, it is set to 0.0. A partially inserted rod is represented by a number density in the range 0.0 to 1.0. The actual cross sections then, are interpreted as changes in the problem's macroscopic constants. The cross section mixing, matrix generation and other routines are not explicitly aware of control rod cross sections. The control rod "nuclide" is treated in the same way as any other nuclide. The control rod nuclide number density is set on the code's internal number density file along with thermal feedback changes. This means, for example, that control rods may have fission cross sections, $\delta\sigma_j^n$'s, etc. The initial rod positions are set on input and must coincide with mesh points.

Control rod movement is achieved by use of velocity functions. Each control rod group has assigned to it a velocity function (if the rod group does not move, a zero is input meaning no velocity function is used). The same function may be used by more than one rod group. The functions themselves consist of pairs of velocities and times. The velocity is the rod group velocity at that time. In the present version, time is measured relative to the beginning of the transient. Positive velocities denote rod withdrawal, while negative velocities denote rod insertion. By proper specification of the velocity function, step changes can be simulated. In many cores, rod motion is limited. Control rods cannot extend below the bottom of the active core nor be withdrawn beyond the top of the active core. Using data from an input card, the code checks for these conditions and fixes rod positions so as to prevent such movement.

A8.1 BASIC CONTROL ROD DATA

700000,MAXRF,MAXRR,NRGRPS,IRCOR,INUC,RFPIC,RRPIC

MAXRF Maximum control rod final figure number.
MAXRR Maximum control rod planar region number.
NRGRPS Number of control rod groups.

IRCOR Control rod group correspondence--1/2 by rod figure/by rod region.
INUC Numeric nuclide ID of control rod cross sections.
RFPIC Control rod final figure picture edit--0/1--No/Yes.
RRPIC Control rod planar region picture edit--0/1--No/Yes.

If this card is absent no further control rod data will be processed.

700001,P_1,NV_1,...,P_{NGRPS},NV_{NRGPS}

P Initial position of the tip of a control rod group. Given as a distance from core bottom in cm. For 2-D problems, P=0.0 is a fully inserted rod, while P=1.0 is a fully withdrawn rod. Floating point.

NV Rod velocity function number. If the rod will not be moved, use NV=0.

There are as many P,NV pairs as there are rod groups (NRGRPS).

700002,LPLR,$NGRP_1$,...

LPLR Length of a part-length rod (inches). Floating point.
NGRP Rod group numbers for those rod groups which are part length rods.

Omit this card if there are no part-length rods.

700003,IBOT,ITOP

IBOT Mesh point number for bottom of active core (0 in 2-D).
ITOP Mesh point number at which rod motion stops (1 in 2-D).

The data on this card is used by the code to prevent insertion of a rod below the bottom of the core, or withdrawal of it through the top of the core. The rod position on card 700001 are checked against the positions corresponding to IBOT and ITOP respectively. If a rod tip is below IBOT or

above ITOP, its position is set to correspond exactly with IBOT or ITOP as appropriate. A warning message is printed. In a transient, rod motion stops when the position reaches IBOT or ITOP.

700I01,V_1,T_1,V_2,T_2,... (All floating point) I=1,...,9

V Control rod velocity (cm/sec). A positive velocity causes rod withdrawal.

T Time (sec). T_1 = 0.0 is required.

The V,T pairs define the control rod velocity function I. The velocities are linearly interpolated between points.

700I0,PR_1,PR_2,... I=1,...,9

Rod group number correspondence to rod regions or figures.

I Rod group number.

PR_i Rod region number or rod figure number as specified on card 700000.

A8.2 CONTROL ROD GEOMETRY DATA

9bb000,COLBDY,ROWBDY

Basic figure control card for basic rod figure bb0. Similar to card 8bb000.

9bbass,n_1,n_2,n_3,n_4,n_5 (01≤ss≤99)

Initial figure bba overlay set (similar to card 8bbass). The basic figure is specified on subseries bb0. Any auxiliary figures, which are modifications of the basic figure, are specified on subseries bba (a=1-9). Any number of five-word sets (n_1,...n_5) may be specified in each subseries where

n_1 rod region number
n_2 left column
n_3 right column; $0 \leq n_2 < n_3 \leq$ COLBDY
n_4 bottom row
n_5 top row $0 \leq n_4 < n_5 \leq$ ROWBDY

18ssss,N_1,N_2,N_3,N_4,N_5,N_6 (0001$\leq$ssss$\leq$9999)

Final rod figure overlay data (similar to card 17ssss). Any number of six-word sets (N_1,...,N_6) may be specified on the series where

N_1 final rod figure number
N_2 initial rod figure number, bba
N_3 origin column (any integer, +, 0, or -)
N_4 origin row (any integer)
N_5 rotation number (0, 1, 2, or 3)
N_6 reflection number (0 or 1)

A9.0 EDIT CONTROL DATA

The integration editing includes power fractions and average macroscopic parameters.

An edit set is a collection of final figure numbers together with a collection of planar region numbers. Each edit set defines a region of the mesh, not necessarily connected, which is to be treated as a unit for integration editing purposes. A particular mesh rectangle belongs to each edit set whose definition includes both the final figure number and the planar region number of the mesh figure. Every integral quantity is calculated for each edit set in each plane. Note that the edit sets are the same in every plane since they depend only upon final figures and planar regions.

A plane grouping is a collection of planes, not necessarily connected, which is to be treated as an axial editing unit. Note that a particular plane may belong to any number of plane groupings. All edit sets are summed over the planes comprising a plane grouping before being printed. Thus, to identify the region of integration for a single printed quantity requires a list of final figures, a list of planar regions, and a list of planes. The program solves this identification problem by numbering both the edit sets and the plane groupings. The definition of each of these is printed once, and integral quantities are then identified by edit set number and plane grouping number.

Edit control data is specified using card series number 01. Subseries 100-499 are used for edit sets and subseries 500-599 are used for plane groupings.

The data for each edit set subseries is of the form

$$f_1, \pm f_2, \pm f_3, \ldots, \pm f_m, 0, r_1, \pm r_2, \pm r_3, \ldots, \pm r_n$$

where the zero is used to separate a collection of planar region numbers from a collection of final figure numbers. A negative figure number designates all figures from the previous figure number through the negative figure number, and similarly for a negative region number. For both the figures and the regions,

the numbers must be strictly increasing in absolute value, there may not be two consecutive negative numbers, and the first number must be positive. As an example, the sequence 3, 5, -7, 0, 2, -4, 9 specifies figure numbers 3, 5, 6, and 7 and region numbers 2, 3, 4, and 9.

01100S to 01499S Planar Edit Sets

The subseries are separated into four ranges: 100-199, 200-299, 300-399, and 400-499. Any (but not all) of the ranges may be omitted and the first missing subseries in each range terminates the range. Each of subseries 100-199 specifies a single edit set. In each of subseries 200-299, the figure numbers are expanded to remove negative signs and an edit set of the form

$$f_i, 0, r_1, \pm r_2, \pm r_3, \ldots, \pm r_n$$

is constructed for each figure number. Similarly, in each of subseries 300-399, the region numbers are expanded and an edit set of the form

$$f_1, \pm f_2, \pm f_3, \ldots, \pm f_m, 0, r_j$$

is constructed for each region number. Finally, in each of subseries 400-499, both the figure and region numbers are expanded and an edit set of the form

$$f_i, 0, r_j$$

is constructed for each figure-region pair.

010017 Axial Editing and Thermal-Hydraulic Block Boundaries

This card identifies axial blocks used for editing and for the thermal-hydraulic mesh. This card is required for all one-dimensional and three-dimensional problems, whether or not a thermal-hydraulic calculation is being performed.

These boundaries are column (for one-dimensional problems) or plane (for three-dimensional problems) mesh points. Column or plane 0 and the corresponding boundary point from card 010001 are required. Other mesh points must correspond to finite element mesh points listed on card series 040105 (one-dimensional) or 040305 (three-dimensional). For example,

```
040301,0,1,3,5,7,9,10
010017,0,1,5,9,10
```

One mesh point each must correspond exactly to the bottom and top of the active core. (There is no automatic checking for this requirement).

01500S to 01599S Plane Groupings

At least one plane grouping subseries is required in three-dimensional problems and the subseries numbers present must be sequential. The data for each subseries specifies a single plane grouping and is of the form

$$p_1,-p_2,p_3,-p_4,\ldots,p_{n-1},-p_n.$$

The plane numbers in a subseries must be strictly increasing in absolute value and occur in plus-minus pairs, each pair designating the axial region between the two planes. The sequence 0, -3, 5, -8, for example, specifies a plane grouping consisting of planes 0-3 together with planes 5-8. The plane numbers used on this card series must correspond to axial editing and thermal-hydraulic block boundaries from card 010017.

A10.0 THERMAL-HYDRAULIC DATA

The thermal-hydraulic model in HERMITE divides the active core into thermal channels whose horizontal cross sections correspond to selected planar edit sets. A single channel is defined for one-dimensional problems. There are two types of channels, primary and secondary. Each planar mesh rectangle in the active core must be included in exactly one primary channel. Additional secondary channels may be defined corresponding to planar edit sets which overlap the primary channels. Primary channels are used in certain integrations over the active core and only primary channels are used as the basis for modifying cross sections in thermal feedback calculations. In one or three dimensions the core is also divided into axial blocks which consist of one or more mesh intervals of the finite element (coarse) mesh. The bottom and top reflector (if present) are each assigned an axial block.

The coolant flow model assumes axial flow in closed channels with no cross-flow or pressure balancing. The model recognizes subcooled, saturated, superheated, and supercritical water and steam. Inlet flow and temperature are input by channel. The code solves the one-dimensional continuity and conservation of energy equations. Heat is added directly to the coolant as a fraction of node power and through the clad surface as determined by the heat transfer model. Coolant density and temperature are passed to the cross section routines.

The present version of HERMITE models two heat transfer regimes which determine the clad surface temperature and, in a transient, the surface heat flux.

The fuel pin heat conduction model uses finite difference equations to solve for the fuel pin temperature distribution and average fuel temperature.

As an alternative to solving the heat transfer and heat conduction equations, the user may select one of two correlations giving average fuel temperature as a function of linear heat rate. This option is available for steady state problems only.

010016,IPLT(0),IEDIT(0),MXTHSS(5),EPSTH(.001),ITFMAX(5),EPSTF(.1),
IDTMOD(88),IDDENS(89),IDTFUL(98)

Default values are indicated in parentheses. If the indicated variable is missing (too few numbers on card) or is ≤ 0, the default is set.

IPLT Not used, supply 0 if further data is provided.

IEDIT
- 0 - No thermal-hydraulic data edited.
- 1 - Selected information - one line per channel.
- 2 - Above plus fuel pin temperature distribution (°F).
- 3 - Above plus conductivities (Btu/hr-ft-°F).
- 4 - Above plus volumetric heat capacities (Btu/°F-in^3). (transient only)

WARNING: IEDIT = 2,3,4 result in increasingly large output files and should be reserved for debugging purposes.

MXTHSS Maximum number of steady state thermal-hydraulic passes (i.e., maximum number of values used from card 010030 below).

EPSTH Steady state thermal-hydraulic convergence criterion. Thermal-hydraulic convergence is assumed if at the n^{th} thermal-hydraulic pass,

$$\underset{\text{all T-H nodes}}{\text{MAX}} \left\{ \left| \frac{T_{FUEL}^{n} - T_{FUEL}^{n-1}}{T_{FUEL}^{n-1}} \right| , \left| \frac{\rho_B^{n} - \rho^{n-1}}{\rho_B^{n-1}} \right| , \left| \frac{T_B^{n} - T_B^{n-1}}{T_B^{n-1}} \right| \right\} < EPSTH$$

The maximum of each of the three ratios is printed after each T-H pass with an indication of whether convergence has been satisfied. Floating point.

ITFMAX Maximum number of iterations on the steady state fuel pin temperature distribution allowed to obtain consistent conductivities.

EPSTF Criterion in °F for convergence of steady state fuel pin temperature distribution. Floating point.

IDTMOD
IDDENS
IDTFUL Numeric nuclide ID's for the three thermal-hydraulic feedback variations (ΔX_n's): moderator temperature (°F), moderator density (gm/cc) and square root of average fuel temperature in °K (NOTE: T_{FUEL} reference value is input in °F--not square rooted; the code makes the necesssary conversion internally).

The code reads this card (if present) regardless of whether a thermal-hydraulic calculation is specified. This allows the cross section routines to identify IDTMOD, IDDENS and IDTFUL. The associated variables may be given initial number densities in the absence of a thermal-hydraulic calculation. See card 100tts under section A7.7.

010020,IFT,C_1,C_2,C_3,C_4,C_5 (1 to 6 entries required; all C's are floating point.)

IFT=0 *Full steady state and transient fuel temperature distribution* calculated using finite differences.

IFT=1: Correlation 1

$$T_{FUEL} = C_1(1-C_2\, e^{-C_3 \cdot KW/FT}) - C_1\,(1-C_2) + T_{WALL}$$

IFT=2: Correlation 2

$$T_{FUEL} = C_1 + KW/FT\,(C_2 + KW/FT\,(C_3 + KW/FT \cdot C_4))$$

where KW/FT is the local linear heat rate (kw/ft) and T_{WALL} is the clad surface temperature.

010030,N_1,N_2,N_3,...,N_{20} default N_1 = 10

N_i number of outer (source) iterations in steady state neutronics calculation prior to i^{th} thermal-hydraulic pass. If only j numbers are present, then the code uses $N_i=N_j$ for all $j \geq i$ ($j \leq 20$ allowed). If more than MXTHSS (see card 010016) values are present, they are ignored.

If $N_j \leq 0$ no source iterations are performed before the j^{th} thermal-hydraulic pass. This allows the user to set $N_1=0$, for example, and force a thermal-hydraulic calculation based on the initial flux guess. The initial flux guess is uniform flux unless a guess has been input.

010031,TLOW,INCL,THI,INCH (Water Property Tables)

TLOW and THI are the floating point lower and upper temperatures for subcooled and superheated water property tables, repsectively. The subcooled table extends from TLOW to the saturated liquid temperature in INCL increments. The superheated table extends from the saturated vapor temperature to THI in INCH increments. If INCH=0 then THI is ignored and one entry is made for saturated vapor.

For supercritical pressures (over 3208.23474 psia), only TLOW, INCL, and THI may be present. A table in INCL increments from TLOW to THI is created.

500110,PRES,WIN,0. (All floating point)

PRES System pressure (psia)
WIN Core inlet flow (lbm/hr)
0. A value must be supplied but is not used.

500120,DUO2,TG,TC,HEIGHT,RC,0.,RHOUO2(10.4215),NFUEL(3),NCLAD(3)
(All but NFUEL,NCLAD floating point)

DUO2 Fuel pellet diameter (in.)
TG Gap thickness (in.)

TC — Clad thickness (in.)

HEIGHT — Active core height (in.).

RC — Fraction of heat deposited directly in coolant.

0. — A value must be supplied (but is not used) if RHOUO2, NFUEL, or NCLAD are input on this card.

RHOUO2 — Fuel stack height density in gm/cc.

NFUEL, NCLAD — Number of radial temperature points (not increments) in fuel ($\geq$3) and clad ($\geq$2) respectively.

The centerline and all physical surfaces are counted in determining NFUEL and NCLAD. For example, to have five regions in the fuel, specify NFUEL=6. To have one region in the clad, specify NCLAD=2.

Defaults, where allowed, are indicated in parentheses. A value of zero or too few numbers on the card (minimum 5) will result in the default being set.

501sss,TIN,WP,PINS,AC,GIN (All floating point) sss=001,...,999

Each card defines thermal channel type sss

TIN — Inlet temperature (°F)

WP — Wetted perimeter (ft)

PINS — Number of fuel pins (floating point number--fractional values allowed)

AC — Coolant flow area (ft^2)

GIN — Relative mass velocity. The code will multiply all GIN's by a normalization factor so that

$$\sum_{\text{primary channels}} GIN \cdot AC = WIN$$

See card series 502sss below for discussion of primary and secondary channels.

502sss,±NTYPE,EDITSET,±NTYPE,EDITSET (all integers)

This card series associates channel type descriptions (from series 501sss) and planar edit sets (from series 011sss to 014sss) with thermal channel numbers. The following convention is used for the sign of NTYPE:

NTYPE>0 The channel is a primary thermal channel. Its values for TFUEL, TMOD, and DENS are used to modify cross sections in feedback calculations. The planar edit sets for all primary channels must exactly span the active core area with no overlap and no unrepresented areas. (WARNING: there is no automatic error checking for this requirement.) Areas outside the active core may be included, but AC and GIN must represent only the active portion of the channel. Only primary channels are used to normalize GIN.

NTYPE<0 The channel is a secondary thermal channel for which the user desires thermal calculations but which presumably duplicate areas covered by primary thermal channels. Results from secondary channels are not used for feedback, and the area of secondary channels area is not considered in normalizing GIN. Their input value of GIN is, however, multiplied by the same normalization factor computed for primary channels.

Channel Numbers For reasons of efficiency the code resequences the data on series 502sss so that all primary channels are listed first and all secondary channels last. The channels are then assigned thermal channel numbers in the new sequence. If the user desires to avoid confusion by having the channel numbers correspond to the sequence on series 502sss he should list primary channels first.

NTYPE=0 is permitted but is interpreted to mean that the listed edit set is not a thermal channel. No channel number is assigned. Use of NTYPE=0 has the same effect as not listing the edit set on card 502sss.

503000,HGAPC1,HGAPC2,ID_1,...,ID_N (Gap Conductance Input)

All entries must be provided. N is the number of thermal channels. The user is reminded of the MØDEL repeat notation, e.g., /5/1→1,1,1,1,1.

HGAPC1,HGAPC2 floating point constants for the transient temperature dependent HGAP calculation

$$HGAP = HGAPSS \left\{\frac{TGAP + HGAPC1}{TGAPSS + HGAPC1}\right\}^{HGAPC2}$$

TGAPSS and HGAPSS are steady state values of the average gap temperature and gap conductance, TGAP, and HGAP, respectively.

ID_j=KKK indicates use card 503KKK for determining steady state value of HGAP as a function of KW/FT. Use of multiple tables is envisioned for representation of fuels of different type or burnup.

503KKK, KW/FT_1, $HGAP_1$,KW/FT_2,$HGAP_2$,... (all floating point)

KKK HGAP table number. The tables must begin with 001 and be sequential. It is not required that a table be used on card 503000, so dummy tables may be entered. At least one table is required.

A minimum of two KW/FT, HGAP, pairs is required. The KW/FT entries must be in ascending order. Steady state HGAP as a function of KW/FT for a given thermal-hydraulic node is determined by linear interpolation.

A11.0 INPUT AND OUTPUT FILES

Permanent files are stored and retrieved through the IFM File Manager system. Briefly, this system permits a program to process files in terms of their logical structure, with no knowledge of the physical format of the files required. File processing is also independent of the physical device used, which may be either a magnetic tape or a disk.

Three levels of identification are associated with each file: the seven-character user name of the person creating the file (see section A2.0) a FILEID of up to ten characters supplied as input by the user, and a file type number supplied by the program. Thus, files created by different individuals are distinguished by user name, files created in different jobs or different cases of the same job are distinguished by file ID, and files created in the same case are distinguished by type number.

HERMITE will accept flux, concentration, and thermal-hydraulic data files as input and will store flux, concentration, thermal-hydraulic data, and thermal-hydraulic plot files for subsequent use. Input files are retrieved near the beginning of a case, and a comment is added to the printed output after each file has been successfully read. Input files are required to be on disk. An auxiliary program, TCOPY, is available for moving such files from tape to disk.

An input flux file must be compatible with the current problem in number of groups, finite element columns, rows and planes. If an input flux file is not used, the flux is set to zero at all zero flux boundary points and to one everywhere else.

An input concentration file must be compatible in number of nuclides, number of mesh points per plane, and number of planes. In addition, the order in which the nuclides are listed in the input must not be changed.

An input thermal-hydraulic data file must be compatible in the number of channels, the number of axial thermal-hydraulic blocks and the number of fuel and clad mesh intervals.

Output files are saved at the very end of a steady-state case and at selected time points during a transient. Each may be stored on tape or disk or both. A comment is added to the output after each file has been successfully written on either device. Thus, if there is a failure during filing, the comments indicate which files had been saved before the error occurred. In the case of a tape failure, an attempt should not be made to write on the tape in any subsequent job. Note that there is no provision in the program for using more than one reel of tape in a single job.

0100IS,USER,FILEID S=1,2,3,5

USER Name on USER control card of job where files were saved.
FILEID 1-10 character alphanumeric identification of the file to be input for this case.
S=1 ⇒ Input flux file.
S=2 ⇒ Input number density file.
S=3 ⇒ Input thermal-hydraulic data file.
S=5 ⇒ Input transient restart files.

For a summary on use of initial guesses and on restarts see Section A13.

010021,FILEID

FILEID 1-10 character alphanumeric file identification for output files. These files are written at the end of the steady-state calculation. In the case of transient restart files, only the first 6 characters will be used (the last four are overwritten with zsss where z is the time zone number and sss is 1 + the time step number in the time zone z. sss is right justified and blank filled so there may be embedded blanks in the file identification of transient restart files).

010022, File Writing Flags

Up to five numbers may be present on this card to request that files be saved at the end of the steady state calculations or to indicate the disposition of any transient restart files saved. There is one number for each file in the order: flux file (type 220), number density file (type 221), thermal-hydraulic data file (type 224), thermal-hydraulic plot file (type 223), and transient restart files, (types 220, 221, 224, and 323). The first three files may be used as steady state input to a transient calculation (IC(1) = 2 on card 010000). The values of the flag for each file are:

0 ⇒ do not save file
1 ⇒ save file on tape only
2 ⇒ save file on disk only
3 ⇒ save file on both disk and tape.

See card 021007 under Section A5.2 for specification of time steps when transient restart files are written.

A12.0 PLOT FILE CONTROL DATA

HERMITE has the capability of saving data on disk for plotting. In order to limit the amount of data saved, the user is required to specify the items to be saved and the time points at which these items are to be saved. The specified information is written on a random access file and can be retrieved and plotted by the Physics Integrated Plotting System (PIPS). On any given run the user may attach and overwrite or extend an existing plot file or may catalog a new plot file.

More than one selection of data may be saved on the plot file and each selection is specified by a different identifier or RECID. This feature allows the user some flexibility in trading off spatial detail for frequency in time without saving excessive quantities of data. For example, the user may wish to save detailed spatial data at steady state, and maybe a few selected time points while saving smaller amounts of data at close enough time intervals to obtain smooth plots in time. For this purpose he would require two RECID's. Each different RECID requires a complete plot file description beginning with card 019P00 (P = 0,1,...,9 for up to 10 RECIDS).

The user may also add new RECID's to an existing plot file which he is extending.

Data saved on the plot file is in compressed format to save disk space. Compressed format retains only about 6-1/2 significant decimal digits of information.

In the present version of the code, it is necessary to perform a thermal-hydraulic calculation in order to obtain spatial information.

In addition to the data selected by the user, the following data is always saved.

ID	Variable
1	Time (sec)
2	Power (watts)
3	Pressure (psia)
9	Height of middle of each axial block (cm). All thermal hydraulic variables saved are calculated at, or interpolated to the center of the axial block. See card 019P60, below.

010019, {ATTACH, (pfn) / CATALOG, [(pfn)]}

If this card is missing, no further plot file information is read.

ATTACH — Attach existing plot file for rewriting or extending. pfn required.

CATALOG — Catalog a new plot file with either the default or the supplied pfn. If a file with the same pfn already exists, the operating system will modify the first character, trying A, B, C and so on until a unique name is found.

pfn — Permanent file name, 1 - 40 characters. If missing on CATALOG mode, the following unique default pfn is generated

(NUAHERMITEPLTEDTFILEttttttttttmm-dd-yy-jj)

where,
t...t is columns 10 - 19 of title card
mm-dd-yy is the date
jj is the last two characters of the job identifier (supplied by the system)

019P00, RECID, IFORM, ITPRGM

P — 0,1,...,9 one subseries 019P for each RECID.

RECID — Unique 1- 10 character hollerith identification for this selection of data.

IFORM — Data format (hollerith character).

S indicates all data saved on a single record for steady state or for each time point.

Z indicates multiple records saved at each time point including steady state. A global record followed by one axial record per axial thermal block is saved at each time point. This option is used to break the information into smaller records if the S format record would contain more than 8190 numbers. S format should be used whenever possible.

ITPRGM — Time program. (Two hollerith characters).

T0 (T-zero) Save data for this RECID at steady state only.

T1 Save data for this RECID at steady state and at all time points selected on card 021005 (see Transient Program Control Cards, Section A5.2).

T2 Save data for this RECID at steady state and at all time points selected on card 021006.

019P20 (Optional)

List rod group numbers whose height is to be saved (up to NRGRPS numbers - see card 700000). Must be in increasing order.

019P50 (Optional)

List all thermal-hydraulic channel numbers for which data is to be saved. Must be in increasing order.

019P60

List variable ID's for all thermal-hydraulic variables to be saved. Must be in increasing order. The selected variables are saved for all axial blocks of the selected channels. The following thermal hydraulic variable ID's are defined in the current version of the code.

ID	Definition
11	Average fuel temperature (°F)
12	Moderator temperature (°F)
13	Moderator density (lbm/ft^3)
14	Void fraction
15	Not available
16	Enthalpy (Btu/lbm)
17	Quality
18	Not available
19	Linear heat rate (nuclear) (kw/ft)
20	Heat flux into coolant (Btu/hr-ft^2)
21	Not available
22	Not available
23	Mass flow rate (lbm/hr)
24	Not available
25	Gap conductance (Btu/hr-ft^2-°F)
26	Centerline fuel temperature (°F)
27	Pellet surface temperature (°F)
28	Inside clad surface temperature (°F)
29	Clad coolant surface temperature (°F)
30	Flow velocity (ft/hr)

A13.0 RESTART CAPABILITIES

Information necessary to restart calculations is scattered throughout this input description. In order to assist the user in saving the necessary files and in using them to restart calculations, the relevant information has been extracted and amplified below.

There are three basic restart situations. In situation 1 the user has saved a steady state solution from a previous run but either wishes to perform further iterations, or intends to modify some of the input parameters slightly and use the original solution as an initial guess. In situation 2, the user has a completed steady state calculation and wishes to initiate a transient calculation with no further steady state computations. In situation 3, the most complicated situation, the user wishes to continue a transient calculation which is already in progress. He may be running the transient in segments so that he may analyze the results before proceeding to the next segment, he may be restarting a transient which aborted due to computer failure, or he may be changing the sequence of events (such as rod motion) at times after the restart. Each situation will now be discussed separately below.

Situation 1 or 2 - Saving Steady State Files

To save steady state results the following cards are necessary:

USER(name) in job control deck
010021,FILEID (1-10 characters - 6 characters recommended)

010022,I_1,I_2,I_3,I_4

- I_1 = 2 saves flux file on disk
- I_2 = 2 saves number density file on disk
- I_3 = 2 saves thermal-hydraulic file on disk (if a thermal-hydraulic calculation was performed)
- I_4 = 0 thermal-hydraulic plot file, not required for restarts. Use 1, 2 or 3 to save the file on tape, disk or both, respectively

I_1,I_2, or I_3 may also be 1 or 3 to save the data on tape or on both disk and tape but it is required that the files be on disk when they are read to perform the restart. Only the flux file is necessary for the purpose of continuing the steady state iterations (Situation 1) although use of input number density and thermal-hydraulic data files will save a small amount of computer time.

Situation 1 - Continuing Steady State Iterations

The following cards may be needed to continue steady state iterations.

010011, USER, FILEID

Designates input flux file to use for initial guess. Required.

010012, USER, FILEID

Designates input number density file. May be omitted -- see card 010030 below. Should be omitted if thermal-hydraulic channels, edit sets, table sets, initial number densities, or compositions have been changed.

010013, USER, FILEID

Designates input thermal-hydraulic data file. May be omitted. Serves no purpose in Situation 1. Should be omitted if any data affecting the thermal-hydraulic calculation has been changed.

010030, n_1,n_2,n_3,...,n_{20}

This card controls the number of outer (source) iterations before each thermal-hydraulic pass in a problem with thermal-hydraulic feedback. If card 010012 is omitted, n_1 should be set to zero. This will cause one thermal-hydraulic pass to occur before any neutronics iterations are

performed and will save iterations by creating a number density file consistent with the initial flux guess (and its implied power distribution).

010019, {ATTACH, pfn / CATALOG, [pfn]}

If the original run of the problem wrote a plot file and it is desired to overwrite the original plot file, change CATALOG to ATTACH. If it is desired to write a new plot file, CATALOG a new pfn (or allow the code generate a new unique default pfn). If it is desired to use the same plot file with a new RECID, ATTACH the old file but change cards 019P00.

If an attempt is made to catalog a second file with the same pfn, a new pfn will be created by the system by changing the first character to A, B, C and so on until a unique name is found.

Situation 2 - Initiating a Transient From Saved Steady State Files

The following changes and cards are required to initiate the transient.

010000,2,...

Set item 1 to 2 to indicate transient calculation only.

010011, USER, FILEID	(required)
010012, USER, FILEID	(required)
010013, USER, FILEID	(required if thermal-hydraulic calculation is being performed)
010019, . . .	(same as for situation 1)

If the old plot file pfn and RECID are used, the steady state results will be overwritten and the transient results added on.

Situation 3 - Saving Transient Restart Data

To save transient restart data the following cards are needed.

USER(name) in job control deck

010021, FILEID (1 - 10 characters, only 6 will be used)

010022, I_1, I_2, I_3, I_4, I_5

I_1 - I_4 affect steady state files only (see Situations 1 and 2)

I_5= 1/2/3 Save transient restart files on tape only/disk only/ or both. Files must be on disk to be read for restarting the transient. Note that four files are actually saved if $I_5 \neq 0$

021007, n_1,n_2,...

Gives frequency at which restart files are saved during each time zone. For example, if n_2 = 5, restart files are saved after every 5 time steps during and at the end of the second time zone. For details on the use of this card see Transient Program Control.

Situation 3 - Restarting a Transient Already in Progress

To continue a transient already in progress the following cards are needed.

010000, 3, ...

Change item 1 to 3 to indicate restarted transient in progress.

010015, USER, FILEID

FILEID is aaaaaazsss where aaaaaa are the first six characters of the FILEID given on card 010021 on the original run (left-justified, blank filled). z is the number of the time zone during which the file was saved (a file saved at the end of time zone k has z = k). sss is one plus the time step number, counted from the beginning of the time zone after which the file was saved (right-justified, blank filled). Files saved after the

25th step of time zone 2 have zsss = 2b26 where b represents a blank. The user is advised to check the output of the job which saved the file to ensure he has the correct FILEID.

010019, ATTACH, pfn (if plotting)

The mode must be ATTACH and the pfn must agree with the pfn cataloged. Use of CATALOG will yield unpredictable results. Any time steps which exist on the file after the restart point will be destroyed and overwritten by new results.

019PSS

These cards may not be altered except that an entire subseries 019P may be deleted.

The following additional cards may require modification:

010010, item 3, NTZ = number of time zones

020004, TZ(1),TZ(2), . . . (time zone widths)

The last zone before the restart may be lengthened. Subsequent zones may be altered, added, or deleted.

020005, DELT(1),DELT(2), . . . (time step widths)

May be altered for zones which have not been processed.

021001 - 021007,J_1,J_2, . . . (transient program control)

Frequencies may be altered for any zone, but only the uncompleted portion of the transient is affected. Frequencies for a zone in progress may be changed. If this occurs, the code counts from the beginning of the zone in

determining when every n^{th} time step is completed. For example, say the new frequency is every 8 time steps and the restart was taken after 20 steps. The selected event (depending on the card number) will occur next after step 24 - the next even multiple of 8.

0211SS, n_1,n_2,... (transient iteration control)

May be altered. Changes affect the portion of transient not yet completed.

022002, CHGTF, CHGTC, CHGRHO (feedback override limits)
022004, CHGROD (feedback override limit)

May be changed. Changes affect uncompleted portion of transient. Since feedback is computed immediately after the restart, cumulative changes start at zero.

700I01, V_1,T_1,V_2,T_2,... (control rod velocity functions)

Recall that the data on this card represent points in a piecewise linear function of time. Careless alteration of a point after the restart was taken may affect the value of the function before the restart. Unpredictable results will occur if the function is altered for times preceding the restart. The following is a legal change for a restart taken at .7 seconds. Note that the data are v,t pairs.

Old

700201, 0., 0., 150., 1., -250., 1.5

New

700201, 0., 0., 120., .8, 140., 1., -250., 1.5

ABB Combustion Engineering Nuclear Operations
Combustion Engineering, Inc.
2000 Day Hill Road
Post Office Box 500
Windsor, Connecticut 06095–0500
Telephone: (860) 285–9678
Fax: (860) 285–4117